



SAPIENZA
UNIVERSITÀ DI ROMA

Scuola di Dottorato di Ricerca in **Neuroscienze**

Curriculum di **Psicobiologia e Psicofarmacologia**

**Morphofunctional impairment of neuronal and glial cells in
the developing cerebellum of a mouse model of Niemann-
Pick type C1 disease**

PhD student: **Francesco Bruno**

Tutor: **Prof.ssa Maria Teresa Fiorenza**

Index

Chapter I. The Niemann-Pick type C disease

1.1.	Historical background and definition	5
1.2.	Epidemiology	7
1.3.	Clinical manifestations	8
1.3.1.	Systemic symptoms	9
1.3.2.	Neurological symptoms	9
1.3.3.	Psychiatric manifestations	11
1.3.4.	Cognitive impairment and neuropsychological profile	12
1.4.	Genetics of NP-C disease	13
1.4.1.	Structure of NPC1 protein	13
1.4.2.	Structure of NPC2 protein	14
1.4.3.	<i>NPC1</i> and <i>NPC2</i> gene mutations	15
1.4.4.	NPC1 and NPC2 function: a key role in the intracellular trafficking of lipids	18
1.4.5.	Consequence of NPC1 and NPC2 mutations on lipids trafficking	22
1.5.	Murine models of NP-C1 disease	24
1.6.	Diagnosis	25
1.7.	Differential diagnosis	30
1.8.	Prognosis	30
1.9.	Treatments	31

Chapter II. The cerebellum: involvement in NP-C1 disease

2.1.	The cerebellum	37
2.1.1.	Cerebellar neurons	40
2.1.2.	Cerebellar glia	42
2.2.	Origin of cerebellar neurons and glia	46
2.3.	Interaction between Bergmann glia and Purkinje cells	49
2.4.	The scaffolding role of Bergmann glia during granule neuron and Basket/Stellate interneuron migration	50

2.5.	The involvement of astrocytes and microglia in NP-C1 disease	54
2.6.	Oligodendrocyte differentiation: implication for NP-C1 disease	55
2.7.	Sonic hedgehog patterning during cerebellar development: implications for NP-C1 disease	59
2.8.	The importance of BDNF signaling pathway in cerebellar development and current knowledge of its role in NP-C1 disease	62

Chapter III. The research project

3.1.	Background and aims	65
3.2.	Materials and methods	67
3.2.1.	Mice	67
3.2.2.	Genotyping	67
3.2.3.	Treatments	68
3.2.4.	Western blot assays	70
3.2.5.	Brain collection and sectioning	70
3.2.6.	Immunohistochemistry	70
3.2.7.	Histological analyses	73
3.2.8.	Behavioral assessment	74
3.3.	Statistical analyses	
3.4.	Results	77
3.4.1.	The overall cerebellar size is reduced in <i>Npc1^{nmf164}</i> and is rescued by CD treatment	78
3.4.2.	<i>Npc1^{nmf164}</i> mice display a reduced density of GNs in the external granule layer (EGL)	80
3.4.3.	The reduced density of GNs in the EGL is due to defective proliferation of precursors	83
3.4.4.	GN precursor proliferation defect results in a disorganized cellular architecture of the EGL	85
3.4.5.	<i>Npc1^{nmf164}</i> mice display abnormal Bergmann glia morphogenesis and early astrocyte activation that are not rescued by the CD treatment	87
3.4.6.	Bergmann glia functions are defective in <i>Npc1^{nmf164}</i> mice	91
3.4.7.	The cerebellar cortex of PN15 <i>wt</i> and <i>Npc1^{nmf164}</i> mice displays similar densities of Bergmann glia, Purkinje cells and Basket/Stellate interneurons	94

3.4.8. Purkinje cells of <i>Npc1^{nmf164}</i> mice display a reduced number of glutamatergic and GABAergic inputs which is rescued by the CD treatment	96
3.4.9. <i>Npc1^{nmf164}</i> mice display defective myelin maturation	101
3.4.10. <i>Npc1^{nmf164}</i> mice display normal levels of activated microglia but a reduced microglia-mediated phagocytosis	107
3.4.11. <i>Npc1^{nmf164}</i> mice display an abnormal BDNF signaling pathway	109
3.4.12. <i>Npc1^{nmf164}</i> mice show a delay in the acquisition of complex motor skills requiring fine motor coordination and balance	111
3.4.13. Motor deficits of <i>Npc1^{nmf164}</i> mice become more severe in the adulthood	116
Discussion and conclusions	118
References	124

Chapter I

The Niemann-Pick type C disease

1.1. Historical background and definition



Albert Niemann
(1880-1920)

The first case of an individual affected by the then unknown Niemann-Pick disease has been described by the German pediatrician **Albert Niemann** in 1914. Niemann described a child that died at 18 months and had an abnormal enlargement of liver and spleen, swelling and darkening facial skin and several alterations of nervous system (Niemann, 1914).

Later on, in 1927, the German pathologist **Ludwig Pick** studied *post-mortem* tissues of several children who had similar symptoms (Pick, 1927). From their pioneering work was coined the eponym **Niemann-Pick disease**.

For many years, this eponym was used to define a heterogeneous group of lipid storage diseases, with the common characteristic of hepatosplenomegaly and sphingomyelin accumulation in the reticuloendothelial and parenchymal tissues, with or not neurological involvement (Vanier, 2010).



Ludwin Pick
(1868-1944)

In 1958, **Crocker and Farber** discovered that the disease had a variable age of onset, clinical manifestations and sphingomyelin accumulation levels in tissues (Crocker and Faber, 1958). This led the researchers to classify Niemann-Pick disease into four subgroups (types A, B, C and D), each characterized by specific pathological features (Crocker, 1961).

In particular:

- the **Type A** is landmarked by a severe and early deterioration of the central nervous system (CNS) and a massive accumulation of sphingomyelin in bowels and brain;
- the **Type B** shows a chronic course with a marked involvement of bowels in spite of a small involvement of CNS;
- the **Type C** and the **Type D** are characterized by a sub-acute involvement of CNS, a slower progression of the disease and a more moderate and mild visceral accumulation. Noteworthy, Type D patients share a common geographical origin, Nova Scotia.

In 1966, the research group lead by Brady demonstrated that type A (NP-A) and type B (NP-B) are very different from type C (NP-C) and -D, the first two types being characterized by a specific severe deficiency in lysosomal sphingomyelinase activity (Brady et al., 1966).

Further investigations indicated that the prominent feature of NP-C and -D disease was an impairment in the intracellular trafficking of cholesterol and other lipids (Pentchev et al., 1984).

In 1997, it was discovered that most of NP-C patients had a common genetic trait: a mutation in the gene, later termed *NPC1*, located on chromosome 18q11 (Loftus et al., 1997; Carstea et al., 1997).

Three years later, it was found that a small proportion of patients who showed the characteristic symptoms of NP-C disease but had no mutations in the *NPC1* gene, had a mutation in *HE1* gene, subsequently renamed *NPC2*, located on chromosome 14q23.3 (Naureckiene et al., 2000).

These discoveries led to the distinction of two groups of Niemann-Pick disease: acid sphingomyelinase deficiencies (due to *SMPD1* mutations, including types A, B and intermediate forms) and alterations in trafficking of endocytosed cholesterol in Niemann-Pick type C disease (due to *NPC1* or *NPC2* mutations). Type D is a distinct entity is no longer considered (Vanier, 2010).

In summary, **Niemann-Pick type C disease** is an inherited lysosomal storage disorder, with autosomal recessive transmission, ultimately fatal and presenting variable neurovisceral symptoms, age of onset and life span (Pentchev et al., 1984; Vanier, 2010). It is caused by mutation of the genes ***NPC1*** (~95% of cases) or ***NPC2*** (~5% of cases), encoding for two proteins that cooperatively mediate the egress from endosomes/lysosomes of exogenous cholesterol (Vance, 2006; Peake and Vance, 2010).

The reduced functionality of these proteins causes an accumulation of cholesterol and other lipids such as sphingosine and gangliosides (GM2 and GM3) in late endosomal/lysosomal compartments (Pentchev and Tagle, 1996; Peake and Vance, 2010). This impairment leads to hepatosplenomegaly and progressive neurodegeneration that causes premature death (Peake and Vance, 2010).

Although *NPC1* and *NPC2* complementation groups are indistinguishable from a biochemical and clinical point of view, in literature is usually referred to them as NP-C1 and NP-C2 disease (Vanier et al., 2016).

1.2. Epidemiology

It is very difficult to estimate the real incidence and prevalence of the NP-C disease due to poor clinical knowledge of the disease combined with the relative difficulty in conducting appropriate biochemical tests (Vanier, 2010). The most recent incidence estimated worldwide is **1.12** affected patients **per 100.000 live births** (lb) (Wassif et al., 2016).

However, in **Portugal** 9 cases were reported between 1985 and 2003 (prevalence 2.20 per 100.00 lb) (Pinto et al., 2004). Prevalence estimates vary between **0.66** and **0.83 per 100.00** lb in **France, England** and **Germany** on the basis of the diagnoses made between 1988 and 2002 (Patterson et al., 2001; Vanier and Millat, 2003). In **Australia** were reported only 20 cases between 1980 and 1996 (prevalence 0.47 per 100.000 lb) and in **Low Countries** only 25 cases during the period 1970-1996 (prevalence 0.35 per 100.000 lb) (Meikle et al., 1999; Pinto et al., 2004).

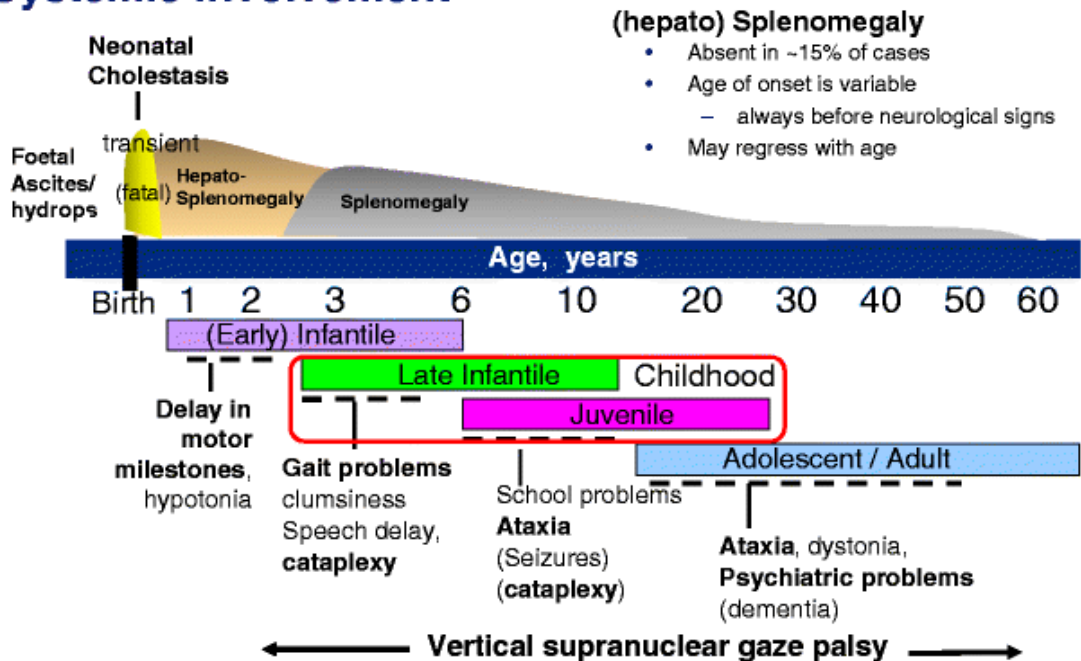
The low prevalence observed in Australia and Low Countries could be explained by misdiagnosis; the broad clinical spectrum of NP-C disease wasn't recognized until the 90s of the last century and up to the mid-80s specific laboratory tests weren't available (Vanier, 2010).

1.3. Clinical manifestations

The NP-C disease is a **neurovisceral condition** that clinically manifests with **systemic, neurological** and **psychiatric symptoms** and **cognitive impairment**. Since the disease has different clinical features depending on the age of onset, some authors have proposed **5 different subgroup classification** (Wraith et al., 2009) (Figure 1):

- **Pre-peri natal** (before 3 months of age);
- **Early infantile** (between 3 and 12 months of age);
- **Late infantile** (between 2 and 6 years of age);
- **Juvenile** (between 6 and 15 years of age);
- **Adolescent/Adult** (after 15 years of age).

Systemic involvement



Neurological involvement

--- Period of onset [Purple] [Green] [Pink] [Blue] Duration

Figure 1. Schematic representation of clinical manifestations of NP-C disease (Vanier, 2015).

1.3.1. Systemic symptoms

Systemic symptoms of NP-C disease mainly include **hepatosplenomegaly**, an abnormal simultaneous increase of spleen (splenomegaly) and liver (hepatomegaly) volumes, and associated symptoms. Pulmonary infiltration with foam cells are usually present only in early onset forms and in subjects with mutation in *NPC2* gene (Griese et al., 2010; Bjurulf et al., 2008). Usually, in late onset forms, hepatosplenomegaly is asymptomatic and often is not clinically recognized. Data suggest that it occurs in the 85% of patients (Vanier, 2010), whereas isolated hepatomegaly is less common in adults (Sèvin et al., 2007).

Often, patients with severe pre-/peri-natal onset have a history of **neonatal jaundice** (Iturriaga et al., 2006; Imrie et al., 2007) and can manifest other systemic symptoms (Vanier, 2010; Garver et al., 2007; Spiegel et al., 1999; Sedel et al., 2008) such as an abnormal storage of fluid in fetal compartments (**fetal hydrops**) and/or in peritoneal cavity (**ascites**), accumulations of bile components in bloodstream (**neonatal cholestasis**) and **hepatic failure**.

However, when systemic symptoms occur, they always precede the onset of neurological signs that may also start after several years (Vanier, 2010) (**Figure 1**).

1.3.2. Neurological symptoms

The **neurological manifestations** occur along a continuous spectrum and there is a considerable overlap between the various forms regardless the age of onset. Often, the onset of neurological manifestation is insidious, with subtle signs such as the presence of a low muscle tone (**central hypotonia**) or frequent falling.

The prominent neurological hallmark of NP-C disease is identifiable in **oculomotor abnormalities** that are present in the 81% of subjects and usually emerge in late childhood with a reduction of saccadic eye movements (Garver et al., 2007). Initially, the ocular disturbance affects vertical saccadic movement and subsequently also the horizontal ones, reflecting the progressive degeneration of the brain stem (Abel et al., 2009; Solomon et al., 2005). Over the time these abnormalities may progress and cause **vertical supranuclear gaze palsy** (VSGP) that begins with a gradual reduction of the speed of saccadic movement (while the saccadic latency remains normal) and leads to a **saccadic palsy** (Solomon et al., 2005; Lengyel et al., 1999). The vestibulo-ocular reflex appears normal until the terminal stage of degeneration.

In the early infantile onset cases, there is a **delay in the developmental milestones**. These include **speech, oculo-motor** and **social delay** and in particular **motor delay** such as slow movements, clumsiness and poor head control (Mengel et al., 2013). Most of these children fail to reach some developmental milestones in the following order: delay in grasping and moving object, lack of visual attention, falls and tendency to cling parents and objects to maintain balance (Mengel et al., 2013). Often, they never learn to walk. During disease progression there is a loss of poorly acquired motor skills followed by spasticity and death within 5 years of age (Vanier, 2010).

In the forms with late onset, several **striatum signs** appear, such as dystonia and **cerebellar signs**, such as cerebellar ataxia, dysarthria and dysphagia (Sarna et al., 2003; Walkley and Suzuki, 2004) (**Figure 1**).

Dystonia consists in an abnormal involuntary muscular contraction, causing inappropriate and repetitive tremulous and twisting movements, which can affect hands and face or influencing posture (Sedel et al., 2008; Albanese et al., 2013). A typical dystonic sign that occurs in NP-C patients is a forced smile during speaking (Mengel et al., 2013). In the terminal stage of the disease, dystonia may also involve trunk and neck (Sedel et al., 2008).

Cerebellar ataxia is the lack of coordination of voluntary movement associated with the loss of cerebellar Purkinje cells (PC) (Sarna et al., 2003; Mengel et al., 2013). It occurs in the 76% of cases with adolescent/adult onset (Sèvin et al., 2007). NP-C subjects manifest a “slow” ataxia characterized by slow movements compared to other ataxic patients. Children suffering from a mild form of the disease may appear slower than healthy ones. For example, they walk instead of running and grab objects cautiously. Usually, ataxia appears after dystonia. Since ataxia may have different etiologies, if it is the only neurological manifestation, it’s better to wait the onset of additional symptoms prior to suspect that the patient is affected by NP-C disease (Mengel et al., 2013).

Dysarthria is a motor speech disorder characterized by a poor articulation of phonemes due to a loss of control of the motor-speech system. It occurs in the 63% of cases with adolescent/adult onset and results from the combination of ataxia and dystonia (Sèvin et al., 2007).

Dysphagia, consisting in difficulty swallowing, begins to manifest with coughing or choking during feeding. It can occur early in the course of the disease and represents a serious problem in the clinical management and a risk factor for mortality because it may result in the interruption of feeding and in fluid or food aspiration (Chien et al., 2007;

Fecarotta et al., 2011). It occurs in the 37% of cases with adolescent/adult onset (Sèvin et al, 2007).

Other less common symptoms include **cataplexy, seizures, sensorineural hearing loss** and **peripheral neuropathy** (Yanjanin et al., 2010; Zafeiriou et al., 2003).

Cataplexy is a relatively specific and common sign of NP-C disease (Garver et al., 2007). It's manifested by the loss of muscular tone of legs and sometimes of neck and jaw, in response to emotions that produce laughter (**gelastic cataplexy**). This symptom is often overlooked, erroneously as the consequence of ataxia or seizures (Vanier, 2010). It occurs in half of the patients with late infantile and juvenile onset and in the 16% of the cases with adolescent/adult onset (Sèvin et al, 2007).

However, **seizures** occur mostly in late infantile and juvenile forms and only in 4% of cases with adolescent/adult onset (Sèvin et al., 2007). They can be both partial and generalized, myoclonic, tonic-clonic and absence (Mengel et al., 2013).

Sensoriniural hearing loss is the loss of hearing or deafness caused by inner ear, sensory organ or vestibule-cochlear nerve disorders. It affects the 20% of patients and can be light or severe (Vanier, 2010). Because proper cholesterol trafficking is crucial in auditory physiology (Ward et al., 2010; Crumling et al., 2012), this symptom is strictly associated to NP-C disease.

Lastly, **peripheral neuropathy** is a rare complication of NP-C disease; some patients have a reduced nerve conduction velocity due to a mild demyelination (Zafeiriou et al., 2003).

1.3.3. Psychiatric manifestations

Psychiatric manifestations often occur in patients with adolescent/adult onset of NPC (Vanier, 2010; Imrie et al., 2007; Sèvin et al., 2007). However, juvenile onset cases with a history of behavioral problems may develop psychiatric disorders during adolescence (Turpin et al., 2003; Sandu et al., 2009).

The most prominent **behavioral problems** of juvenile onset cases are **Attention Deficit Hyperactivity Disorder (ADHD), learning impairment, deficit in expressive language, aggression** and **self-mutilation**. In the 25% of cases with late onset is present a **schizophrenia-like psychosis**, which manifests with visual and/or auditory hallucinations, disorganized thinking and behavioral impairment (Vanier et al., 1991; Walterfang et al., 2009).

Other psychiatric disabilities reported in the literature are **major depression**, **bipolar disorder** and **obsessive-compulsive disorder** (Zafeiriou et al., 2003; Trendelenburg et al., 2006).

1.3.4. Cognitive impairment and neuropsychological profile

The impairment of cognitive functions is observed in all patients with adolescent/adult onset (Imrie et al., 2002; Sèvin et al., 2007) and is less commonly recognized in early childhood forms of the disease.

However, patients with late infantile and juvenile onset may be display **poor school performance**, **learning impairment** and **intellectual disability** (Imrie et al., 2007). **Cognitive dysfunction** in NP-C disease usually begins with fronto-subcortical deficits characterized by deficits in **executive functions**, **reduced processing of language** and **verbal working memory** deficits (Sèvin et al., 2007; Klarner et al., 2007). With the progression of the disease, patients experience a more general cognitive decline, leading in many cases to **dementia** with prominent dysexecutive syndrome and verbal memory disorders in spite of normal visuospatial memory skills (Hulette et al., 1992). The **dysexecutive syndrome** is characterized by inhibition deficits, planning and organization, diminished comprehension and cognitive flexibility (Klarner et al., 2007). The analysis of clinical history of patients revealed the presence of some typical **neuropsychological abnormalities**, including:

- deterioration of fine and gross motor skills, with indistinct articulation;
- alterations of logical and abstract thinking, difficulty in complex associations and divided attention;
- difficulty concentrating and limited memory (specially working memory);
- lack of distance (often interpreted as a sexually uninhibited behavior);
- deficit in word retrieval, followed by the use of stereotyped expression;
- the ability to perform activities of daily living like bathing, dressing autonomously with gradual loss of personal hygiene.

Some authors have proposed a classification system in 5 phases to categorize the severity of the NP-C disease (Higgins et al., 1992):

Phase 0. The disease is diagnosed by biochemical, histological, genetic and molecular examination but patients don't manifest typical symptoms of the disease, yet;

Phase I. The initial symptoms such as minor disorders of movement and cognitive difficulties are present, but sometimes there are recognized only after a painstaking observation because patients can appear normal. Sometimes the gait can be unstable, a mild ataxia or dystonia can be present, horizontal saccadic eye movements can be slow, vertical supranuclear gaze palsy can be limited in moving down or up and the language may be slowed;

Phase II. The severity of motor and cognitive deficit continues to increase. The gait is increasingly unstable; balance problems are present even though the patient is still able to walk independently for short distances (100 m). Ataxia, dystonia, vertical supranuclear gaze palsy and dysarthria become increasingly serious. The speech, although preserved is poor (reduced sentences to simple grammatical structures and vocabulary with depleted) and is landmarked by articulation difficulties.

Phase III. Significant cognitive and motor dysfunction requiring nursing care. The patient can walk independently only if supported and for a few meters; needs assistance with eating, dressing, bathing and becomes incontinent. The speech becomes very limited and reduced to 1/2-word phrases;

Phase IV. Neurological deficits severely compromise walking abilities or determine a vegetative state. The patient is unable to speak or articulate clearly.

1.4. Genetics of NP-C disease

Linkage studies identified two complementation groups of NP-C disease (Steinberg et al., 1994; Vanier et al., 1996), The **NPC1** one, which is responsible of ~95% of cases (Millat et al., 1999; Carstea et al., 1994) and the **NPC2**, which is responsible for the remaining ~5% of cases (Millat et al., 1999).

1.4.1. Structure of NPC1 protein

The *NPC1* gene includes 25 exons, spanning ~56 Kb region and is located on chromosome 18 in position 11.2 (Vanier and Millat, 2003).

This gene encodes for the endolysosomal NPC1 glycoprotein having a theoretical molecular weight of ~180 kDa and consisting of 1278 amino acids (aa) forming 13 transmembrane domains. Behind its transcription, NPC1 protein is synthesized and N-glycosylated in the endoplasmic reticulum (ER). Subsequently it is transported to the Golgi cisternae, where the

oligosaccharide moieties are further modified. Then, the mature NPC1 form reaches the late endosome/lysosome compartments (Watari et al., 1999).

The NPC1 protein is provided with **signal sequence** (aa 1-24), a **N-terminal domain** between aa 25-264 (**luminal loop-1; LL-1**) that binds cholesterol and two large loops (LL-2; LL-3) located in the vesicle lumen. **LL2** (aa 371-615) corresponds to the binding domain for NPC2 protein and Ebola virus (Lu et al., 2015). **LL3** is a cysteine-rich loop (aa 855-1098) containing the ring finger motif that mediates protein-protein interactions. Between these two luminal loops (aa 616-791) there is a **putative sterol-sensing domains (SSD)**. The **C-terminal** is rich in leucine residues protruding into the cytoplasm and necessary for the proper functioning of protein in the endocytic pathway (**lysosomal targeting motif; LLNF**) (Watari et al., 1999; Davies et al., 2000) (**Figure 2**).

The sterol sensing domain shares a 30% identity with the sterol-sensitive domain of 3-hydroxy-3-methylglutaryl-coenzyme A reductase (HMGR) enzyme, the cutting-activating protein (SCAP) and the Sonic Hedgehog receptor *patched* (Davies et al., 2000).

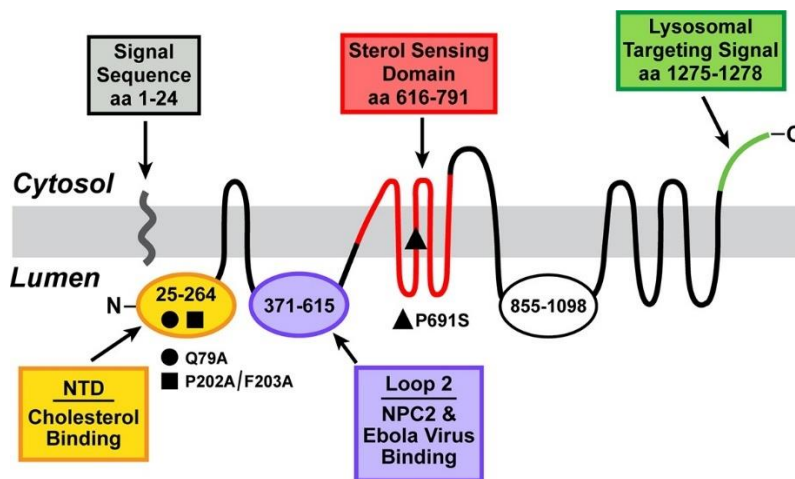


Figure 2. Schematic representation of NPC1 protein structure (Lu et al., 2015).

1.4.2. Structure of NPC2 protein

The *NPC2* gene includes 5 exons spanning a ~13.5 Kb region and is located on chromosome 14 in position 24.3 (Vanier and Millat, 2003). This gene encodes for a small soluble 132 aa glycoprotein, formerly *He1*, having a predicted molecular weight of ~18 kDa (Vanier et al and Millat, 2004; Lu et al., 2015).

The NPC2 protein contains a proline-rich region (PVPFPIP), six cysteine residues and 1 to 3 glycosylation sites (Larsen et al., 1997; Friedland et al., 2003; Vanier and Millat, 2004).

The 3D structure of the bovine protein shares an 80% sequence identity with the human protein and is provided with 7 h-strands arranged in 2 h-sheet stabilized by 3 disulfide bonds, conferring to the protein an immunoglobulin-like β -sandwich fold (Friedland et al., 2003). NPC2 protein is characterized by several cholesterol-binding sites (**Figure 3**).

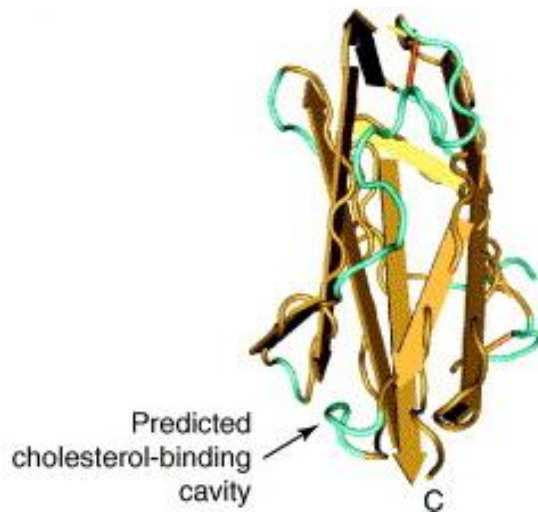


Figure 3. Secondary structure of the bovine NPC2 protein. The cholesterol-binding cavity are reported in light blue (Adapted from Ioannou and Yiannis, 2005).

1.4.3. NPC1 and NPC2 gene mutations

Currently, 380 and 22 distinct mutations in *NPC1* and *NPC2* genes, respectively, (Runz et al., 2008; Stenson et al., 2009; Vanier et al., 2016) are recorded in mutation database. Most of these mutations are missense (71%) and nonsense, although genomic deletions and intronic mutations have been also reported (Bauer et al., 2002; Millat et al., 2005; Runz et al., 2008; Macias-Vidal et al., 2011).

The **mutations in NPC1 gene** can be localized and negatively affect all functional domains except the leucine zipper motif. More than a third of the mutations occur in the cysteine rich luminal loop, mostly in the region between aa 927-958 (Vanier and Millat, 2003), the most frequent ones are: I1061T, P1007A and G992W (**Figure 4**).

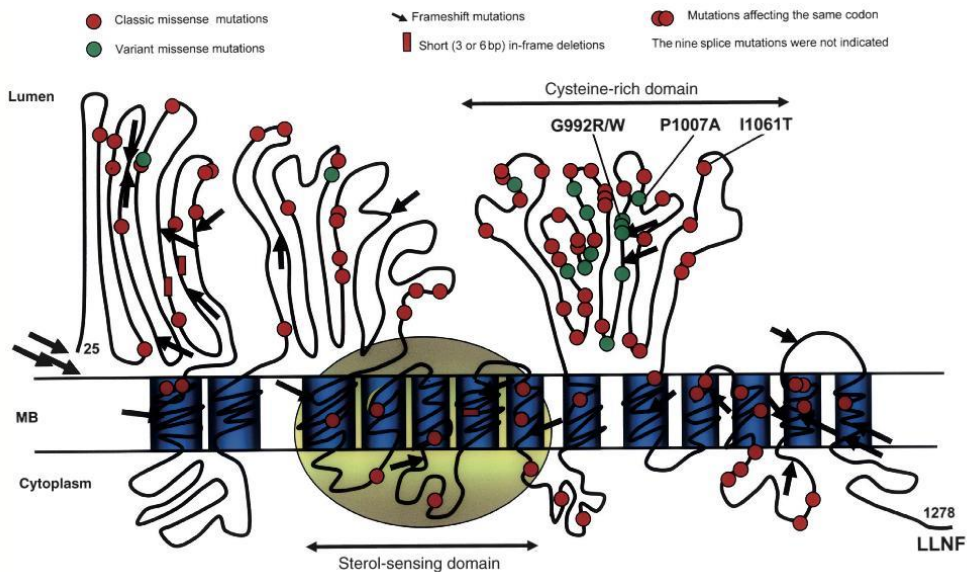


Figure 4. Topology of the most common *NPC1* mutations (Vanier and Millat, 2003).

The **I1061T** mutation occurs mainly in Western European descent patients (20% of France-UK and 15% of USA patients) and is very common in patients from the Spanish-American isolate, southern Colorado and New Mexico (Klünemann et al., 2002; Vanier and Millat, 2003).

The **P1007A** mutation is the second most common mutation in European patients, while the **G992W** one is typically found only in Nova Scotia patients (Greer et al., 1999; Yamamoto et al., 2000; Sun et al., 2001; Meiner et al., 2001; Millat et al., 2001a; Bauer et al., 2002; Tarugi et al., 2002; Vanier and Millat, 2003).

In Japanese patients is very prevalent the **R518Q** mutation, while in Italian patients the **P474L** (Tarugi et al., 2002; Yamamoto et al., 2000). Other common missense mutations are: R404Q, Y852C, D874V, S940L, D948N, S954L, R978C, M1142T, N1156S, and R1186H (see **Table 1**, for details).

While missense mutations of *NPC1* gene are associated to more severe and late onset disease forms, nonsense mutations are typical of infantile onset disease forms, which also display particularly severe neurological impairment (Millat et al., 2001a).

Loop A	Loop C	Loop I	Loop I (cont.)	TM domains	Other
C63R	V378A	D874V	R978C	M272R (1)	I642M
C74Y	L380F	P888S	G986S	M631R (3)	S652W
Q92R	A388P	V889M	G992W/R	G640R (3)	L724P
C113R	R389C	Y890C	M996R	G660S (4)	S734I
T137M	P401T	Y899D	S1004L	V664M (4)	R789C/G
P166S	R404Q/W	G910S	P1007A	C670W (4)	Y825C
C177Y/G	P433L	A927V	G1012D	G673V (4)	C1168Y
N222S	E451K	L929P	In frame del. of 1015–1032	L684F (5)	R1186H
G231V	S473P	R934Q	H1016R	P691L (5)	E1189G
In frame del. of S230, V231	P474L	S940L	V1023G	L695V (5)	
P237S	Y509S	W942C	A1035V	D700N (5)	
D242N/H	H510P	I943M	A1054T	F703S (5)	
C247Y	H512R	D944N	R1059Q	In frame del. of F740, S741 (6)	
G248V	R518W/Q	D945N	I1061T	E742K (6)	
	A521S	D948Y/N	F1087L	A745E (6)	
	P543L	V950M	Y1088C	A767V (7)	
	A605V	S954L	E1089K	Q775P (7)	
	E612D	C956Y	I1094T	S849I (8)	
	R615C	R958Q/L	M1142T	Y852C (8)	
		C976R		N1137I (10)	
				G1140V (10)	
				M1142T (10)	
				N1150K (11)	
				N1156S (11)	
				V1165M (11)	
				T1205R/K (12)	
				L1213F (12)	
				G1236E (13)	
				S1249G (13)	

Table 1. Missense mutation of *NPC1* gene (Scott and Ioannou, 2004).

At least 30 families have been identified worldwide with **mutations in the *NPC2* gene**. In most cases, the mutation generates a truncated protein due to a premature stop codon (Vanier and Millat, 2004). In a first study, the prevalence of **E20X** nonsense mutation, which is associated with infantile onset and a very severe clinical phenotype, was estimated at 50%, but more recent investigations have made it to come down to 30% (Millat et al., 2001a; Vanier and Millat, 2004). Missense mutations are associated with more variable phenotypes and age of onset (Millat et al., 2001a; Park et al., 2003; Chikh et al., 2005); **V39M** is associated with the adult onset of neurological features and a slow progression of disease, while the **C99R** causes a very severe neonatal/infantile disease (Vanier and Millat, 2004). **Figure 5** shows the most common *NPC2* mutations.

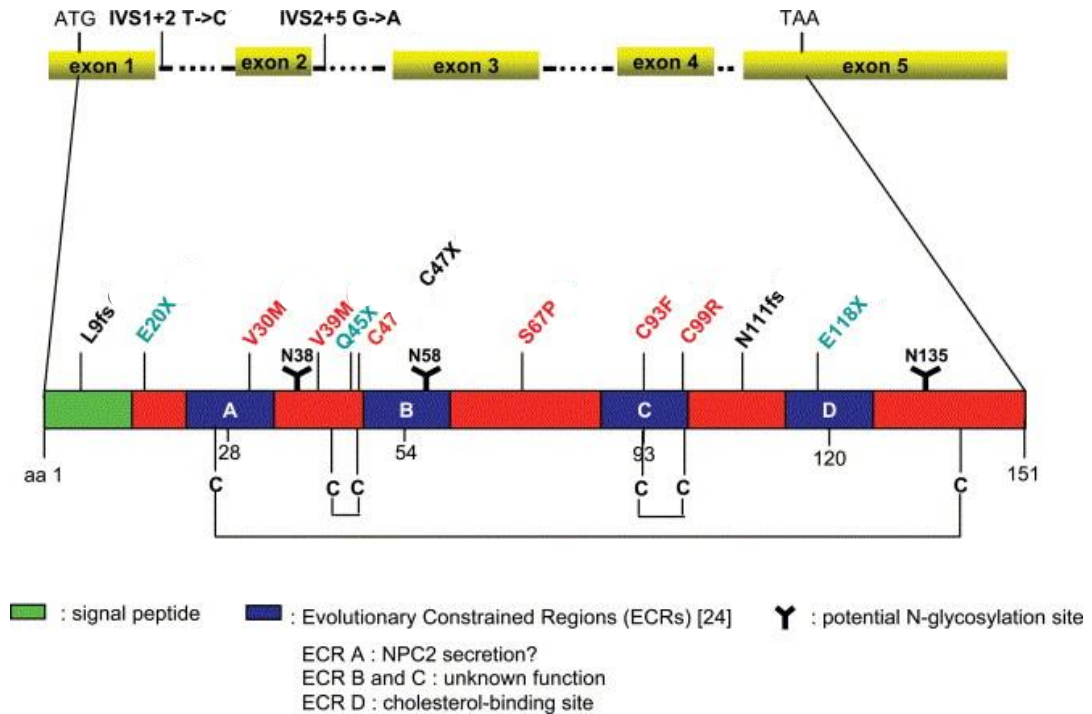


Figure 5. Schematic representation of *NPC2* gene (upper) and *NPC2* protein (lower), showing the localization of *NPC2* mutations (Adapted from Vanier and Millat, 2004).

1.4.4. NPC1 and NPC2 function: a key role in the intracellular trafficking of lipids

It has been shown that NPC1 and NPC2 proteins cooperatively mediate the egress from endosomes/lysosomes of exogenous cholesterol brought to the cells by the low-density lipoprotein (LDL) (Peake and Vance, 2010).

Cholesterol ($C_{27}H_{45}OH$) is a polycyclic aliphatic alcohol, belonging to the family of sterols. Usually in cells it is present as unesterified, or free, cholesterol (an amphipathic molecule with the polar hydroxyl group in position 3 and the remaining part of the molecule apolar). However, it can also be present as esterified cholesterol, or cholesterol ester, in which the hydroxyl group is bound to a carboxylic acid, giving rise to a completely apolar molecule (**Figure 6**).

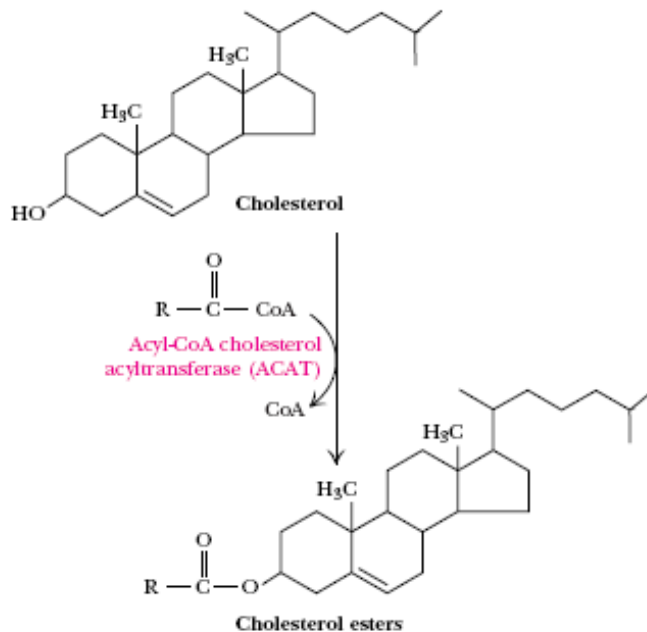


Figure 6. Chemical structure of cholesterol and cholesterol esters. The cholesterol consists of three regions: a hydrocarbon tail, a ring structure region with 4 hydrocarbon rings and a hydroxyl group. The enzyme Acyl-CoA cholesterol acyltransferase (ACAT) catalyzes the condensation reaction between cholesterol and a fatty acid leading to the formation of an ester bound between the carboxyl group of the fatty acid and the hydroxyl group in position 3 of cholesterol.

The brain is the most cholesterol-rich organ of the human body: about 25% of whole-body cholesterol is localized in the brain while the brain represents only the ~2% of body mass (Vance, 2006).

Within the brain cholesterol performs important functions relating to cells architecture and structure. In fact, it is involved in neuronal development, synapses formation and transmission, maintenance of synaptic plasticity, neurite growth, transport of synaptic vesicles and release of neurotransmitters. It is also an essential component of the plasma membrane (PM) and is involved in the formation and maintenance of lipid rafts defined as small and high dynamic domains (10-200 nm), rich in sterols and sphingolipids that compartmentalize cellular processes. In the cytoplasm, cholesterol is the precursor for the synthesis of bile acids, steroid hormones, oxysterols, myelin and Vitamin D (Miller and Strauss, 1999; Kusters et al., 2003; Ikonen, 2006). Because of these pleiotropic functions, an imbalance in the homeostasis of cholesterol severely affects proper brain functioning.

All cells are provided with the biochemical machinery needed for cholesterol synthesis starting from acetyl CoA, although cholesterol synthesis is prominent in liver cells.

Cholesterol does not cross the blood-brain barrier once it is fully established after birth (Abbott et al., 2010) making the adult brain mostly dependent on endogenously-derived cholesterol. Accordingly, cholesterol *de novo* synthesis occurs in neurons, astrocytes and oligodendrocytes during early postnatal neurogenesis, thereafter becoming most prominent in astrocytes that provide it to neurons (Benarroch, 2008).

In astrocytes, cholesterol is synthesized by the HMGR enzyme, which is regulated by a negative feedback mechanism through the sterol-regulated element binding protein (SREBP) that binds to the sterol -regulated element- 1 (SRE-1) in the promoter of the HMGR gene. Then, cholesterol is complexed with Apolipoprotein E (APOE), the largest apolipoprotein expressed in the central nervous system, and is secreted *via* adenosine triphosphate (ATP) binding cassette (ABC) transporter family member A1 (ABCA1), also known as cholesterol efflux regulatory protein (CERP) (Beffert et al., 1998; Karten et al., 2000). The APOE-cholesterol complex is then uptaken by neurons *via* binding low density lipoprotein receptor (LDLR), and once released in late exosomes/lysosomes compartments (LE/L) the cholesterol is de-esterified by the action of lysosomal acid lipase enzyme (LAL) (Herz, 2009) (Figure 7).

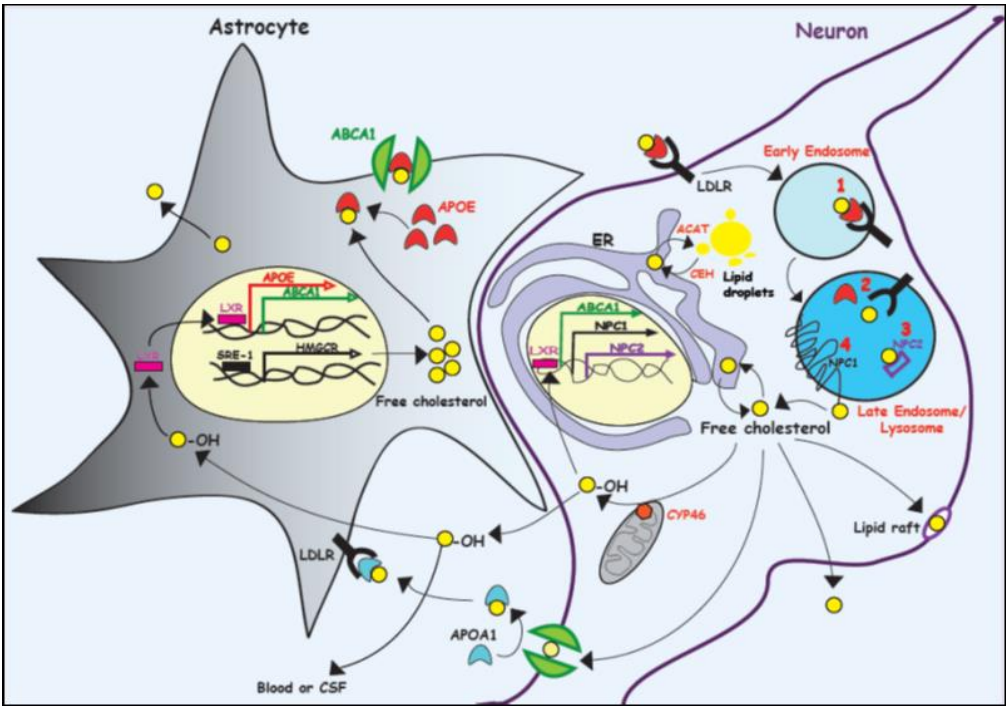


Figure 7. Cholesterol metabolism in mature Central Nervous System (CNS) (Fiorenza et al., 2013).

As already pointed out, NPC1 and NPC2 proteins mediate the egress of cholesterol from endosomes/lysosomes by ways not fully characterized yet. Two possible mechanisms regarding the sequential action of these two proteins have been proposed (Infante et al., 2008) (**Figure 8**). According to the first model (**Model A**), cholesterol stored in vesicles binds to the NPC2 protein localizing in the lumen of LE/E. Subsequently, NPC1 receives cholesterol from NPC2 and transfers it across membranes delimitating LE/E, making cholesterol available to others cellular compartment, including the ER, PM and mitochondria (Vance, 2006; Wang et al., 2010). The second model (**Model B**) predicts that NPC1 removes cholesterol from LE/E vesicles and releases it to NPC2 localizing on the membrane surface of LE/E. Both models predict the participation of an additional protein, not yet identified, which transport cholesterol from LE/E membrane to other sites (Karten et al., 2000).

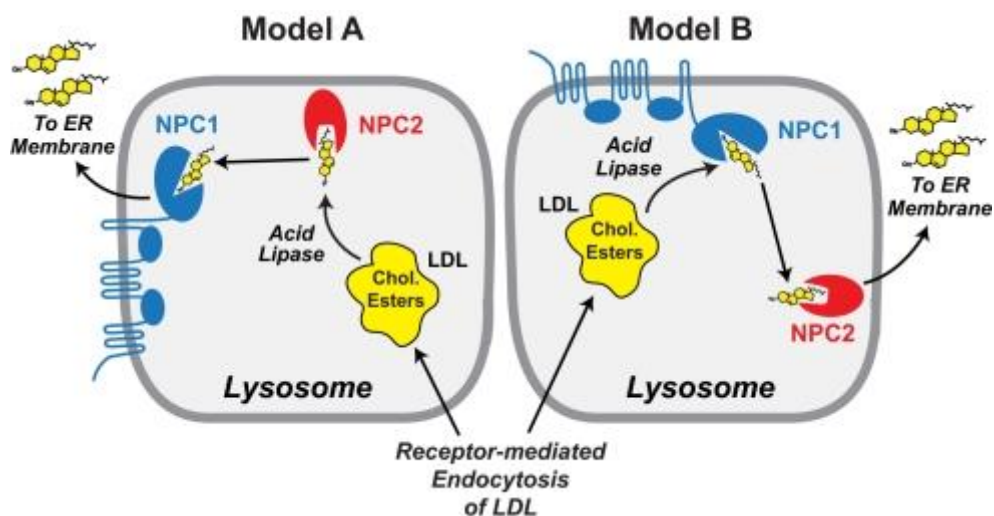


Figure 8. Models for the efflux of cholesterol from LE/E compartment (Infante et al., 2008).

In ER cholesterol is re-esterified by the action of cholesterol acyltransferase (ACAT) and stored as cholesteryl ester; alternatively, it is released by neurons through APOA1-ABCA1 complex or included in lipid rafts. In mitochondria cholesterol is hydrolyzed to 24-hydroxy cholesterol (24-OHC) by the cytochrome P450 (CYP) family member (CYP46), and therefore it can freely cross the blood brain barrier or be released into the plasma. Moreover, when 24-OHC is internalized by astrocytes or neurons it binds the liver X-activated receptors (LXRs), important member of the nuclear receptor that regulates cholesterol homeostasis,

enters in the nucleus to induce the expression of the gene that regulates LXR, APOE and ABCA1 (see **Figure 7**) (Fiorenza et al., 2013).

Besides that, NPC1 protein plays a key role in the LE/L efflux of **sphingosine** and **α -tocopherol**, as well as in the retrograde trafficking of **GM2** and **GM3** gangliosides (Lloyd-Evans et al., 2008; Zhou et al., 2011; Yèvenes et al., 2012).

1.4.5. Consequence of NPC1 and NPC2 mutations on lipids trafficking

Although in NP-C disease the endocytic uptake of LDL-cholesterol and the hydrolysis of LDL-derived cholesteryl esters to unesterified cholesterol in LE/E are normal, the egress of unesterified cholesterol from LE/L is impaired (Sokol et al., 1988; Liscum, 2000; Neufeld et al., 1996). This causes an accumulation of cholesterol, sphingolipids (sphingosine and sphingomyelin), glycolipids (glucosylceramide, lactosylceramide, gangliosides GM2 and GM3), and other lipids such as bis(monoacylglycerol)phosphate (BMP) and lysosome-specific phospholipid (LBPA) in LE/L (Watanabe et al., 1998; Kobayashi et al., 1999; Liscum and Munn, 1999; Zervas et al., 2001b; te Vruchte et al., 2004).

Therefore NP-C disease is mainly conceived as a cholesterol storage disease, although it is still unclear why the defective function of NPC1/NPC2 proteins causes the accumulation of other lipids. In this respect, several studies indicate that cholesterol could not be the primary toxic metabolites of NP-C disease (Davies et al., 2000; Sun et al., 2001; Infante et al., 2008).

In 2008, Lloyd-Evans et al., proposed that NP-C disease is a **sphingosine storage disease**. Sphingosine, with chemical formula $\text{CH}_3\text{-(CH}_2\text{)}_{12}\text{-CH=CH-(CHOH)-(CHNH}_2\text{)-CH}_2\text{OH}$), is an 18-carbon amino alcohol with an unsaturated hydrocarbon chain, that form the primary part of sphingolipids (Figure 9).

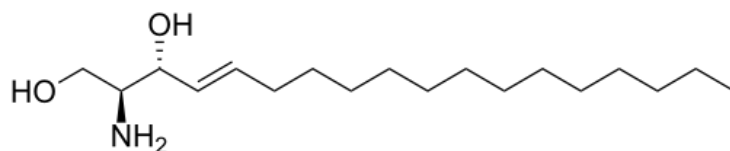


Figure 9. Chemical structure of sphingosine

The sphingosine efflux from LE/L is a key step in the salvage pathway of GSL biosynthesis and promotes the sphingosine-1-phosphate (S1P) protein synthesis, which in turns regulates the transcription of several enzymes implicated in the biosynthesis of cholesterol (Tettamanti et al., 2003; Ozbay et al., 2004).

After the inactivation of NPC1 protein, the first event observed is the accumulation of sphingosine in lysosomes and the concomitant reduction of sphingosine efflux from lysosomes. Subsequently, sphingosine storage causes an impairment of calcium homeostasis, indicated by the low calcium levels measured in acidic compartments, that may cause defective endocytosis (Lloyd-Evans et al., 2008) (**Figure 10**). The sphingosine storage may also explain the accumulation of sphingomyelin and glycolipids (GLs), as they have all a sphingosine backbone (Erickson, 2013).

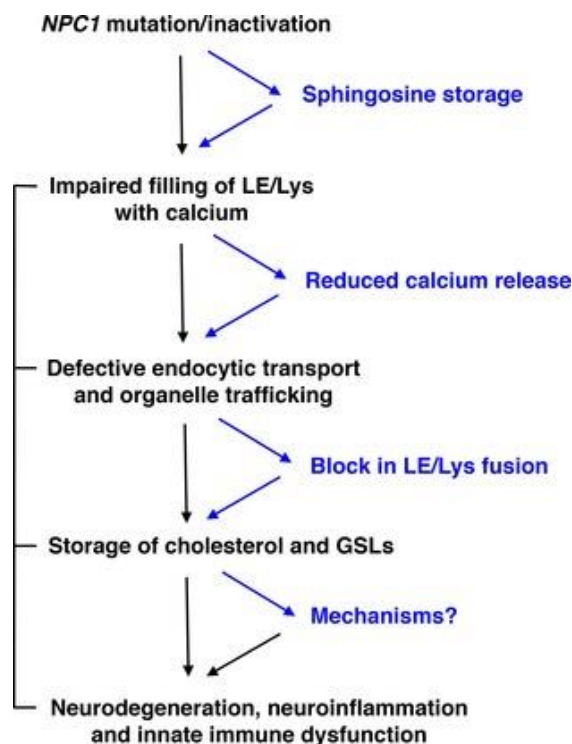


Figure 10. Proposed pathological cascade in NPC1-cells (Platt et al., 2016).

In addition, it was also reported that α -tocopherol (**Figure 11**, a naturally-occurring form of vitamin E with potent antioxidant properties) accumulates in LE/L (Yévenes et al., 2012).

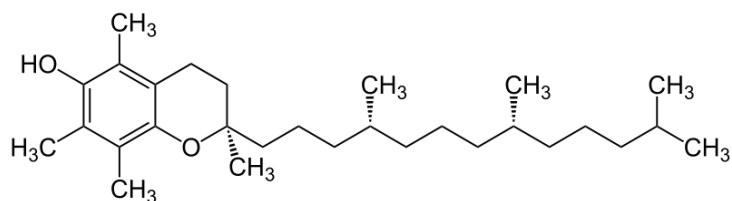


Figure 11. Chemical structure of α -tocopherol (α -TOH), consisting of 2 benzene rings bound to a hydrocarbon chain.

The intracellular trafficking of α -TOH requires the activity of several proteins that also participate in the cholesterol trafficking pathways, such as NPC1L1 protein, which has extensive homology with NPC1 (Siato et al., 1993; Davies et al., 2000; Reboul et al., 2006; Reboul et al., 2009).

The intracellular accumulation of α -TOH in LE/L of NPC1-deficient cells (Yévenes et al., 2012), emphasizes the role of NPC1 in its intracellular trafficking, also suggesting a block of endocytosis, which in turn would hinder the antioxidant functions of α -TOH in other cellular compartments.

1.5. Murine models of NP-C1 disease

Several animal models, including feline (Lowenthal et al., 1990), canine (Kuwamura et al., 1993) and murine (Pentchev et al., 1984; Maue et al., 2012), have been developed during the last three decades.

One of the first murine model of NP-C1 disease, known as ***Npc1^{spm}***, was developed in 1982 by Miyawaki on C57BL/KsJ strain mice (Miyawaki et al., 1982). It was generated by inserting a 43 base pair (bp) following codon 971, thus generating a frame shift mutation and a premature termination codon within the LL1 domain of the protein, which contains the cholesterol binding site.

Concomitantly, Pentchev and coll. characterized the knock out model of NP-C1 disease, known as ***Npc1^{nih}***, on BALB/C strain mice, that has become the most widely used model (Pentchev et al., 1984). This mouse line originated from a spontaneous mutation due to a retroposon insertion of 1100 bp of DNA, causing a frame shift that almost completely abrogated the *Npc1* gene (Loftus et al., 1997). Western blot analysis (WB) revealed the total absence of Npc11 protein in these mice, indicating the complete loss of function and making this model a true “knock out” (Maue et al., 2012).

In 2012, a novel mouse model commonly referred to as *Npc1^{nmf164}* was generated and phenotypically characterized at the Jackson Laboratory (Maue et al., 2012). This mouse model was generated by *N*-ethyl-*N*-nitrosourea (ENU) mutagenesis of C57BL/6J strain mice and later transferred to BALB/c mouse strain. *Npc1^{nmf164}* mice carry a point mutation in the *Npc1* gene, consisting in a single nucleotide substitution (A to G in the cDNA 3163 bp) that leads to a change from aspartate (coded by GAT codon) to glycine (coded by GGT codon) in position 1005 (D100G) of the protein. This change occurs in the cysteine-rich luminal loop of the NPC1 protein, where about one-third of human mutations identified up to now are located (Vanier, 2010; Maue et al., 2012). Although quantitative real-time polymerase chain reaction (qRT-PCR) revealed a slight reduction of *Npc1* mRNA level (a roughly 20% reduction), WB analysis showed a significant reduction of protein level (Maue et al., 2012). Histological analysis of liver, spleen and brain revealed that the abnormal accumulation of cholesterol and the loss of Purkinje cells proceeded at a slower rate in *Npc1^{nmf164}* compared to *Npc1^{nih}* mice. Therefore, while *Npc1^{nih}* model mimics severe and early onset forms of the disease, the *Npc1^{nmf164}* model mimics the late-onset and slower progressive forms of NP-C1 disease, which include most of the human cases (Maue et al., 2012).

1.6. Diagnosis

As already pointed out, the clinical presentation of NP-C disease is extremely heterogeneous and is characterized by a wide range of symptoms, whose progression depends on the age of onset (Patterson et al., 2001; Imrie et al., 2007; Vanier, 2010). This hampers the possibility to achieve an early diagnosis and often causes misdiagnosis. For this reasons the diagnosis of NP-C disease can require a very long time (years) and the intervention of specialists in different disciplines (Vanier, 1997; Patterson et al., 2001; Wraith et al., 2009).

In addition, the rarity of the NP-C disease and the lack of clear guidelines on therapeutic monitoring, represent significant challenges in the clinical management of the disease. In most countries the NP-C disease is managed in non-specialist centres.

Initial screening assessment of patients is aimed at distinguishing the disease from other lysosomal storage disorders and represents a prerequisite for a careful evaluation of the onset and evolution of symptoms and signs over the time (Wraith et al., 2009; Vanier, 2010).

In 2009, Wraith and coll. proposed an **ideally series of analyses** to be carried in individuals possibly affected. These tests can be grouped into three micro-areas of investigation: reconstruction of medical history, clinical investigation and execution of laboratory tests.

The reconstruction of the patient's **medical history** includes the analysis of the first appearance of neurological manifestations, the presence of splenomegaly and neonatal cholestasis, as well as coordination, muscle tone and posture problems., It also considers if the patient had poor school performance or limited work ability and if he/she had episodes of cataplexy and/or seizures.

The **clinical investigation** includes at first a physical examination (vital signs, body weight, head circumference) and a comprehensive neurological examination with the aim of identifying the presence of characteristic signs and symptoms. The presence of NP-C disease is easily inferred in patients that show the most typical symptoms of the pathology, such as the simultaneous presence of splenomegaly, ataxia, and VSGP (Vanier, 2010). From a neurological point of view, it is important to evaluate muscle tone, strength and motor reflexes by specific tests, along the assessment of movement (ataxia and dystonia) and swallowing tests (Wraith et al., 2009; Vanier, 2010). Because abnormal saccadic movement (SEM) is often among the first neurological symptoms of the disease, ophthalmological assessment is also particularly relevant. The clinical examination includes an ultrasound evaluation of liver and spleen size, psychometric assessment and a psychiatric evaluation. Sometimes patients are also subjected to hearing tests (audiogram and/or brainstem evoked potential) and nerve conduction analyses (electromyography) to assess the presence of peripheral neuropathy.

Given that routine laboratory tests often reveal no anomaly, Wraith and coll. (2009) proposed a **specific laboratory algorithm (Figure 12)**.

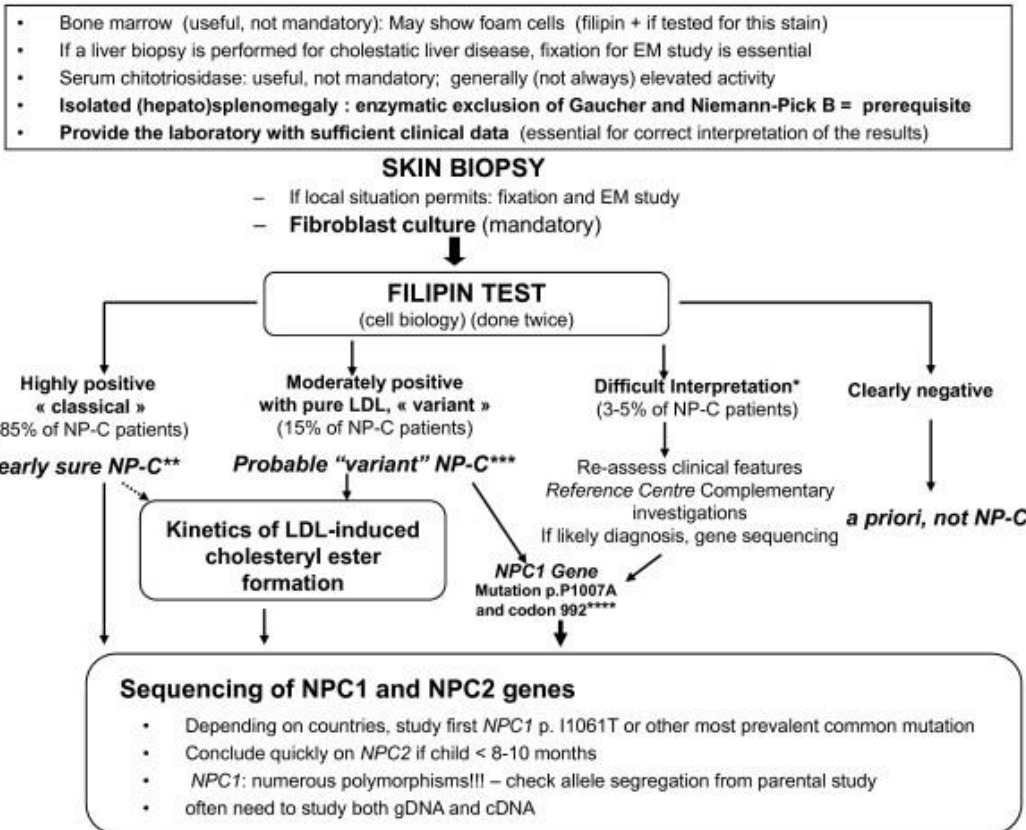


Figure 12. Laboratory diagnosis algorithm (Vanier, 2010).

The ultimate diagnostic test to diagnose NP-C disease must be able to detect the presence of an impairment in the intracellular trafficking and homeostasis of cholesterol. Up to now, the **Filipin test** represents the most sensitive and specific assay for NP-C disease diagnosis (Vanier et al., 2016).

Filipin is an antifungal antibiotic forming specific complex with unesterified cholesterol that can be observed by fluorescence microscopic examination (Vanier, 2010). While in fibroblast cultures of NP-C patients nearly all cells are display fluorescent perinuclear vesicles, in normal subject only about the 10% of cells are filipin-positive (Vanier et al., 2016). Although the 85% of NP-C patients display the “classical” storage pattern, about the 15% of them shows a “moderate” profile with only a small number of positive cells and the remaining 5 % of cases is completely negative.

In any case, the diagnosis requires the detection of mutations in *NPC1* or *NPC2* genes (Millat et al., 2005; Wraith et al., 2009; Vanier, 2010; Vanier et al., 2016) by **Sanger and next-generation sequencing (NGS) methods** (Bounford and Gissen, 2014).

More recently a **cholesterol esterification test**, evaluating the cholesterol ester formation and the re-esterification of cholesterol by ACAT that are particularly impaired in NP-C cells was developed (Pentchev et al., 1987; Vanier et al., 1991; Vanier, 2016). It is considered a useful test to be performed, in addition to the filipin test and prior the identification of possible mutations in the *NPC1* or *NPC2* genes (Vanier et al., 2016). However, both filipin and cholesterol esterification tests are invasive because require fibroblast isolation from skin biopsies.

In the last few years, many researchers have sought to identify **specific biomarkers** possibly allowing the diagnosis by blood or urinary tests, thus reducing time and costs (Vanier et al., 2016).

The first approach measures the **plasma chitotriosidase activity** that represents a valid biomarker of Gaucher disease and is typically increased in lysosomal storage diseases, including NP-A -B and -C, compared to normal subjects (Ries et al., 2006). However, an increase in plasma chitotriosidase activity level occurs in other and more common conditions such as stroke and type 2 diabetes mellitus. Moreover, in NP-C1 patients with late onset its level can be normal (Bustamante et al., 2014; Elmonem et al., 2016; Vanier et al., 2016).

A more recent approach proposed for diagnosis is the **plasma oxysterol-based tests**. Although there are many oxysterols, whose levels are increased in NP-C1 patients, cholestane-3 β ,5 α ,6 β -triol (**C-triol**) and 7-ketocholesterol (**7-KC**), appeared of particular interest for diagnosis (Vanier et al., 2016). The blood plasma levels of these two metabolites are significantly increased in both *Npc1*^{-/-} mice and NP-C1 patients (Zhang et al., 2008; Porter et al., 2010; Jiang et al., 2011; Pajares et al., 2015).

Evidence suggests that C-triol has a greater discriminatory power than 7-KC (Porter et al., 2010; Jiang et al., 2011; Pajares et al., 2015; Boenzi et al., 2014; Reunert et al., 2016). However, it has been shown that the levels of both metabolites are high in other pathological conditions such as Niemann-Pick disease type A (NP-A), Niemann-Pick disease type B (NP-B), LAL deficiency and cerebrotentinus xanthomatosis (Klinke et al., 2015; Romanello et al., 2016).

Another promising approach for the NPC diagnosis is the **analysis of lysosphingolipids plasma levels**. Lysosphingolipids are toxic metabolites which contribute to the pathophysiology of several diseases (Suzuki,1998; Sueyoshi et al., 2001).

Globotriaosylsphingosine and glucosylsphingosine belong to this class of molecules and are great plasma biomarkers for Fabry disease and Gaucher disease, respectively (Aerts et al., 2008; Dekker et al., 2011).

Galactosylsphingosine and sphingosylphosphorylcholine (SPC; lysosphingomyelin) are suitable markers for the screening of NP-B and Krabbe disease (Chuang et al., 2013; Chuang et al., 2014). Preliminary studies have shown that SPC plasma levels are also increased in patients with NP-C disease (Welford et al., 2014; Kuchar et al., 2015; Piraud et al., 2015) and even more increased levels were found in patients suffering for NP-A and NP-B (Raymond et al., 2015; Motta et al., 2016).

An emerging approach is the **analysis of bile acid metabolites** that could replace the analysis of oxysterol in the near future (Vanier et al., 2016). The bile acid 3β -sulfooxy- 7β -*N*-acetylglucosaminyl-5-cholen-24-oic acid (SNAG- Δ^5 -CA) and its glycine-and taurine-conjugates is particularly high in the urine of NP-C patients (Alvelius et al., 2001; Maekawa et al., 2013). In addition, other authors found an increase of two bile acid metabolites: 3β -hydroxy- 7β -*N*-acetylglucosaminyl-5-cholenic acid and *N*-($3\beta,5\alpha,6\beta$ -trihydroxycholan-24-oyl) glycine (Jiang et al., 2016; Mazzacuva et al., 2016).

Recently, it has been shown that an isoform of **Bis(monoacylglycero)phosphate** (BMP or LBPA) named **di-22:6-BMP** displays a 50-fold increase in the urine of NP-C patients (Liu et al., 2014). BMP is a phospholipid that plays a key role in both cholesterol processing and sphingolipids degradation in the LE/L (Vanier, 2015). Further studies are needed to prove its usefulness in the diagnosis of NP-C disease (Vanier et al., 2016).

Cluzeau and coll. (2012) reported an increase in serum levels of two proteins: the **pro-inflammatory galectin-3 (LGALS3)**, and the **lysosomal protease cathepsin D (CTSD)**. Elevated serum levels of both proteins appear to correlate with the severity of the neurological deficit and appear to be specific for the NP-C disease and therefore to be a potentially useful for diagnosis.

In 2011, two adult patients with NP-C disease were subjected to the **Magnetization Transfer Ratio (MTR)**, an advanced technique that allows the assessment of the integrity of macromolecules forming the brain tissue (Zaaeaoui et al., 2011). This technique revealed damages in the grey matter of the cerebellar, thalamic and lenticular nuclei in both patients. It is reasonable that the damage of the grey matter is initially localized

in cerebellum and spreads thereafter to the frontotemporal cortex in the later stages of the disease. This hypothetical course of the disease correlates with the clinical features of the disorder in which initially are present sub-cortical signs (dystonia, dysarthria, dysphagia) and later cognitive impairment.

Recently, some authors have tried to set a battery of tests suitable for the neuropsychological evaluation of the NP-C disease (Klarner et al., 2007). Because the cognitive changes that occur in patients with NP-C disease are similar to those occurring in elderly patients with dementia, similar tests can be used for both disorders. The *Trial Making Test* (A & B) and the *verbal fluency tests* are sensitive indicators of the early stages of the NPC. In later stages of the disease patients have a reduced performance in *Corsi Block-Tapping*, *Mini Mental State Examination (MMSE)* and *Clock Drawing*. Due to their compromised motor skills Grooved Pegboard, Trail Making and Mosaic's tests are not suitable for evaluation in the advanced stages of the disease.

1.7. Differential diagnosis

For early onset NP-C disease forms the differential diagnosis should consider all possible causes of **cholestatic jaundice**, such as idiopathic neonatal hepatitis.

Among other lipid storage diseases, the differential diagnosis must be performed especially with NP-B, which presents in bone marrow similar foam cells, and **Gaucher disease**, which can present many symptoms in common including ataxia, VSGP and splenomegaly (Pandi et al., 2014).

For late onset forms, the differential diagnosis should be performed from all those conditions that can causes the most prominent neurological signs (Schiffmann, 1996; Wraith et al., 2009; Vanier, 2010).

1.8. Prognosis

Generally, NP-C patients **die prematurely** between **10 and 25 years of age** (Vanier, 2010). However, the rate of disease progression and life expectancy vary greatly depending on the age of onset and the severity of symptoms.

Patients with pre/peri-natal onset, suffering from a severe form of neonatal cholestasis, usually die within 5 month of age.

Subjects with severe early infantile onset die within 5 years of age, while, in late infantile onset form the survival varies between 7 and 12 years of age. The juvenile onset forms display a more variable life span; some patients surviving up to 30 years of age (Vanier, 2010). Finally, in cases with adolescent/adult onset the life expectancy is even better; some patients, who show few neurological symptoms, survive until the sixth or seventh decade of life (Trendelerbug et al., 2006; Dvorakova et al., 2006).

Although the precise **causes of death** are not always reported in the literature, historical and epidemiological data indicate that patients typically die because of **bronchial pneumonia, infections and choking** due to the repeated aspirations caused by the progressive dysphagia (Kelly et al., 1993; Jan et al., 1998).

1.9. Treatments

In the absence of a specific treatment for the NP-C disease, therapeutic approaches attempt to delay the onset and progression of cellular damage and symptoms. In recent years, several therapeutic approaches have been proposed. The most promising are presented below.

Symptomatic therapy involves the use of standard drug treatments for gastrointestinal and neurological manifestations. Dysphagia could cause malnutrition and food aspiration; dietary manipulation, including softening and thickening of food as well as antibiotics treatment to avoid aspiration pneumonia, are widely used. In severe cases it is advisable to perform a gastrostomy to ensure proper daily caloric intake. Atropine can control the heavy drooling of saliva. Seizures and cataplexy can be controlled using antiepileptic drugs and tricyclic antidepressant or CNS stimulants, respectively. Dystonia and tremors respond well to anticholinergic drugs, trihexyphenidyl, benzodiazepines, and Gamma-aminobutyric acid derivatives. Insomnia can be treated using Melatonin. These treatments are usually helped by physiotherapy, physical occupational and language therapy (Alobaidy, 2015).

Miglustat. Miglustat (Zavesca® and Brazaves®) is a small water-soluble iminosugar derived from the glucosidase inhibitor deoxynojirimycin (Lysegn-Williamson, 2014). Up to now, it represents the only drug approved for the treatment of NP-C disease neurological manifestations in EU countries as well as in Argentina, Australia, Brazil,

Canada, Chile, Colombia, Japan, Mexico, New Zealand, Russia, South Korea, Switzerland and Turkey (Lysegn-Williamson, 2014). This molecule inhibits the synthesis of glucosylceramide synthase, the enzyme involved in the first step of glycosphingolipid synthesis and inhibits the glycosphingolipid synthesis (Platt et al., 1994; Lysegn-Williamson, 2014). In both feline and murine models of NP-C disease, miglustat reduces glycosphingolipid accumulations, delays the onset of neurological manifestations and increases the lifespan (Zervas et al., 2001; Lachmann et al., 2004). The oral administration of miglustat to NP-C patients improves the lipid trafficking and storage, protects from oxidative stress and axonal degeneration, and stabilizes the neurological manifestations (Lachmann and Platt, 2004; Maalouf et al., 2011; Ribas et al., 2012). However, the administration causes gastrointestinal disorders such as diarrhea and flatulence (Patterson et al., 2007).

Substrate reduction therapy. The main substrate reduction approaches include the administration of statins and/or ezetimibe and a low-cholesterol diet (Rosenbaum and Maxfield, 2011). These treatments reduce the load of peripheral cholesterol (Patterson and Platt, 2004; Liu et al., 2010). In particular, **statins** inhibit the synthesis of endogenous cholesterol by acting on hydroxymethylglutaryl-CoA reductase, an enzyme that converts HMGR into mevalonic acid, a precursor of cholesterol. Instead, **ezetimibe** selectively inhibits the intestinal absorption of cholesterol taken by diet and the biliary cholesterol present in the brush borders of the small intestine, without causing the side effects typical of the resins binding bile acids. The two drugs can be co-administered (Rosenbaum and Maxfield, 2011). An alternative strategy of substrate reduction for lowering visceral symptoms is the **inhibition of cholesterol synthesis** via the hydrolysis of cholesterol esters mediated by LAL. It has been shown that this inhibition causes a significant reduction of cholesterol storage in human NPC-defective cells (Rosenbaum et al., 2009). However, the substrate reduction therapy does not correct the insufficient steroidogenesis, which represents an important feature of NP-C disease neuropathology (Griffin et al., 2004; Rosenbaum and Maxfield, 2011).

Acid sphingomyelinase. Recent investigations have focused on the role of the enzyme acid sphingomyelinase (ASM) in the pathogenesis of NP-C disease. In fact, despite the absence of alterations of the ASM gene, the levels of this enzyme activity are decreased in NP-C patients compared to normal subjects (Devlin et al., 2010). The recovery of the

levels of ASM activity by recombinant enzyme re-introduction has led to the reversal of the classic phenotype of NPC1 cells. This observation encourages the use of parallel treatment approaches acting on different aspects of the NPC disease, and on the sphingolipid storage associated with its neuropathology.

Chemical Chaperones. The three-dimensional control of the organization of proteins by chemical chaperones has been proposed as a treatment for a variety of disease, including lysosomal storage disorders (Balch et al., 2008). Cultured cells obtained from a mouse model of NPC1 carrying the I1061T mutation and treated with chemical chaperones have shown an improvement of the folding of NPC1 protein and a rescue of lysosomal trafficking (Gelsthorpe et al., 2008). **Arimoclomol** is a drug that induces the expression of an important group of chaperone proteins known as heat shock proteins (HSPs). It has been shown that in several neurodegenerative diseases, including amyotrophic lateral sclerosis (ALS), the upregulation of HSPs reduces the cellular damage, prevents protein misfolding, aggregation and abnormal degradation (Kalmar et al., 2014). Also, the HSPs upregulation improved the intracellular accumulation of lipids in NP-C cells (Kierkegaard et al., 2010). Presently, an observational study of Arimoclomol effects in NP-C patients is ongoing (ClinicalTrials.gov identifier: NCT02435030).

Curcumin. It has been shown that the active principle of turmeric, known as curcumin, increases cytosolic calcium levels *in vitro* and enhances the cellular phenotype of *Npc1*^{-/-} mice (Lloyd-Evans et al., 2008). In addition, Lloyd-Evans and coll. reported that curcumin increases of 35% the survival of *Npc1*^{-/-} compared to *wild-type* mice. However, a second study using the same mouse model, reported a lengthening of life span of 19%, leading to the conclusion that curcumin is not a highly efficacious treatment for NP-C disease (Borbon et al., 2012).

Histone deacetylase (HDAC) inhibitors. HDACs are a family of enzymes that play a key role in a multitude of biological processes by influencing gene transcription. It has been shown that HDACs increase the expression of NPC1 protein, thus correcting the intracellular accumulation of cholesterol in human fibroblasts (Munkacsi et al., 2011; Pipalia et al., 2011). In addition, the treatment with the HDAC valproic acid (VPA) has been shown to promote the differentiation of neural stem cells in *Npc1*^{-/-} mice (Kim et al., 2007).

Acetyl-DL-leucine. Recently, the administration of a modified amino acid, known as Acetyl-DL-leucine was tested in 12 NP-C patients, whose age varied between 13 and 32 years. An improvement in cerebellar signs of disease, such as ataxia was observed after a month of treatment. Also, this treatment was well tolerated by patients, with only one of them developing transient dizziness as side effect. This makes this amino acid one of the most promising treatments (Bremova et al., 2015; Papandreou and Gissen, 2016).

Cyclodextrins are cyclic oligosaccharides formed by a hollow cone-like toroid structure with a hydrophobic cavity and a hydrophilic exterior and composed by several linked glucopyranose moieties. The number of glucopyranose moieties determines the cyclodextrins nomenclature (α , β , γ) as well as its cavity size (**Figure 13**) (Liu, 2012). These structural features make cyclodextrins useful molecules to solubilize various pharmaceuticals (Davis and Brewster, 2004).

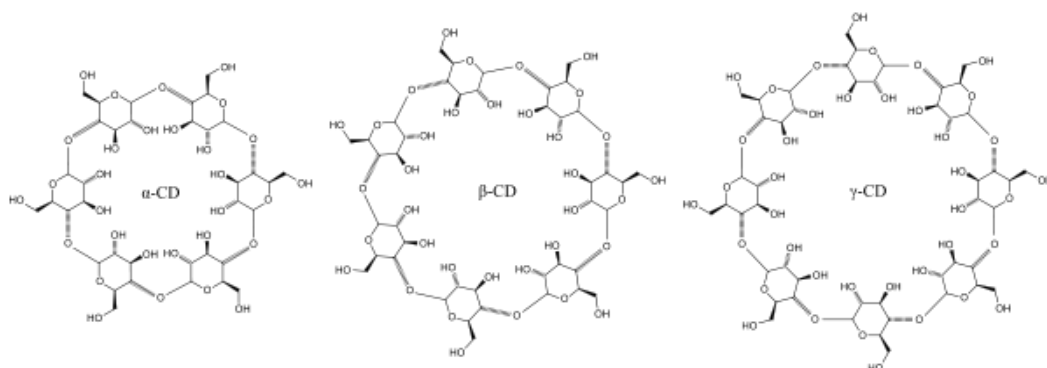


Figure 13. Chemical structure of cyclodextrins.

The discovery of their efficacy in treating NP-C disease has been accidental. In fact, a single subcutaneous injection of the neurosteroid **allopregnanolone (ALLO)**, which levels are reduced in NP-C disease, solubilized in 20% 2-hydroxypropyl- β -cyclodextrin (CD) increased life span and improved neuropathology in *Npc1*^{-/-} mice (Griffin et al., 2004). Several subsequent studies have shown that CD injections alone were responsible for the effects of CD+ALLO administration (Liu et al., 2010, Davidson et al., 2009). These investigations have demonstrated that a single injection of CD (4 mg/Kg body weight) performed at post-natal day 7, significantly reduced the NPC-phenotype in brain, liver, spleen, lungs and bone marrow and extend the life span by nearly 50% of *Npc1*^{-/-} mice (Liu,

2012). Also, CD treatment decrease cholesterol and glycosphingolipids storage and prevents Purkinje cells death on both feline and murine models of the disease (Xie et al., 2011; Davidson et al., 2009; Raminetz et al., 2010; Liu, 2012; Vite et al., 2015).

However, preclinical studies carried out in animal models, showed that young animals responded better to CD treatment than the older ones (Liu et al., 2008; Vite et al., 2015). The closure of the blood-brain barrier that cyclodextrins are not able to cross because of their chemical structure, likely explains this finding (Liu, 2012).

Despite their inability to cross membranes, CDs can be delivered via pinocytosis to LE/LY, where they can replace the function of NPC1 and NPC2 proteins (Rosenbaum et al., 2010b) and promote cholesterol esterification by acetyl CoA:acyl transferase (Abi-Mosleh et al., 2009). The exact nature of CD's mechanism of action to replace NPC1 and NPC2 function in LE/LY is yet to be determined.

One possibility would be that CD solubilizes cholesterol and thus promote its efflux via vesicular transport. Alternatively, CD action might act catalytically to shuttle cholesterol from LAL directly to the limiting membrane of the lysosome, bypassing the potential requirement for NPC2-NPC1 interaction (Rosenbaum and Maxfield, 2011). Once delivered to the luminal leaflet of the limiting membrane, cholesterol can then spontaneously flip to the cytosolic leaflet and be carried away to various compartments within cells, *via* still poorly characterized transport processes (Maxfield and Menon, 2006) (**Figure 14**).

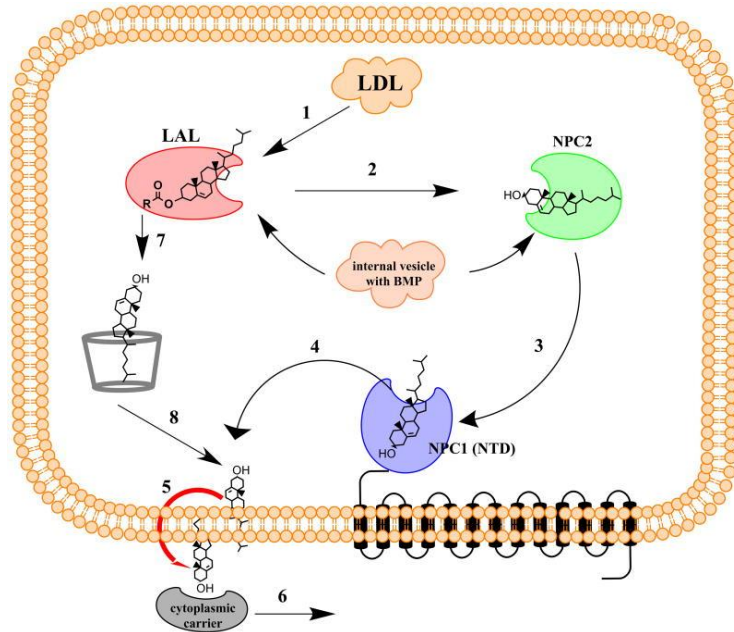


Figure 14. Model for cyclodextrin action in cholesterol efflux from late endosomes/lysosomes. In normal cells, cholesteryl esters are hydrolyzed by LAL to produce free cholesterol and fatty acid (1), then free cholesterol is transferred to NPC2 (2), and subsequently to the N-terminal domain of NPC1 (3). Free cholesterol is then delivered to the luminal leaflet of the limiting membrane of late endosomes/lysosomes (4), where it can spontaneously flip to the cytosolic side (5) and then be carried to its various destinations in the cell by cytoplasmic carriers (6). In the absence of functional NPC2 or NPC1, cyclodextrins can replace their functions in promoting cholesterol efflux (7, 8), bypassing steps 2–4 (*Rosenbaum and Maxfield, 2011*).

In 2010 the U.S. Food and Drug Administration (FDA) approved the **CD compassionate use** in humans and in recent years it has been administered to a number of pediatric patients (*Garcia-Robles et al., 2016*)

These studies have shown that treatment with CD stabilizes or improves the health of young patients (*Hastings, 2010; Matsuo et al., 2013; Matsuo et al., 2014; Maarup et al., 2015*).

In 2016, was published the first study on treatment with CD in two female adult patients that received NP-C disease diagnosis only several years later the onset of first symptoms (*Garcia-Robles et al., 2016*). In both patients CD were intrathecally administrated in the framework of FDA compassionate use clinical study protocol (*Hastings, 2010*). Although the treatment duration was relatively short, it didn't stabilize or decrease the progression of the disorder, resulting in a worsening of neurological symptoms in both

patients. In addition, a patient refused dropped out of the treatment while the other developed severe adverse reactions, such as toxic meningitis, probably due to method of CD administration (García-Robles et al., 2016).

Chapter II

The cerebellum: involvement in NP-C1 disease

2.1. The cerebellum

The **cerebellum** (“little brain”) is the part of central nervous system (CNS) located in the posterior cranial fossa (Buckner, 2013). Macroscopically the cerebellar anatomy consists of two hemispheres connected by a midline structure known as vermis (**Figure 15A**).

The cerebellum is divided into three lobes by two deep fissures: anterior, posterior and flocculonodular lobes. The primary fissure separates the anterior and posterior lobes, whereas the postero-lateral fissure divides the posterior from the flocculonodular lobe. More superficial fissures divide these regions in sub-lobules, known as folia, which represent the gyri on the cerebellar surface.

All mammals have a similar *10-folia structure*, denoted by Roman numerals, suggesting that foliation is genetically determined (Sudarov and Joyner, 2007; Cerminara et al., 2015) (**Figure 15B**).

Anatomically, the **cerebellar cortex** is formed by 8 different neuronal cell types (Purkinje, Golgi, Lugaro, Granule, Basket, Stellate, Unipolar brush and Candelabrum cells) and glial cells (Bergman glia, protoplasmic and fibrous astrocytes, oligodendrocytes and microglia) (Cajal, 1911; Lainè and Axelrad, 1994; Mugnaini and Floris, 1994; Vela et al., 1995; Buffo and Rossi, 2013).

In the brain of adult mammals these cells are arranged in three layers (**Figure15C**):

- The **Molecular layer (ML)**, located under the pial surface and formed by the dendritic tree of several neurons (Purkinje, Golgi, candelabrum cells), by the cells bodies and dendritic tree of basket/stellate interneurons, Bergmann glia fibers and parallel/climbing fibers;
- The **Purkinje cell layer (PCL)** contains the soma of Purkinje cells, Bergmann glia and candelabrum cells, part of the dendritic tree of Golgi cells and it is crossed by parallel/climbing fibers;
- The **Internal granule layer (IGL)**, also called Granule cell layer (GCL), contains the cell bodies of granule neurons and Golgi cells, Lugaro cells, unipolar brush cells, Purkinje cell axons, mossy/climbing fibers, protoplasmic astrocytes. The granule layer parallel fibers also originate in this layer.

Beneath the GCL resides the white matter (WM), where the cerebellar deep nuclei and fibrous astrocytes are located. Instead, microglia and oligodendrocytes are localized in both cortical layers and white matter (Vela et al., 1995; Buffo and Rossi, 2013; D'Angelo and Casali, 2013).

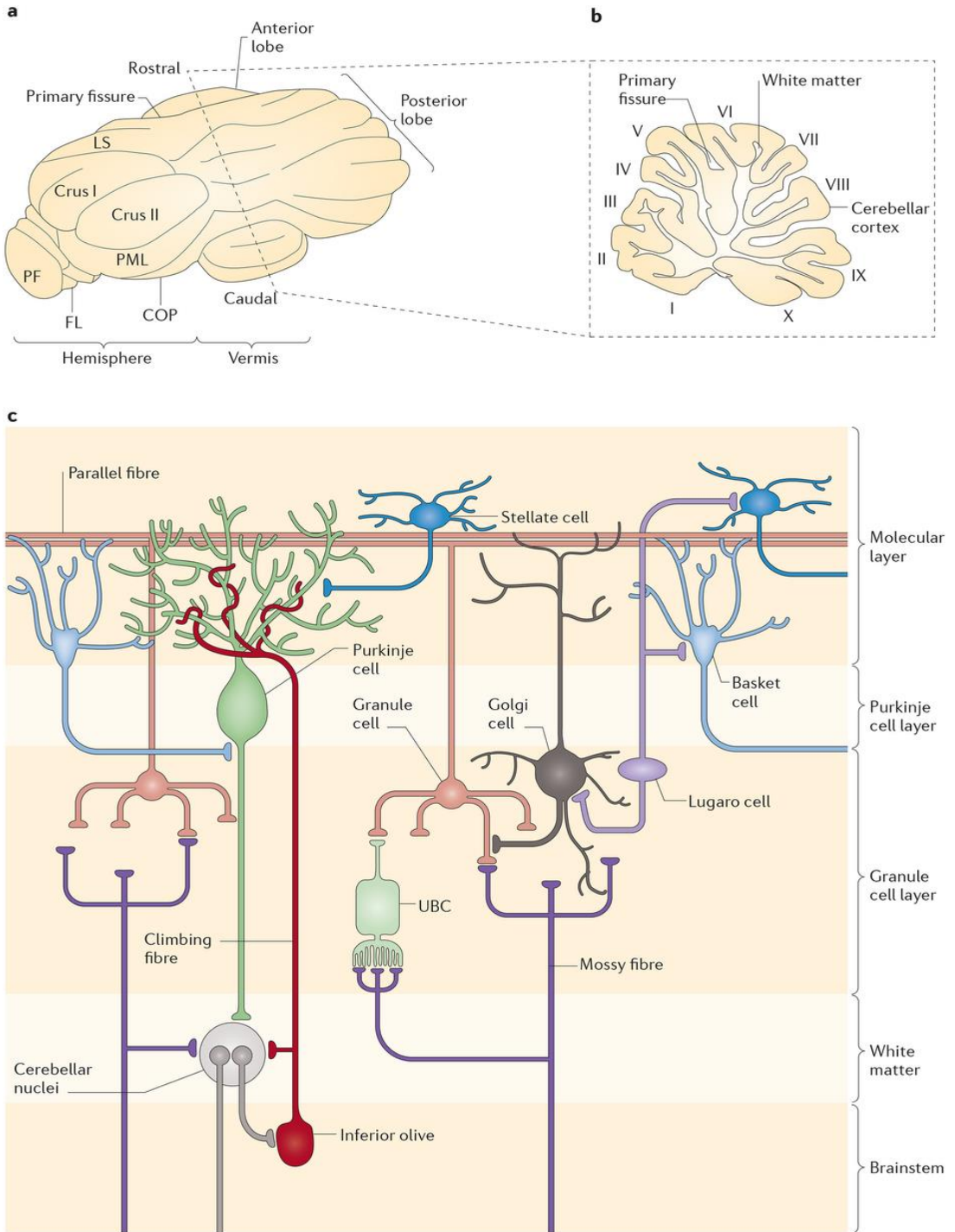


Figure 15. Cerebellar cytoarchitecture (Cerminara et al., 2015).

2.1.1. Cerebellar neurons

The most important neuronal class is the GABAergic **Purkinje cells (PCs)** that represent the sole output of cerebellar cortex (D'Angelo and Casali, 2013). The cell bodies of PC (~18 μm diameter in mouse) have a flask shape and are arranged in the PCL monolayer. Multiple primary dendrites emerge from the neck of PC cell body and extend upward contributing to the formation of the ML (Weber and Schachner, 1984; Nakagawa et al., 1998).

Each PC receives over 100,000 inputs from parallel fibers (PFs) and inhibitory interneurons, and about 500 inputs from a single climbing-fiber (CF) (Ito, 2006) and has a single axon emerging from the bottom of the cell body, descending through the GCL and WM and terminating in one of the deep cerebellar nuclei (Monsivais et al., 2005).

To send the appropriate output to deep cerebellar nuclei, PC cells need to receive an appropriate excitation/inhibition by different classes of cerebellar neurons. Among these, **Granule neurons (GNs)** represent the most abundant neuronal population of the cerebellum (Fox and Barnard, 1957). They are characterized by a small cell body (5-8 μm diameter) from which emerge 4/5 dendrites that receive excitatory and inhibitory inputs from mossy fibers (MF) and Golgi cells. These synapses give rise to typical structures known as **glomeruli** (Buffo and Rossi, 2013). GNs are provided with unmyelinated axons extending upward to the upper ML, where they split in two arms each and elongate horizontally to form the so called parallel fibers (Vranesic et al., 1994). Being glutamatergic, GNs exert excitatory effects on PCs, whereas receive inhibitory inputs from Golgi cells and excitatory input from Unipolar brush cells.

The **Golgi cells (GCs)** are the most common and numerous GABAergic interneurons of the GCL, mainly located in the upper GCL (~6000 in cat; ~1200 in humans; ~400 in rats) (Palkovits et al., 1971; Andersen et al., 1992; Korbo et al., 1993; D'Angelo and Casali, 2013). GCs are landmarked by a soma of irregular shape (diameter 10-30 μm), a branched axon, some basal dendrites that form synaptic contacts within the GCL and by two/three apical dendrites that ascend to the molecular layer and form synaptic contacts with parallel fibers (Dieudonné, 1999; Barmack and Yakhnitsa, 2008). It has been shown that GCs receive excitatory inputs from MF and GABAergic or mixed GABAergic/glycinergic inputs from Basket/Stellate interneurons and Lugaro cells, respectively (Dumoulin et al., 2001; D'Angelo and Casali, 2013). GCs represent the sole output that inhibits GNs in cerebellar

glomeruli through both feedforward and feedback loops, regulating and controlling the MF-GN synapses (Rossi et al., 2003; D'Angelo and Casali, 2013).

The **Unipolar brush cells (UBCs)** are the only glutamatergic interneurons of cerebellar cortex, mainly localized in the lobule IX (~24%) and X (~42%) (Altman and Bayer, 1996; Sekerková et al., 2004). They are very small neurons that present a single thick and stubby dendrite which terminates in a brush-like spray (Schilling et al., 2008). UBCs receive input from a single MF that provides vestibular afferents and send an excitatory input to GNs. Their single axon takes a tortuous course in the GCL and shapes a rosette-like protrusions that form the central component of glomeruli (Schilling et al., 2008). It has been shown that their principal function is to coordinate the synchronized activity of a group of GNs, which in turn regulate the activity of a small group of PCs (Nunzi et al., 2001). PCs also receive GABAergic inputs from Basket/Stellate interneurons and Lugaro cells.

The **Basket and stellate cells (BC/SCs)** in turn receive excitatory inputs from parallel fibers and, in addition to PCs, also inhibit GCs (Dumoulin, 2001; Cameron et al., 2009). It is unclear whether they represent two distinct classes of cells; currently their subdivision is based on morphological features and their localization in the ML (Schilling et al., 2008). Basket cells have a stellate shape and localize in lower ML (Rakic, 1972). They are slightly more numerous than PCs (about 15-20%) and their dendritic tree does not extend beyond the lower ML and is provided with scattered spines. Their axons have numerous ascending collaterals that form a kind of basket surrounding the soma of PCs (Rakic, 1972). Stellate cells are mostly located in the upper ML and even if dendrites and spines are similar to those of the BC, the trajectory and the branching of their axons confer to these cells a star-like shape (Eccles, 1967; Rakic, 1972). **Lugaro cells (LCs)** represents 1/3 of inhibitory interneurons of GCL in mice, while in other species, such as rats and cats, they seem to be less abundant (Sahin and Hockfield, 1990; Dieudonné and Dumoulin, 2000; Simat et al., 2007). Like GCs, they are mainly located in the upper GCL and are characterized by a fusiform cell body, whose size is in between that of GN and GC (Schilling et al., 2008). A single fiber originates from the LC cell body, reaches the ML and emanates two pairs of long dendrites which send GABAergic and a GABAergic/glycinergic inputs to PC and BC/SC, respectively (Lainè and Axelrad, 1996; Dieudonné and Dumoulin, 2000). In the GCL they provide inhibitory inputs to GC: it was estimated that one LC takes contacts with ~100 GCs (Dieudonné and Dumoulin, 2000). LCs are the primary target of serotonergic input in the cerebellar cortex and also receive inputs from collateral axons of PC and Basket

interneurons (Fox and Barnard, 1957; Palay and Chan-Palay, 1974; Dieudonné and Domulin, 2000).

In 1994, an additional class of cerebellar neurons, known as **Candelabrum cells (CCs)**, was discovered (Lainè and Axelrad, 1994). These cells are characterized by a small and pyriform soma located between PC soma. CCs have 1-2 branches dendrite ascending into ML and 3-5 short dendrites projecting in the GCL (Lainè and Axelrad, 1994; Schilling et al., 2008). Lainè and Axelrad (1994) named these cells “candelabrum” because their axon projects horizontally to ML and emit here multiple branches that ascend vertically for the entire ML. Some evidence has shown that they are distributed in all parts of the cerebellar cortex and that they use a GABA/glycine transmission (Schilling et al., 2008). However, their afferents and efferents have not yet been identified, even if their dendritic structure suggests that CCs may receive inputs by climbing/parallel fibers, ascending GN axons and BC/SC and send output to PC dendrites (Schilling et al., 2008).

Interestingly, both histological and immunohistochemistry analyses have suggested that **other neuronal type** exist in cerebellar cortex, although they have been not yet characterized. In 2003, it has been shown that the incubation of mouse cerebella with NeuN antibody marks a class of neurons located in the lower ML. This study also established that NeuN does not stains cerebellar inhibitory interneurons such as PCs and UBCs (Weyer and Schilling, 2003).

In addition, at least two additional neuronal types might exist; the first are Npas3-positive, while the second are cat-301-positive. Both are located in the GCL but are distinct from other neurons actually known (Erbel-Sieler et al., 2004; Crook et al., 2007; Schilling et al., 2008).

2.1.2. Cerebellar glia

Based on their morphology and anatomical location cerebellar **astrocytes** can be divided into two main classes: Bergmann glia and intraparenchymal astrocytes (protoplasmic and fibrous astrocytes) (Buffo and Rossi, 2013).

Bergmann glial (BG) is a highly diversified unipolar astrocyte type, essential for neuron migrations during development and performing an important role for extracellular ion homeostasis (Wang et al., 2012), synapse stability (Iino et al., 2001; Saab et al., 2012), plasticity (Balakrishnan and Bellamy, 2009; Balakrishnan et al., 2014), and metabolic

function and neuroprotection (Poblete-Naredo et al., 2011; Jakoby et al., 2014) in the adult cerebellum.

BG cell bodies are located around the PCs bodies and extend several fibers that traverse the ML and terminate in the pial surface, taking contacts with the blood vessels of the ML (Buffo and Rossi, 2013). The shaft fibers form a palisade-like glial framework.

The dendritic tree of each PC is covered with longitudinal glial columns made by several BG fibers (Yamada and Watanabe, 2002). It was estimated that in rodent cerebellum there are ~8 BG cells *per* PC and that each BG cell enwraps 2000-6000 PC synapses (Reichenbach et al., 2010). Thus, BG processes provide a structural substrate for the directional growth of PC dendrites, influencing the shape of the dendritic tree (Lordkipanidze and Dunaevsky, 2005; Buffo and Rossi, 2013).

Protoplasmic astrocytes localize in the GCL and display the classical stellate shape with several stem branches that give rise to many finely branching processes in a uniform globoid distribution (Cajal, 1909).

Fibrous astrocytes localize in the white matter and are characterized by many long fiber-like processes (Cajal, 1909) (**Figure 16**).

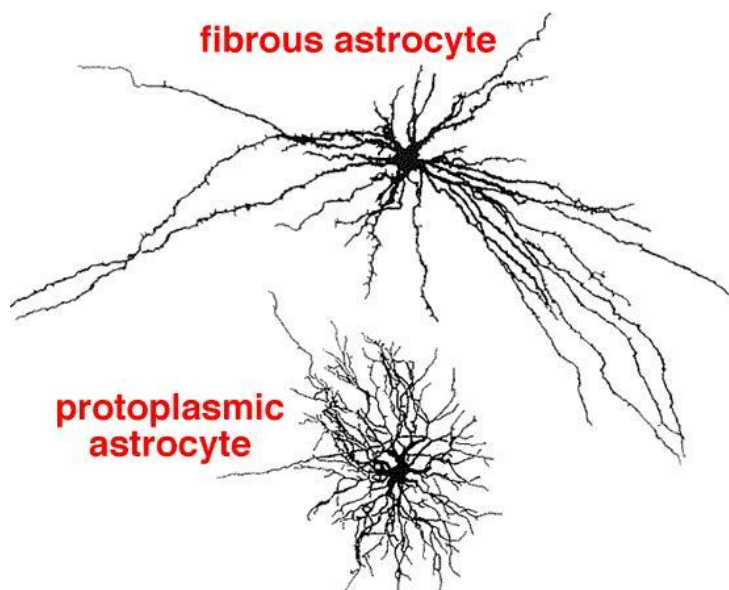


Figure 16. Intraparenchymal astrocytes morphology.

Both types of astrocytes contact blood vessels and form gap junctions with the distal processes of neighboring astrocytes (Peters et al., 1991).

Recent findings show that astrocytes produce and release several molecular mediators, such as prostaglandins (PGE), nitric oxide (NO), and arachidonic acid (AA), that increase or decrease blood vessel diameter and blood flow in response to neuronal activity changes (Gordon et al., 2007; Iadecola and Nedersaard, 2007; Kohler et al., 2009).

Astrocytes contribute to CNS metabolism taking up glucose from blood vessels and providing energy metabolites to different neural populations in both gray and white matter. Electron microscopy analyses revealed that, while processes of fibrous astrocytes take contacts with nodes of Ranvier (Peters et al., 1991), the processes of protoplasmic astrocytes border with a small group of GN and enwrap the glomeruli to isolate synaptic complexes and mossy fibers (Palay and Chan-Palay, 1974; Hoogland and Kuhn, 2010).

Each protoplasmic astrocyte extends five-to-ten main stem branches, each of which gives rise to many finely branching processes that are distributed throughout the astrocyte domain in the gray matter and contact several hundred dendrites from multiple neurons enveloping about 100,000 synapses (Bushong et al., 2002; Ogata and Kosaka, 2002; Halassa et al., 2007).

Astrocytes express Aquaporin 4 (AQP4) water channel (regulating the fluid homeostasis, Seifert et al., 2006) and transporters for glutamate, GABA and glycine (removing the neurotransmitters for the synaptic cleft (Sattler and Rothstein, 2006)). Astrocytes release energy substrates, neurotransmitters, purines, growth factors (BDNF, $TNF\alpha$) and neurosteroids and express channels for both potassium and sodium. Their excitation, caused by the increase of intracellular calcium concentration, is required for astrocyte-astrocyte and astrocyte-neuron communication (Sofroniew and Vinters, 2010).

During neurodevelopment astrocytes release signaling molecules, such as thrombospondin, essential for the development of synapses and induce the expression of complement C1q that plays a key role in microglia-mediated synaptic pruning (Christopherson et al., 2005; Ullian et al., 2001; Stevens et al., 2007; Barres, 2008). The functions of astrocytes are summarized in **Figure 17**.

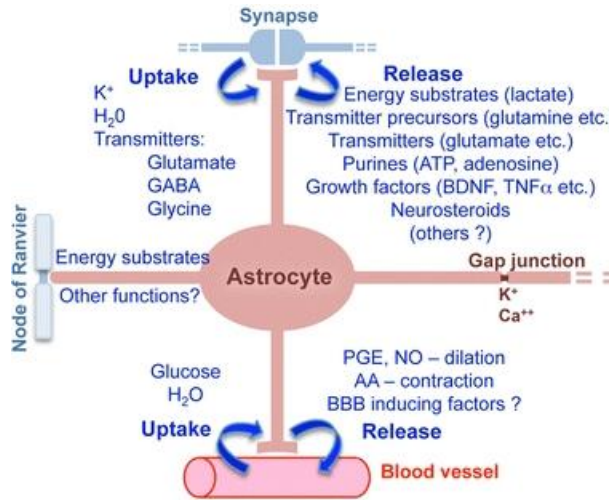


Figure 17. Astrocyte functions in healthy CNS (Adapted from Sofroniew and Vinters, 2010).

In response to CNS injury and disease, astrocytes exhibit different molecular, cellular and functional changes known as **reactive astrogliosis** (Sofroniew, 2009). Reactive astrogliosis can be mild or severe. Mild reactive astrogliosis is landmarked by the up regulation of **glial fibrillary acidic protein (GFAP)** expression, hypertrophy of the cell body and processes with preservation of astrocytes individual domains and little or no astrocyte proliferation (Sofroniew, 2009). In the severe form, there is a strong up-regulation of GFAP expression, more pronounced hypertrophy of the cell body and significantly increased proliferation, causing the disruption of individual astrocytes domains.

Oligodendrocytes are a type of highly specialized glial cells, whose main role is the production of the myelin sheath that electrically insulates axons maximizing the efficiency of action potential propagation (Liu and Zhou, 2013). While oligodendrocytes sit in the white matter and in all cortical layers, myelin formation is restricted to white matter and GCL (Palay and Chan-Palay, 1974; Reynolds and Wilkin, 1988). The only myelinated processes of the molecular layer are PC axons (Palay and Chan-Palay, 1974). It has been shown that PC axons are myelinated from their terminal field to the cell body, while cortical afferents (olivocerebellar axons and mossy fibers) are myelinated in anterograde manner (Buffo and Rossi, 2013).

Microglia are the only resident macrophages of the CNS and their density varies within different areas (Vela et al., 1995; Ginhoux and Prinz, 2015). Microglia exerts a crucial role in both CNS immune defense and homeostasis maintenance (Ginhoux and Prinz, 2015).

Microglia also contributes to brain homeostasis by controlling neuronal proliferation/differentiation and influencing the synapses formation (Lawson et al., 1990; Perry, 1998; Hughes, 2012; Blank and Prinz, 2013).

2.2. Origin of cerebellar neurons and glia

Neurons and glial cells of cerebellum arise from two different germinal zones: the dorsomedial **ventricular zone (VZ)** along the fourth ventricle and the free margin of the hindbrain at the interface between the roof plate and the dorsal neuroepithelium of rhombomere 1, known as **rhombic lip (RL)** (Sotelo, 2004; Kita et al., 2013). Progenitors having a radial glia-like morphology are present in both VZ and RL and give rise to almost all cell types (Kita et al., 2013).

PCs, GCs, LCs, BC/SCs, small-diameter DCNs, intraparenchymal astrocytes, BG cells and some oligodendrocytes originate from the VZ, while UBCs, GNs and large-diameter DCNs originate from RL. The origin of CCs is still unknown. These different cell types begin to differentiate at different stages of embryonic life in mice (Kita et al., 2013) (**Figure 19**).

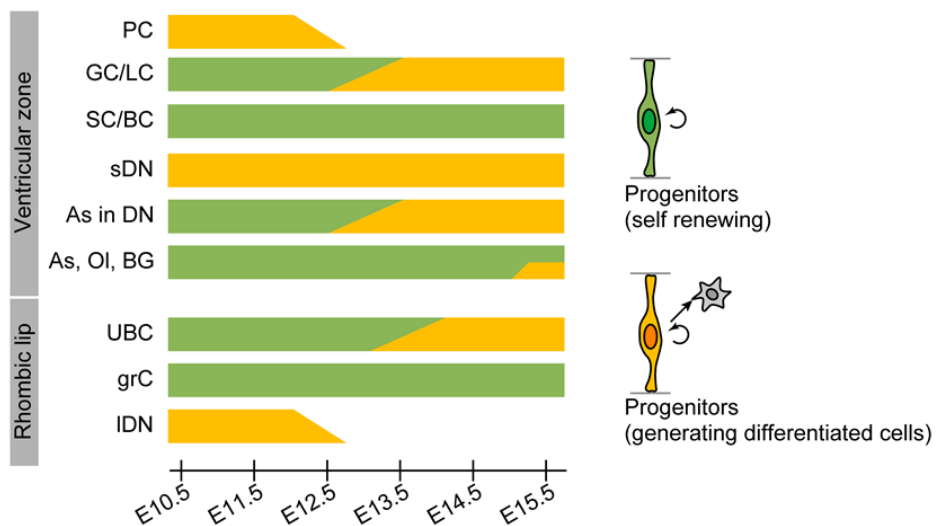


Figure 19. Origin of cerebellar neurons and glia. Green bars indicate that progenitors are self-renewing at indicated stages. Orange bars show stages at which progenitors generate differentiated cells. GC/LC, Golgi cell and Lugaro cell; PC, Purkinje cell; SC/BC, stellate and basket cell; BG, Bergmann glia; As, astrocyte; OI, oligodendrocyte; sDN, small-diameter deep nuclei neuron; IDN, large-diameter deep nuclei neuron; grC, granule cell (Kita et al., 2013).

Neurons of the adult cerebellum follow a temporal sequence of differentiation. Glutamatergic projection neurons (NP), GABAergic nucleo-olivary projection neurons (NO) and PCs differentiate in the early embryonic life, while local interneurons (of both neurotransmitter phenotypes) differentiate in late embryonic and early postnatal life. GABAergic interneurons are generated according to an inside-out sequence, occupying the deep nuclei first, and then the GCL and ML (Carletti and Rossi, 2008; Consalez and Hawkes, 2012).

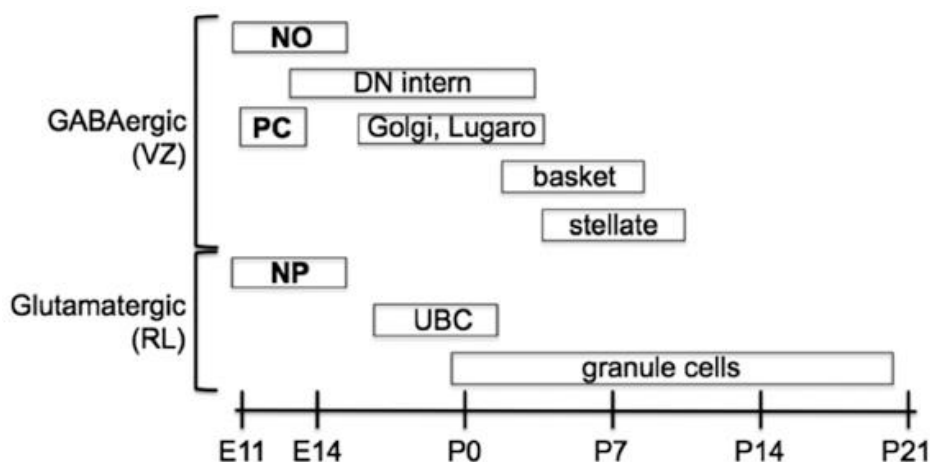


Figure 20. Temporal sequence of differentiation for the main types of cerebellar neurons (Consalez and Hawkes, 2012).

Although both BG and parenchymal astrocytes originate from the radial glia of VZ during late embryonic and postnatal development (Cajal, 1911; Miale and Sidman, 1961; Altman and Bayer, 1996; Sekerkova et al., 2004; Mori et al., 2006), they have a different natural history.

BG arise from the direct transformation of radial glia and continue to proliferate during the late embryonic and early postnatal life to match the simultaneous expansion of cerebellar cortex. Part of VZ radial glia continues to proliferate and then migrates in the PWN where it continues to divide and eventually acquires the mature trait of both fibrous and protoplasmic astrocytes (Buffo and Rossi, 2013). It is still unclear whether PWN progenitors contribute to generate BG or, *vice versa*, if proliferating BG can differentiate in intraparenchymal astrocytes (Miyake et al., 1995; Yuasa, 1996) (**Figure 21**).

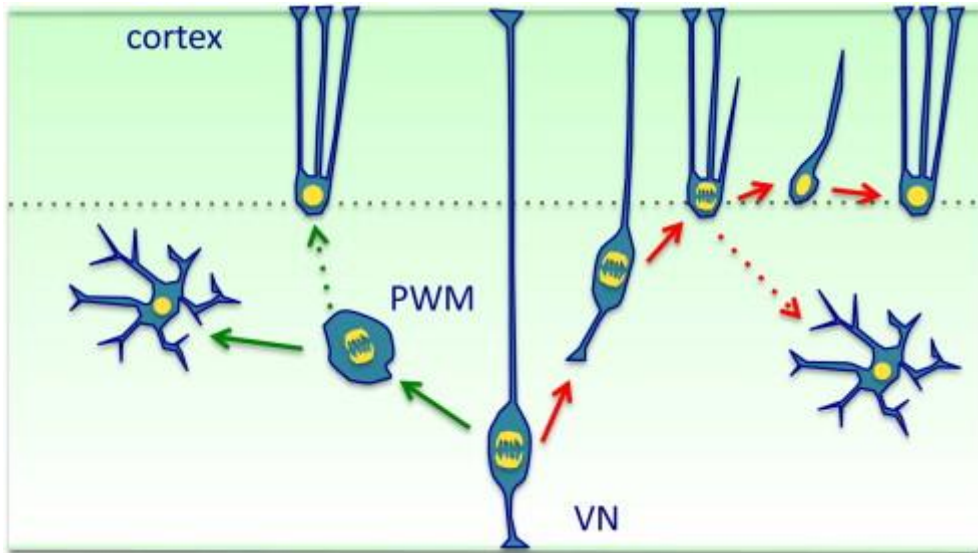


Figure 21. Origin of intraparenchymal astrocytes and BG. Both astrocyte classes originate from the radial glia of the VZ. Part of VZ radial glia continues to proliferate and then migrates in the PWM where it continues to divide, finally acquiring the mature trait of intraparenchymal astrocytes (green arrows on the left side of the picture). It is unclear whether PWM progenitors can differentiate in BG (dashed green arrow on the left side of the figure). BG arises from the direct transformation of BG arising from the direct transformation of radial glia and continues to proliferate during the late embryonic and early postnatal development to match the simultaneous expansion of cerebellar cortex (red arrows on the right side of the figure). It is not clear whether proliferating BG may also differentiate in intraparenchymal astrocytes (dashed red arrows on the right side of the figure) (Buffo and Rossi, 2013).

Although some oligodendrocytes originate from the radial glia of the VZ, they mostly derive from an extracerebellar source (Buffo and Rossi, 2013).

Besides oligodendrocytes, also microglia have an **extracerebellar origin**. Several genetic mapping studies have demonstrated that microglia mainly arise from the yolk sac (YS) primitive macrophages (Ginhoux et al., 2010; Hoeffel et al. 2012; Schulz et al., 2012; Kierdorf et al., 2013; Perdiguero et al., 2015).

During embryonic life, microglia precursors use three different routes to invade the CNS (Jordan and Thomas, 1988; Cuadros et al., 1994; Navascu  s et al., 1996):

- Meninges, by traversing the pial surface;
- Ventricles, by traversing the ventricular layer;
- Blood circulation, by traversing the endothelial wall;

among which the first one is the most common one (Cuadros et al., 1997).

2.3. Interaction between Bergmann glia and Purkinje cells

PC migration is physically supported by the processes of radial glia and involves several adhesion molecules, including reelin released by the EGL, leading them to reach specific cortical domain (Rakic et al., 1970; Yuasa et al., 1991, 1996). Recent studies have shown that some PCs migrate tangentially, initially, and interact with BG only at later stages (Yamada and Watanabe, 2002; Miyata et al., 2010).

In mice, until embryonal day 14 (E14) glial precursors display the morphology of radial glia, with cells bodies localizing in the VZ and radial fibers extending to the mantle zone. Between E14 and E15 PCs are in contact and lean against radial glia fibers, suggesting that radial glial cells are involved in contact guidance of PC migration (Yamada and Watanabe, 2002). Between E15 and PN7, the radial glia becomes BG by losing apical process while cell bodies migrate through the cortex (Buffo and Rossi, 2013). The migration of radial glia cell bodies slows down the migration of PCs; first, PCs move radially to the pial surface giving rise to the PC plate (PCP) below the EGL, whereas BG send several radial processes to the pial surface (Altman et al., 1997; Sotelo et al., 2012). Subsequently PCs migrate from the PCP to the bottom of ML forming the PCL. During the second and third postnatal weeks BG undergoes to cytoarchitectonic changes: the shaft fibers extend lamellate processes changing the palisade-like radial organization to a reticular glial meshwork (Yamada et al., 2000).

The dynamic transformation of BG fibers proceeds in concomitance with dendritogenesis and synaptogenesis of PCs, that in rodents are active in the second postnatal week of life (Altman, 1972b; Yamada and Watanabe, 2002). Thus, the rod-like domain of BG fibers provides a physical, trophic and structural substrate for PC growing dendrites, while the reticular transformation is related to structural maturation of newly formed PC synapses by glial covering (Yamada and Watanabe, 2002).

In particular, BG processes almost completely enwrap PF-PC synapses as well as CF-PC synapses (Palay and Chan-Palay, 1974; Spacek, 1985; Xu-Friedman et al., 2001; Yamada and Watanabe, 2002). At the molecular level, this interaction is mediated by phosphacan/6B4 proteoglycan, a chondroitinsulphate proteoglycan expressed by PCs (Maeda et al., 1992). Phosphacan is a component of the protein tyrosine phosphatase zeta (PTP ζ) receptor that mediates Pleiotropin (PTN) and Midkine (MN) signalling (Maeda et al., 1996, 1999), which are expressed and released by BG (Matsumoto et al., 1994; Wewetzer et al., 1995).

The activation of BG can be elicited by the stimulation of both PFs and CFs, which causes an increased intracellular calcium concentration in BG processes (Clark and Barbour, 1997, Bergles et al., 1997; Grosche et al., 1999; Iino et al., 2001). CFs-mediated stimulation increases the expression of **GLutamate ASpartate Transporter (GLAST)** by BG; GLAST removes glutamate from the synaptic cleft, preventing glutamate spillover between adjacent PCs (Bergles et al., 1997; Takayasu et al., 2009). Within the brain, BG expresses the highest density of GLAST; there are roughly 18000 molecules of GLAST for each μm^3 of tissue, while other glial cells express 4700 molecules per μm^2 (Lehre and Danbolt, 1998). GLAST is expressed from the earliest stages of development (Lehre et al., 1995), but the concentration increases significantly in concomitance with PC synaptogenesis (Ullensvang et al., 1997). In light of these findings, GLAST can be considered as a useful marker to analyze the structural relationship between BG and PCs development (Yamada et al., 2000).

After the uptake into BG, glutamate is converted by the enzyme **Glutamine synthetase** to glutamine and recycled back to synapses for reconversion into active transmitter (Sofroniew and Vinters, 2010).

In addition to GLAST and glutamine synthetase, BG also expresses high Calcium permeable α -amino-3-hydroxy-5-methyl-4-isoxazolepropionic acid (**AMPA**) glutamate receptors. It has been shown that glutamate released by PF/CF terminals acts through calcium-permeable AMPA receptors to regulate the degree of perisynaptic envelopment by BG. This, in turn, modulates the rate of glutamate removal from the synaptic cleft affecting the dynamics of synaptic signaling (Buffo and Rossi, 2013).

2.4. The scaffolding role of Bergmann glia during granule neuron and Basket/Stellate interneuron migration

The scaffolding activity of BG during **GN migration** is probably the most important and most studied example of glial-guided neuronal migration (Rakic, 1971; Buffo and Rossi, 2013).

By E10 GN precursors of the mouse embryo begin to proliferate, then they acquire a unipolar morphology, with a single process that projects away from the rhombic lip.

By E13 GN precursors exit the rhombic lip and migrate tangentially over the surface of the cerebellar primordium following a rostro-medial direction.

By E16 most of the cerebellar surface is covered by GN precursors, forming the EGL. The latter identifies a mitotically active region where GN precursors lose their processes, proliferate and then become post-mitotic, during the first two postnatal weeks (Altman, 1972).

The EGL can be divided in an outer layer (oEGL) containing mitotically-active p27Kip1-negative GNs progenitors and an inner layer (iEGL), in which p27Kip1-positive post-mitotic GNs start to differentiate and extend the bipolar processes of parallel fibers. Finally, GNs extend a third process perpendicular to the parallel fibers (PFs) and start to migrate radially along BG fibers to form the internal granule layer (IGL). GN proliferation is promoted by the Sonic hedgehog (Shh) secreted from PCs (Ruiz i Altaba et al., 2002) **(Figure 22)**.

PFs form glutamatergic synapses with PC dendrites in the ML, while their dendrites in the IGL form synapses with muscoid fibers (MF). The EGL disappears by ~PN15 and both migration and maturation of GNs are complete by PN20 (Goldowitz and Hamre, 1998; Hatten, 1999).

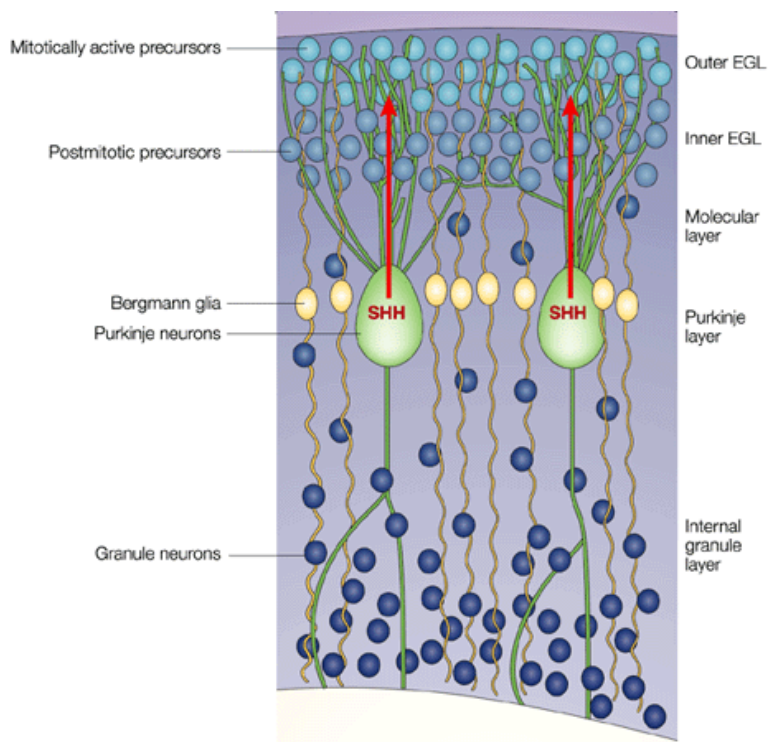


Figure 22. Granule neuron migration (Adapted from Ruiz i Altaba et al., 2002).

It has been suggested that BG also play a role in the **migration of interneurons** of ML (Buffo and Rossi, 2013).

After being generated by the progenitors of the VZ, BS/SC continue to proliferate at the level of prospective white matter (PWM) (Hallonet and Le Douarin, 1993; Zhang and Goldman, 1996a; Maricich and Herrup, 1999) and then, migrate radially and become progressively integrated in the expanding molecular layer (Yamanaka et al., 2004). Time-lapse video microscopy has revealed that the migration of BS/SC is very complex (Cameron et al., 2009). After entering the ML between PN6 and PN14, immature BC/SC exhibit a prolonged migration (~53.7 h) that takes place in four radial and tangential phases (**Figure 23**) (Cameron et al., 2009):

Phase I. BC/SC cross the PCL to enter in the upper ML. At this stage, they have a vertically-elongated soma and a single process orientated towards the pial surface. Once they reach the ML, they change orientation from vertical to horizontal;

Phase II. Cells migrate tangentially in the upper ML, following a rostro-caudal direction. At the end of this phase the cells change orientation from horizontal to vertical with the single processes orientated toward the PCL;

Phase III. BC/SC migrate radially within the ML from the top to the bottom and *vice versa* at a reduced speed, repeatedly extending and withdrawing the leading processes. At the end of this stage the cells turn and change orientation from vertical to horizontal;

Phase IV. Cells migrate tangentially in a rostro-caudal direction reaching their final destination, completely withdrawing the leading process and subsequently extending several dendrite-like processes in multiple directions that take contact with PCs and GCs.

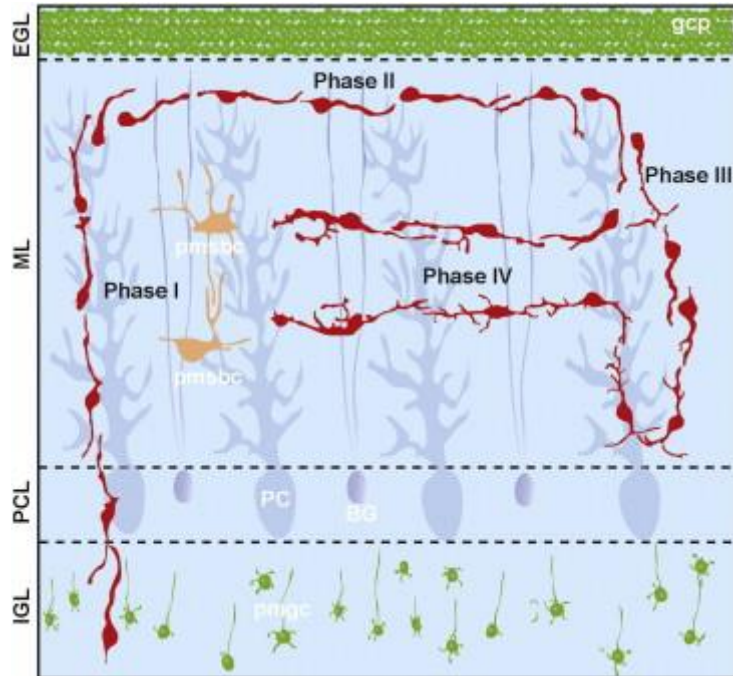


Figure 23. Phases of basket/stellate cell migration in the ML of the developing cerebellum. Abbreviations: gcp, granule cell precursors; pmsbc, postmigratory stellate/basket cells; pmgc, postmigratory granule cells; BG, Bergmann glial cells; PC, Purkinje cells (Cameron et al., 2009).

Accordingly, it has been proposed that migrating BC/SC follow different routes depending on the stage of migration. Probably, young interneurons follow BG fibers along their way from the white matter towards the EGL, while they follow bundles of ascending GN axons and PF to migrate within ML (Guijarro et al., 2006; Simat et al., 2007; Cameron et al., 2009; Buffo and Rossi, 2013). It has been shown that BC axons along PC soma and dendrites are attracted by neurofascin 186 while SC axons and dendrites elongate following the BG scaffold under the guidance of Close Homologue of L1 (CHL1), that is expressed by BG and SCs during postnatal development (Ango et al., 2004; Ango et al., 2008).

2.5. The involvement of astrocytes and microglia in NP-C1 disease

It has been shown that the NPC1 protein is expressed predominantly by astrocytic perisynaptic processes, playing a key role in the vesicular trafficking that is crucial for maintaining the structural/functional integrity of nerve terminals (Patel et al., 1999). Interestingly, in NP-C1 disease the terminal axonal and dendritic tree of neurons, closely associated with perisynaptic astrocytic processes, degenerate earlier than cell bodies (Patel et al., 1999).

Both astrocytes and microglia are mediators of brain inflammation and the premature activation of these two cell types during the early stages of NP-C1 disease, suggests that inflammation plays an important role in the progression of this disorder (Baudry et al., 2003). In particular, reactive astrocytes are already observed nine days after birth in NPC1-KO animals (Reid et al., 2004).

Astrocytosis has been also observed in PN120 *Npc1^{nmf164}* (Maue et al., 2012). However, these authors have not analyzed if this anomaly occurs at earlier disease stages neither the effect of CD treatment in rescuing this defect.

Microglia plays a crucial role in the regulation of brain development and homeostasis, secreting several signaling molecules, such as cytokines, neurotransmitters and trophic factors (e.g. Brain derived neurotrophic factor, BDNF) that regulate neurogenesis, neuronal growth/survival, oligodendrogenesis, synaptic activity and functional plasticity (Tay et al., 2016).

As part of innate immune system microglia detects external or internal danger signals and becomes active, thus eliminating pathogens by phagocytosis and releasing a variety of cytotoxic substances to protect CNS from inflammation and promote tissue repair/remodeling (Minghetti and Levi, 1998; Goldmann and Prinz, 2013).

During development, activated microglia also phagocytes apoptotic neurons and mediates the synaptic pruning to increase the efficiency of neuronal transmissions (Marin-Teva et al., 2004; Peri and Nusslein-Volhard, 2008; Paolicelli et al., 2011; Swinnen et al., 2013).

Although inflammation is a protective mechanism, the molecules produced and released by microglia during an inflammatory response, including glutamate, reactive oxygen species and nitric oxide are potentially cytotoxic.

Microglial activation appears from 2 weeks of age in *Npc1*^{-/-} mice in several regions, such as globus pallidus, ventral lateral thalamus, medial geniculate, cerebellum and DCN (Baudry et al., 2003).

As for *Npc1*^{nmf164} mice, Maue and coll. (2012) have analyzed the microglia activation only in the cerebellum of PN120 mice, finding a high activation. However, it remains unclear, if in this murine model microglia activation also occurs at earlier stages of the disease.

2.6. Oligodendrocyte differentiation: implication for NP-C1 disease

After entering in the central mass of cerebellum, oligodendrocytes, gradually occupy both PWM and all cortical layers, then they undergo a typical maturation that parallels the spatio-temporal pattern of colonization of the cerebellum (Reynolds and Wilkin, 1988).

The **differentiation of oligodendrocytes** is characterized by progressive morphological transformation. In the first differentiation step, oligodendrocyte precursor cells (OPCs) develop multiple immature processes (pro-oligodendrocytes). Then the pro-oligodendrocytes become membrane sheath-bearing mature oligodendrocytes, and, finally, myelinating oligodendrocytes.

Maturing oligodendrocytes express a typical sequence of marker, which reflects their progressive acquisition of mature traits. The OPCs highly express A2B5 antigen, platelet-derived growth factor receptor- α (PDGFR α) and chondroitin sulphate proteoglycan (NG2) while the pro-oligodendrocytes O4. Mature oligodendrocytes are characterized by the expression of galactocerebroside (GC or O1 antigen) and 2',3'-cyclic nucleotide 3'-phosphodiesterase (CNPase), whereas myelinating oligodendrocytes express myelin proteins: myelin-associated glycoprotein (MAG), myelin basic protein (MBP) and proteolipid protein (PLP) (Zhang et al., 2011; Buffo and Rossi, 2013) (**Figure 24**).

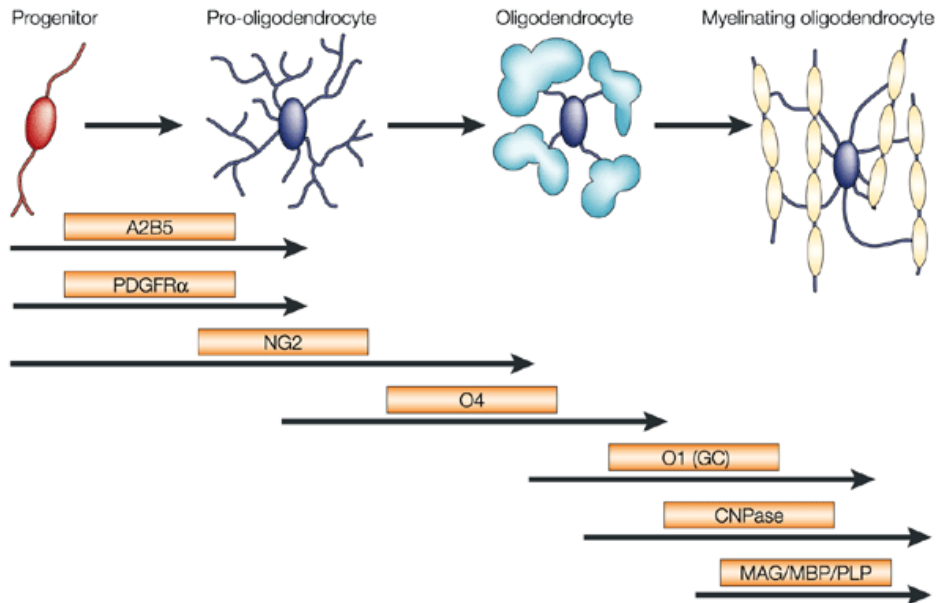


Figure 24. Morphological changes and antigenic markers of developing oligodendrocytes (Zhang et al., 2011).

Oligodendrocyte maturation is regulated by cell-autonomous mechanisms, cell-to-cell interactions and diffusible factors (Chatonnet et al., 2001; Li et al., 2009; Emery, 2010a; Emery, 2010b).

A critical role for oligodendrocyte development is played by **thyroid hormones** that at earliest stage of development indirectly influence oligodendrocytes proliferation/differentiation inducing the release of trophic factors from both PCs and astrocytes. In the adult life, thyroid hormones directly regulate the ability of the remaining precursors to divide or acquire mature traits (Fauquier et al., 2011; Picou et al., 2012).

Evidence suggest that oligodendrocytes are required for neuronal maturation and the appropriate organization of the cerebellar cortex, acting by mechanisms not yet fully characterized (Mathis et al., 2003; Collin et al., 2007; Doretto et al., 2011). Indeed, the of ablation oligodendrocytes in mice at the third postnatal week causes a disorganization of the cortical layers and an abnormal foliation accompanied by decreased GN densities, altered development of PC dendritic tree, impaired migration of BC/SC interneurons and disorganized BG network (Mathis et al., 2003).

The adult cerebellum is characterized by the presence of OPCs in the PWM and in both ML and GCL that maintain a proliferative activity and can differentiate in

oligodendrocytes for myelin remodeling throughout life and to repair myelin damage (Nishiyama et al., 2009; Young et al., 2013).

However, in the adult cerebellum, OPCs express receptors for GABA and glutamate and respond to the gliotransmitter ATP that represents the functional substrate of neuron-astrocyte interaction and promotes their differentiation (Wigley et al., 2007; Mangin and Gallo, 2011; Vèlez-Fort et al., 2012).

It has been proposed that neurons regulate the rate of OPCs proliferation, maturation and migration (Gallo et al., 2008; Mangin and Gallo, 2011; Vèlez-Fort et al., 2012). Each OPC of the ML receives about 70 input from a single CF, weaker inputs from PFs and is innervated by multiple olivary axons (Lin et al., 2005). Unlike synaptic contacts established by PCs, those established by OPCs are not enwrapped by BG (Lin et al., 2005). Although it was demonstrated that the glutamate release by CF causes the activation of calcium-permeable AMPA receptors on the surface of OPCs, the effect of this interaction for neuronal functioning remains unknown (Lin et al., 2005; Buffo and Rossi, 2013).

Among the marker expressed by myelin and oligodendrocytes, in addition to proteolipid protein (PLP), **myelin basic protein (MBP)** represents the second most abundant protein in CNS myelin (about the 30%; Boggs, 2001; Baumann et al., 2001). Various MBP isoforms are generated by alternative splicing and exert specific functions in different intracellular compartments. Namely, the 17.2 and 21.5 kDa isoforms are highly expressed in the cell body and nucleus of developing oligodendrocytes, playing a regulatory role in the genetic program of oligodendrocyte differentiation (Pedraza et al., 1997). In contrast, the 18.5 kDa isoform localizes at the plasma membrane and actively participates in membrane compaction typical of mature myelin (Harauz and Boggs, 2013).

Recently, it has been shown that the intracellular trafficking of lipids mediated by *Npc1* is required for the formation and maintenance of CNS myelin. Indeed, the ablation of *Npc1* in neurons impairs oligodendrocytes maturation and consequentially myelin formation. The ablation of *Npc1* in oligodendrocytes causes a delayed myelination in the forebrain and corpus callosum of PN16 mice, whereas in adult mice causes the loss of myelin proteins which in turn leads to PC degeneration (Yu and Lieberman, 2013).

This finding agrees with previous observations showing the expression of low-/very low-density lipoprotein receptors by oligodendrocytes (Zhao et al., 2007) and the dependence on glia-derived cholesterol of *Npc1*-deficient brains (Borbon et al., 2012; Zhang et al., 2008).

Moreover, dysmyelination and myelin loss were previously reported in prefrontal cortex, corpus callosum and hippocampus of *Npc1*^{-/-} mice (Takikita et al., 2004) and found

to be associated with defective genetic control of oligodendrocyte differentiation (Yan et al., 2011).

In particular, MBP immunohistochemistry revealed that, starting from PN10 both the cerebral cortex and the corpus callosum of *Npc1^{-/-}* mice display hypomyelination that becomes more evident at PN20 (**Figure 25**).

MBP immunoreactivity remains preserved only in the deep layer of somatosensory cortex and cingulate cortex (Takikita et al., 2004). At PN20 *Npc1^{-/-}* mice also display a hypomyelinated septum, whereas no difference was found in the optic chiasma in comparison to *wt* mice. The authors suggest that this deficit can be due to a failure of OPCs to myelinate axons or an axonal incapability to be myelinated (Takikita et al., 2004).

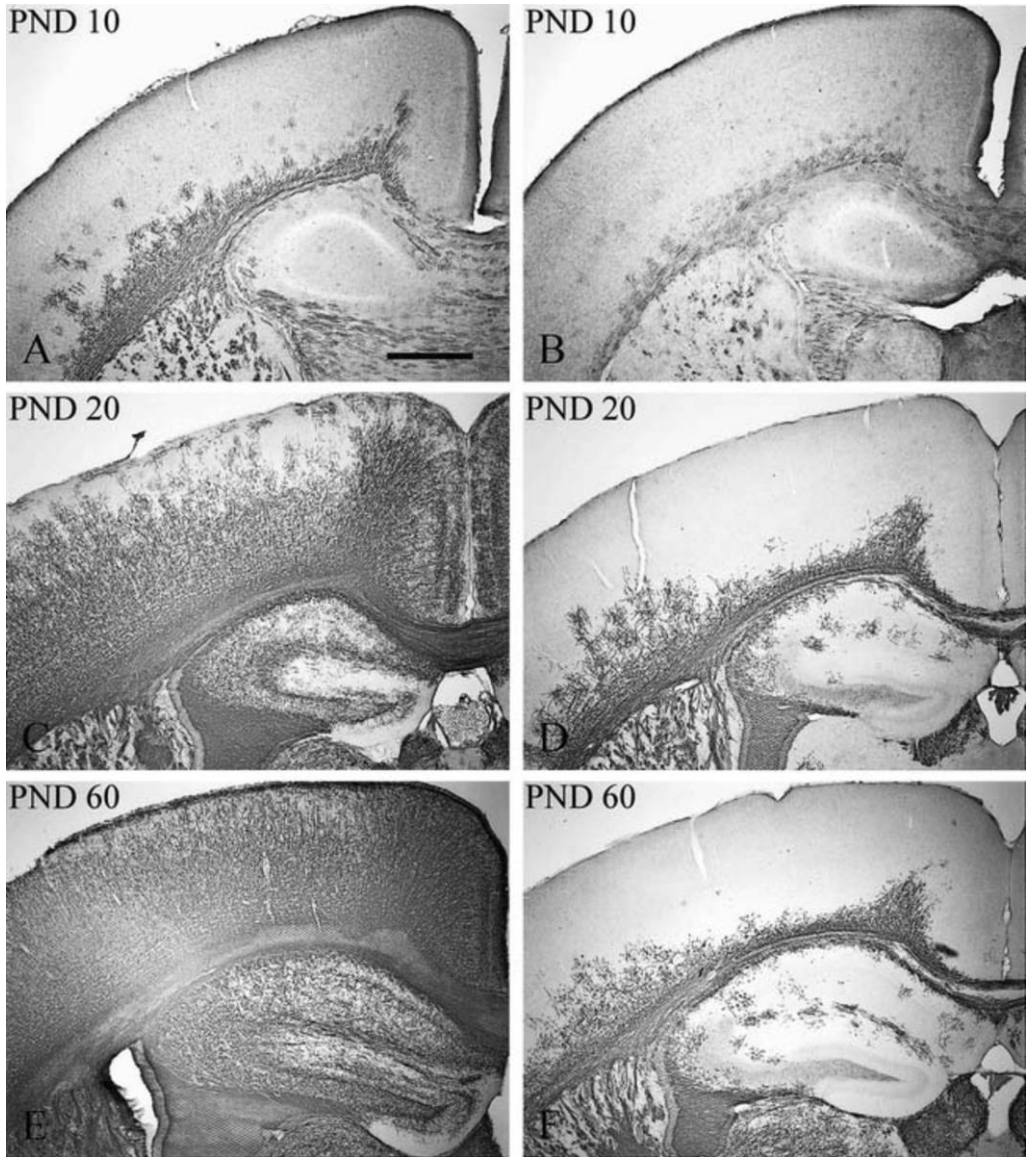


Figure 25. Distribution of myelin basic protein in PN10 (A, B), PN20 (C, D) and PN60 *Npc1^{nih}* mice (E, F). Control mouse, left side (A, C, E); *Npc1^{nih}* mouse, right side (B, D, F). MBP immunohistochemistry reveals obvious hypomyelination of cerebral cortex as well as corpus callosum in the *Npc1^{nih}* mouse brain. Note that almost the entire cortex except the deep layer of somatosensory cortex and cingulate cortex is devoid of MBP immunoreactivity (D, F). Although relative hypomyelination is already recognized in 10-day-old brain (PND10) (A, B), the difference of myelination becomes obvious in the mouse after PND 20. Comparing the images of PND20 and PND60, *Npc1^{nih}* mice show no progress in myelination, whereas myelination extends towards pial surface in control mice (C–F). Similarity of cortical myelin distribution between PND60 *Npc1^{nih}* mice brain (F) and PN10 control brain (A) suggests that unmyelinated cortical area in PND60 *Npc1^{nih}* mouse corresponds to the area of the late-onset myelination (Takikita *et al.*, 2004).

Maue and coll. (2012) have used the diffusion tensor imaging (T2-weighted) by magnetic resonance imaging (MRI) to analyze myelination in *Npc1^{nmf164}* mice, finding no difference between *Npc1^{nmf164}* and *wt* mice for the T2 signal. The issue of whether also *Npc1^{nmf164}* display a deficit in the differentiation of oligodendrocytes and myelin maturation as well as if the myelination deficiency also affects the cerebellum was not investigated yet.

2.7. Sonic hedgehog patterning during cerebellar development: implications for NP-C1 disease

Sonic hedgehog (Shh) is a protein encoded by the SHH gene, which is part of the hedgehog (hh) family that also includes the Desert Hedgehog (Dhh) and the Indian Hedgehog (Ihh) proteins (Echelard et al., 1993).

In mammals, Shh is expressed from early embryogenesis and acts as morphogen, mitogen and guidance molecule for both cerebellar development and maturation (Fuccillo et al., 2006; Yam and Charron, 2013).

Initially, Shh is synthesized as a 45 kDa precursor protein that is auto-proteolytically cleaved into a 19 kDa amino-terminus (Shh-N) with a signaling domain and a 26 kDa carboxy terminus (Shh-C) without signal transduction activity (Porter et al., 1996; Choen, 2004).

Shh-N undergoes to a dual lipid modification, namely the covalent addition of cholesterol and palmitate, becoming an active signaling protein (De Luca et al., 2016).

Shh is then trafficked to the cell surface and released from cells as a multimer (M-Shh-N) (Porter et al., 1996; Chamoun et al., 2001; Pipinsky et al., 1998).

Shh signaling relies on **primary cilium**, a microtubule-based membrane cellular structure essential for signal reception and transduction (Goetz and Anderson, 2010) and on the binding to the transmembrane receptors **Patched (Ptch)**.

In the absence of Shh, Ptch represses **Smoothed (Smo)**, a seven transmembrane G-protein coupled receptor-like protein that represents the transducer of Shh signal inside the cell (De Luca et al., 2016).

Upon Shh binding, Ptch relieves Smo inhibition, which in turn results in the activation of Gli family transcription factors and the activation of genes controlling cell proliferation and differentiation (Huangfu and Anderson, 2006; Ruiz i Altaba et al., 2007).

Besides the need of cholesterol for Shh activity *per se*, the downstream effectors of Shh signaling are cholesterol-dependent. In fact, Smo translocation to the cilium, which is necessary for its activation, is dependent on cholesterol availability (Karpen et al., 2001; Rohatgi et al., 2007).

During the early embryonic life Shh is released by choroid plexus (ChP) and mediate the radial glial cell proliferation and the expansion of the progenitors of GABAergic neurons. Starting from E17.5, Shh is secreted by PCs and promotes the differentiation of radial glia in Bergmann glia. Postnatally, Shh supports the proliferation of both GNs and oligodendrocyte precursor (OPCs) cells in the EGL and PWM, respectively. In the PWM, Shh also promotes the proliferation of neural stem cell-like progenitors that generate both intermediate astrocyte precursors and GABAergic transient amplifying cells (De Luca et al., 2016).

At the end of the first post-natal week, PCs downregulate Shh expression and release vitronectin that induces oligodendrocyte maturation and myelin formation (Boslama-Oueghlani et al., 2012; Sotelo and Rossi, 2012) (**Figure 25**).

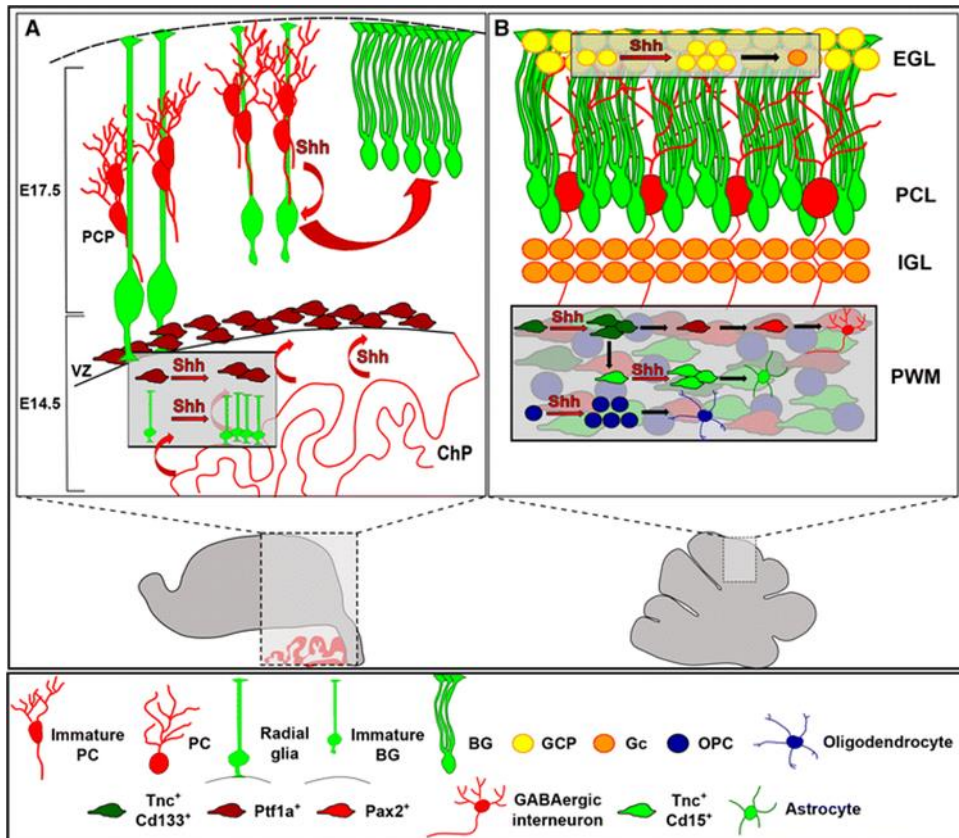


Figure 25. Shh functions during cerebellar development. (A) During the early embryonic life Shh is released by choroid plexus (ChP) and mediates the radial glial cell proliferation and the expansion of Ptf1a⁺ progenitors of GABAergic neurons. Starting from E17.5, Shh is secreted by Purkinje cells and promotes the differentiation of radial glia in Bergmann glia. **(B).** Postnatally, Shh supports the proliferation of both granule neurons and oligodendrocyte precursor cells (GCPs and OPCs), in the EGL and PWM, respectively. In the PWM, Shh also promotes the proliferation of neural stem cell-like progenitors (Tnc⁺CD133⁺) that generate both intermediate astrocyte precursors (Tnc⁺CD15⁺) and GABAergic transient amplifying cells (Ptf1a⁺). PCP Purkinje cell progenitor, ChP choroid plexus, PWM prospective white matter, GL granular layer, PCL Purkinje cell layer, EGL external granular layer (*De Luca et al., 2016*).

Recently we have found that both Shh availability and signal reception at the levels of Patched receptor/Smoothed downstream effector is altered in NPC1 mice causing a defective GN proliferation (Nusca et al., 2014; Canterini et al., unpublished results). This finding suggests that oligodendrocyte and Bergmann glia differentiation, as well as the proliferation of neural stem cell-like progenitors, generating intermediate astrocyte precursors and GABAergic transient amplifying cells could be altered in NPC1 mice.

2.8. The importance of BDNF signaling pathway in cerebellar development and current knowledge of its role in NP-C1 disease

Brain-derived neurotrophic factor (BDNF) is a member of the nerve growth factor gene family and plays a crucial role in the development and maintenance of nervous system. In mice, the *Bdnf* gene consists of many non-coding exons (I, II, III, IV, V, VI, VII, VIII) followed by a single coding exon (IX), which encodes for the pre-pro-protein (pro-BDNF). Although the human gene is very similar, it differs for additional exons V and VIII and for a more complex pattern of alternative splicing involving the exon IX (Koppel et al., 2009) (**Figure 26**).

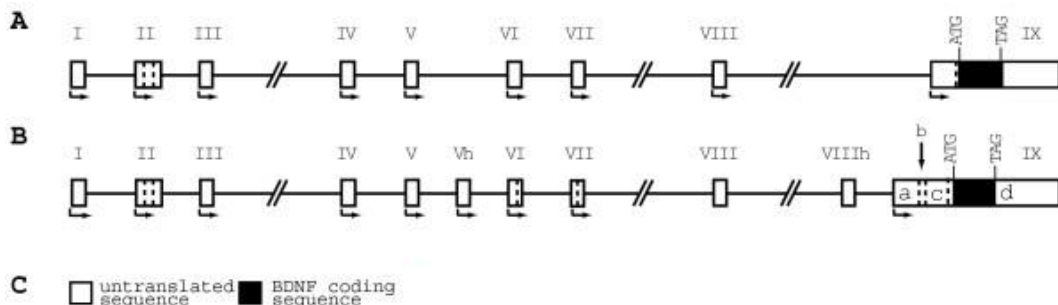


Figure 26. Schematic drawings of rodent and human BDNF genes. (A) Rodent BDNF gene (B) Human BDNF gene (C) Representation of untranslated (white square) and coding sequence (black square) (adapted from Koppel et al., 2009).

Once the **pro-BDNF** is translated, it is converted by the enzyme furin into mature BDNF and directly released exerting its function by binding the tropomyosin receptor kinase B (TrkB). Alternatively, it can be converted into a mature form by proconvertase enzymes and stored in secretory vesicles. Furthermore, cells can directly release unprocessed pro-BDNF. In this case, pro-BDNF can be either converted into mature-BDNF by plasmin or function as a signal molecule *per se* by binding p75^{NTR} receptor (Barker, 2009) (**Figure 27**).

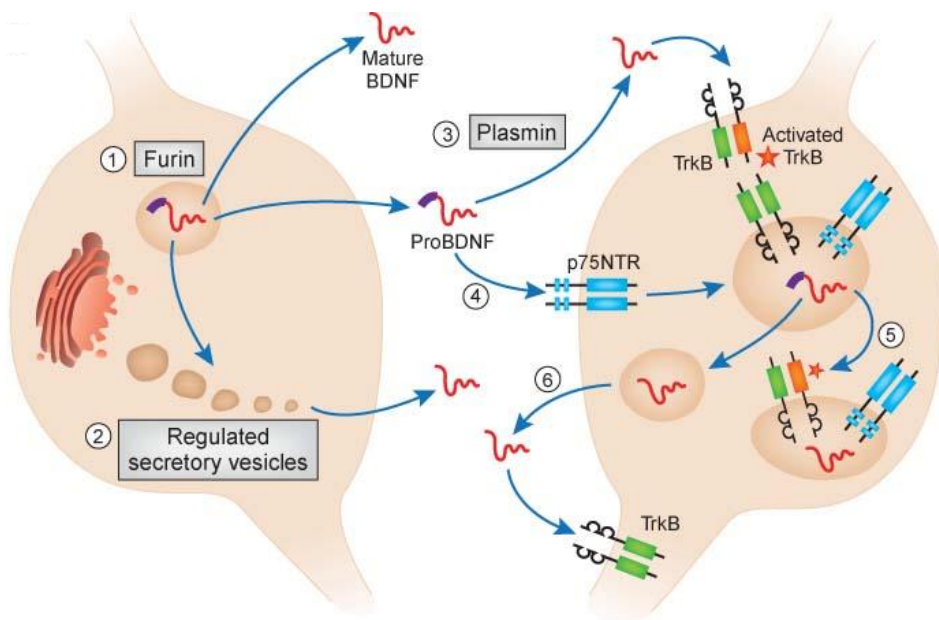


Figure 27. BDNF production and processing in the central nervous system (Adapted from Barker, 2009).

The binding of pro-BDNF to **p75^{NTR}** receptors promotes both apoptosis and cell survival, by the c-Jun N-terminal kinase (JNK) and nuclear factor kappa-light-chain-enhancer of activated B cell (NF- κ b) signaling cascade, respectively. Instead, the binding of BDNF to **TrkB** receptors leads to the activation of three main signaling pathways: 1) Phospholipase C (PLC γ); 2) Phosphoinositide 3-kinase (PI3K); and, 3) extracellular signal-regulated kinase (ERK). These three pathways finally lead to the activation of CREB transcription factor that mediates the transcription of genes essential for both neuronal survival and differentiation (Cunha et al., 2010).

Among signaling pathways controlling cerebellar development, mature-BDNF acts as a chemokinetic factor to induce GN migration and as chemodynamic factor to guide GNs along BGs fibers (Borghesani et al., 2002).

Furthermore, BDNF is required for the development of dendritic spines and arborizations of PCs and axonal growth of GNs, to modulate the dendritic morphology of BCs/SCs and to regulate the cholesterol metabolism for synapses formation (Suzuki et al., 2007a,b; Mertz et al., 2000).

However, during neurodevelopment pro-BDNF mediates opposite effects compared to BDNF, by promoting apoptosis and negatively regulating neurite growth, dendritic spine formation and GN migration (Nagappan and Lu, 2005; Khoshimizu et al., 2009; Xu et al., 2011).

In fact, it has been shown that *BDNF*^{-/-} mice display a defective foliation and development of PC dendritic tree, as well as a reduced thickness of ML, an increased death of proliferating cerebellar neurons and developed ataxia (Schwartz et al., 1997). Instead, TrkB deficient-mice display a multiple CF innervation of a single PC, a reduced thickness of both ML and GCL, altered GABA synthesis and uptake and altered formation and maturation of GABAergic synapses (Rico et al., 2002).

Besides, BDNF elicits neuronal *de novo* synthesis of cholesterol stimulating the transcription of several enzymes involved in the cholesterol biosynthetic pathway (Suzuki et al., 2007a,b). The BDNF-dependent cholesterol biosynthesis plays a critical role for the development of synapses and lipid rafts (Suzuki et al., 2007a,b).

It has been shown that defective cholesterol metabolism of embryonic striatal neurons of *Npc1*^{-/-} mice is associated with a defective neurite outgrowth due to the BDNF failure to activate TrkB receptors (Henderson et al., 2000). It was also reported that neural stem cells of *Npc1*^{-/-} mice show an impaired self-renewal and differentiation, due to the imbalance between histone deacetylase (HDAC) and histone acetyltransferase (HAT) activities, resulting in the down-regulation of the expression of *Bdnf* and *TRKB* genes (Kim et al., 2007).

In spite of this evidence, the issue of whether the BDNF signaling pathway in the developing cerebellum of *Npc1*-deficient mice has not yet been investigated.

Chapter III

The research project

3.1. Background and aims

We have recently shown that in *Npc1*^{-/-} mice there is an overall cerebellar size and external granule layer (EGL) thickness reduction, due to a deficit of the proliferation of granule neuron (GN). This leads to a deficiency of GNs in the Inner Granular Layer (IGL), which may contribute to the later Purkinje cell (PC) degeneration (Nusca et al., 2014).

In line with the robust mitogenic activity Sonic Hedgehog (Shh) exerts on GNs (Wechsler-Reya and Scott, 1999), Shh mRNA levels were found to be significantly reduced in both *Npc1*^{-/-} and *Npc1*^{*nmf164*} mice at the time of final divisions of GN precursors (Nusca et al., 2014; Canterini et al., *manuscript in preparation*). Thus, the reduced Shh availability may cause a GN proliferation deficit in both mouse models.

Among the animal models of NP-C1 disease, the *Npc1*^{*nmf164*} mouse is of particular interest because it harbors a single nucleotide substitution (A to G at cDNA bp 3163) causing an aspartate-to-glycine substitution (D1005G) in the cysteine-rich luminal loop, conferring to the NPC1 protein a partial loss of activity as observed in most common human mutations (Maue et al., 2012).

Besides GNs, also Bergmann glia (BG) responds to Shh (Corrales et al., 2004) by differentiating along with PC maturation, especially promoting PC dendritic tree extension and enwrapping the GABAergic and glutamatergic synaptic contacts that PCs receive from Basket/Stellate interneurons (BCs/SCs) and parallel/climbing fibers, respectively (Yamada and Watanabe, 2002). This suggests that *Npc1*-deficiency also affects the normal pattern of both BG differentiation and functionality.

Shh is required for oligodendrocyte precursors (OPCs) generation and subsequent differentiation into mature oligodendrocytes (Nery et al., 2001). Although previous studies have shown dysmyelination in both NPC patients and *Npc1*^{-/-} mice (Takikita et al., 2004; Walterflang et al., 2010), the effect of *Npc1*-deficiency on oligodendrocyte differentiation has not been well characterized in the cerebellum.

Previous studies have reported that in *Npc1*^{-/-} mice there is an increased number of reactive astrocytes (astrocytosis) starting from nine days after birth in thalamus and cortex (Reid et al., 2004), whereas in *Npc1*^{nmf164} the presence of astrocytosis was analyzed and found only in the adult cerebellum (Maue et al., 2012).

Also, the presence of microglia activation was only investigated in adult *Npc1*^{nmf164} mice.

Besides Shh, also the Brain-Derived Neurotrophic Factor (BDNF) exerts a crucial role for proper proliferation and differentiation of various neuronal and glial cells, likely influencing the overall pattern of synaptic connectivity of the cerebellar cortex.

Mature-BDNF is synthesized from the pro-BDNF but both proteins acts as signaling molecules by binding the TrkB and p75^{NTR} receptors, respectively (Barker, 2009).

However, during the neurodevelopment pro-BDNF mediates opposite effects compared to BDNF, by promoting apoptosis and negatively regulating neurite growth, dendritic spine formation and GN migration. In light of the finding that, BDNF expression is regulated by Shh through post-transcriptional mechanisms (Bond et al., 2013), we have hypothesized that BDNF signaling might be altered in *Npc1*^{nmf164} mice.

Evidence so far obtained prompted us to further investigate above mentioned issues, by addressing the following aims: i) to characterize whether the altered Shh signaling pathway influences Bergmann glia, oligodendrocyte and Purkinje cell differentiation; ii) to characterize the BDNF signaling; iii) to analyze astrocytes/microglia activation and microglia mediated-phagocytosis in the early stage of cerebellar development.

In light of the efficacy of 2-hydroxypropyl- β -cyclodextrin (CD) in rescuing cerebellar anomalies of mouse models (e.g. see paragraph 1.9), these issues were investigated in *Npc1*-deficient mice either treated or untreated with CD.

3.2. Materials and methods

3.2.1. Mice

Npc1^{nmf164/nmf164} mice with BALB/cJ background (hereafter named *Npc1^{nmf164}* mice) were generated by heterozygous crosses and maintained in our animal facility in accordance with Sapienza University guidelines for the care and use of laboratory animals. Experimental protocols and related procedures were approved by the Italian Ministry of Public Health. All efforts were made to minimize animal suffering, according to European Directive 2010/63/EU.

3.2.2. Genotyping

Genotypes were identified by PCR analysis accordingly to Maue et al., (2012). Genomic DNA was extracted from tail biopsy using the HotShot method (Truett et al., 2000).

~1ul of DNA was used for to generate a 176 bp PCR product using the following primer pairs and conditions:

- Reverse primer: 5'-AGGACCCTTCCGTACAAGC-3'
- Forward primer: 5'-GGCCTCCAGGGGAAAGAATT-3'

Cycle step	Temperature	Time	Number of Cycles
Pre-denaturation	95 °C	1 min	1
Denaturation	95 °C	16 sec	38
Annealing	62 °C	16 sec	
Extension	73 °C	15 sec	
Final extension	72 °C	3 min	1
Hold	12 °C	5 min	1

To discriminate the single base change (A to G) PCR product was then incubated at 37 °C for 1 h with the restriction enzyme BstEII that generates two fragments of 128 and 48 bp in the presence of the G allele.

3.2.3. Treatments

The treatment schedule was the following: both *Npc1^{nmf164}* and *wt* pups received two consecutive subcutaneous injections at PN4 and PN7 of 2-hydroxypropyl- β -cyclodextrin in PBS (hereafter named CD; average degree of substitution of 0.67 of hydroxypropyl groups per glucose unit, MW ~1369 Da, catalog number H-107, Sigma Aldrich, Milan, Italy) (w/v; 4000 mg/Kg body weight) (Palladino et al., 2015). Age-matched control mice received plain PBS injections (sham animals).

For CD/sham administration, pre-weaning pups were separated from the mother, weighed, injected at the scruff of the neck (Liu et al., 2008), monitored for complete absorption of the injection bolus and finally returned to the home cage. The entire injection procedure lasted approximately 15–20 min, giving each pup a similar treatment, inclusive of maternal separation, handling and injection.

3.2.4. Western blot assays

For Western blot analyses, total proteins of PN11 and PN15 *Npc1^{nmf164}* and *wt* littermates cerebella (4 mice/genotype/age) were extracted with RIPA buffer (Sigma Aldrich, Milan, Italy) supplemented with protease and phosphatase inhibitors (Roche Life Science, Indianapolis, IN, USA). The protein concentration was routinely determined by Bradford's colorimetric assay (Bio-Rad, Milan, IT).

Equal amounts of total protein/lane were fractionated by electrophoresis on a 4–12% gradient SDS-polyacrylamide gel (Bolt® Bis-Tris Plus gels, Life Technologies, Carlsbad, CA, USA) or 10 % gel pre-cast (Bio-Rad). Fractionated proteins were transferred to PVDF membranes (GE Healthcare, Little Chalfont, UK) and then processed for Western blot analyses.

When proteins of interest had very different electrophoretic migrations, such as in the case of Glutamine synthetase and MBP, membranes were cut into strips to be probed with different antibodies. The primary and secondary antibodies used are reported in **Table 1**.

Table 1. Antibodies used

Antibody		Company	Dilution	
			WB ^a	IHC ^a
Primary	anti-GFAP	Santa Cruz Biotechnology, Santa Cruz, CA, USA; #sc-33673	1:500	1:50
	anti-EAAT1 or GLAST	AbCam, Cambridge, UK; #ab416	1:1500	1:250
	anti-Glutamine Synthetase	AbCam; #ab73593	1:2000	1:333
	anti-VGluT2	Thermo Fisher Scientific, Rockford, IL; USA; #PA5-25653	1:1000	1:50
	anti-GAD65	AbCam; #ab26113	1:2000	1:200
	anti-MBP	Sigma-Aldrich Inc., St. Louis, MO, USA; #M3821	1:500	1:100
	anti-p27Kip1	Epitomics, Burlingame, CA, USA; #P46414	-----	1:75
	anti-parvalbumin	Sigma-Aldrich Inc., #P2088	-----	1:700
	anti-CD11b	AbCam; #ab133357	1:1000	-----
	anti-CD68	Santa Cruz Biotechnology; #sc-59103	1:100	-----
	anti-BDNF	Santa Cruz Biotechnology; #sc-546	1:250	-----
	anti-p75 ^{NTR}	Santa Cruz Biotechnology; #sc-271708	1:1000	-----
	anti-TrkB	Santa Cruz Biotechnology; #sc-377218	1:1000	-----
	Anti-BrdU	Immunological science, Milan, Italy; #IK-11143	-----	1:100
	anti-β-actin	AbCam; #ab6276	1:1000	-----
Secondary	Horseradish peroxidase-conjugated goat anti-rabbit IgG	Thermo Fisher Scientific; #32460	1:200	-----
	Horseradish peroxidase-conjugated goat anti-mouse IgG	Thermo Fisher Scientific; #32430	1:650	-----
	Horseradish peroxidase-conjugated goat anti-mouse IgG2a	Santa Cruz Biotechnology; #sc-2061	1:3000	-----
	Biotinylated goat anti-rabbit IgG	Vector Laboratories, Burlingame, CA; #PK-6101	-----	1:200
	Biotinylated goat anti-mouse IgG	Vector Laboratories; #PK-6102	-----	1:200

3.2.5. Brain collection and sectioning

PN11 and PN15 *Npc1^{nmf164}* and *wt* littermates untreated, sham- or CD-treated (4 mice/genotype) were deeply anaesthetized by intraperitoneal injection of a mixture of xylazine (20 mg/Kg) and ketamine (34 mg/Kg) and then transcranially perfused with 4% PFA in 0.1 M PBS. Brains were removed and post-fixed overnight at 4 °C in 4 % PFA. PFA-fixed brains were dehydrated, embedded in Paraplast Tissue Embedding Medium (Leica Biosystems, Milan, Italy) and serially sectioned (slice thickness 8 µm). Sagittal sections were mounted on X-tra Adhesive glass slides (Leica Biosystems), de-waxed with xylene, rehydrated and washed in PBS.

Alternatively, the detection of some markers was performed on cryosections. For this reason, PFA-fixed brains were cryoprotected with sucrose (30 %, w/v, in PBS), embedded in FSC22 Clear R Frozen Section Compound (Leica Biosystems) and sagittally sectioned (slice thickness 8 µm) using a Leica CM 1900 cryostat. Sections were mounted on X-tra Adhesive glass slides (Leica Biosystems) and washed in PBS.

3.2.6. Immunohistochemistry

For p27kip1 immunostaining rehydrated paraffin sections of PN15 *wt*, *Npc1^{nmf164}* and *Npc1^{nmf164}* CD-treated mice were incubated (5 minx2) in 10 mM sodium citrate, pH 6.0 in a microwave for epitope unmasking. Hence, sections were incubated first with Trypsin working solution (0,05% trypsin, 0,1% calcium chloride in dH₂O) for 15 minutes at room temperature (RT) and then with 2M HCl for 20 minutes to permeabilize tissue. To inactivate endogenous peroxidase, sections were incubated in 5% hydrogen peroxide for 15 minutes and then subjected to a blocking/permeabilization (30 min incubation in a buffer containing 6% goat serum and 0,3% Triton X-100 in PBS). Incubation with rabbit monoclonal primary antibody against p27kip1 was carried out overnight at 4°C. After 3 washes in PBS, sections were stained using first the rabbit Vectastain Elite ABC Kit (Vector Laboratories Inc., Burlingame, CA, USA), allowing specific ABC complex development, and then the DAB Peroxidase Substrate Kit (Vector Laboratories Inc., Burlingame, CA, USA) acc. to the protocol supplied by the manufacturer. Nuclear counterstaining was performed by incubating sections with 0,5% Methyl Green solution (0,5% Methyl Green, 0,1M sodium acetate buffer in water, pH 4.2) for 5 minutes at 60°C. After dehydration, slices were mounted with Eukitt mounting medium (Electron Microscopy Sciences, Hatfield, PA, USA).

For parvalbumin immunostaining, rehydrated paraffin sections of PN15 *wt* and *Npc1^{nmf164}* were subjected to a blocking/permeabilization step consisting in a 30 min incubation in PBS supplemented with 5% normal goat serum, 0.3% Triton X-100. Sections were then incubated with a monoclonal antibody directed to parvalbumin, supplemented with 3% normal goat serum, overnight at 4°C, washed 3-4 times with PBS and stained using the mouse Vectastain Elite ABC kit and the DAB peroxidase substrate kit (Vector Laboratories Inc., Burlingame, CA, USA) according to the protocol supplied by the manufacturer. After dehydration, slices were mounted with Eukitt mounting medium (Electron Microscopy Sciences, Hatfield, PA, USA). The number of PCs and basket/stellate interneurons was determined in 0.04 mm² regions randomly selected in each field of anterior (I-V) and posterior (VI-X) lobules of *wt* and *Npc1^{nmf164}* mice (*N* = 3 mice/genotype; 3–4 sections/mouse) using the function “cell counter” of ImageJ NIH software. Histological observations/evaluations were blindly and independently performed by two investigators.

MBP immunostaining was carried out using rehydrated paraffin sections while the detection of other glial and neuronal cell markers (GLAST, GFAP, Glutamine synthetase, VGluT2 and GAD65) was performed on cryosections of PN15 *wt* and *Npc1^{nmf164}* mice, untreated, sham- or CD-treated.

For GLAST detection, cryosections were subjected to 20 min fixation in acetone (–20 °C), which significantly improved antigen detection (Finckbone et al., 2009). Paraffin sections and cryosections were then processed for epitope unmasking and endogenous peroxidases inactivation.

For antigen unmasking, sections were incubated (5 min x 2) in 10 mM sodium citrate, pH 6.0 in a microwave and then incubated in 0.3% H₂O₂ for 15 min at RT to inactivate endogenous peroxidases. A 2 h incubation in a blocking solution made of 0.5 % BSA in PBS preceded the incubation of sections with anti-GLAST and anti-MBP antibodies.

For the detection of VGluT2, GFAP, Glutamine synthetase and GAD65 the blocking solution was supplemented with 0.1% Triton X-100. The incubation of sections with primary antibodies lasted approximately 18 h at 4 °C and was followed by several washes in PBS before exposure to the appropriate secondary antibody (see **Table 1** for details).

Antibody-antigen complexes were revealed with Vectastain Elite ABC Kit (Vector Laboratories Inc., Burlingame, CA, USA) followed by DAB Peroxidase Substrate Kit (Vector Laboratories Inc.), according to manufacturer’s instructions.

After dehydration, slices were mounted with Eukitt mounting medium (Electron Microscopy Sciences, Hatfield, PA, USA). Images were obtained using a Zeiss Axioplan

microscope equipped with a Sony nex-3 N mirror-less camera (Sony Europe Limited, Milano, Italy) and processed using ImageJ NIH software (National Institutes of Health, Bethesda, MD).

VGluT2- and GAD65-positive puncta were quantitated in 3–4 sagittal sections of 4 mice/genotype as previously described (Grimes et al., 2003; Lin et al., 2014) with slight modifications.

Images were acquired using a Zeiss Axioplan microscope at 100X magnification (Neofluar, 0.7–1.30) and a Sony nex-3 N mirror-less camera. For each antibody, at least 8 image fields of lobule II and lobule X were acquired along the molecular layer starting from the pial surface.

The abundance of VGluT2- and GAD65-positive puncta was determined in regions of interest (ROI) of 6500 μm^2 and 3200 μm^2 , respectively, randomly selected in outer and inner molecular layers by the “cell counter” function of ImageJ NIH software. The number of GAD65-positive puncta around the PC's soma was also determined. Only VGluT2- and GAD65-positive puncta having a high-to-moderate staining and a diameter of 0.3–1.3 μm were counted. All determinations were performed blindly and independently by two investigators.

Because no significant difference was observed between counts of lobule II and lobule X microscopic fields of *wt* or *Npc1^{nmf164}* mice, data were pooled.

To assess GN proliferation, brains were dissected from PN13 and PN15 *wt*, *Npc1^{nmf164}* and *Npc1^{nmf164}* CD-treated mice that had received a single BrdU injection 20 h before and processed as previously described (Nusca et al., 2014). Briefly, epitopes were unmasked by heating sections 2 × 5 min in 10 mM sodium citrate, pH 6.0, in a microwave oven and tissue permeabilization was achieved by incubation in trypsin solution (0.05% trypsin, 0.1% CaCl₂ in water) for 15 min at room temperature (RT) and then in 2 M HCl for 30 min. Histological sections were then incubated overnight at 4 °C with a monoclonal anti-BrdU antibody in PBS supplemented with 0.5% Tween 20, and then for 45 min with an anti-mouse IgG antibody (Alexa Fluor-555 Invitrogen, Milan, Italy; 1:1500 final dilution). After counterstaining with 0.5 $\mu\text{g}/\text{mL}$ Hoechst (Hoechst-33258, Invitrogen, Milan, Italy) for 4 min, sections were mounted with Prolong Gold Antifade Reagent and analyzed with an epifluorescence Zeiss microscope.

For quantification of BrdU-immunopositive cells, regions of interest were randomly selected from bases and crowns of the anterior (I-V) and posterior (VI-X) lobules of 4 cerebella for each developmental stage. The total number of cells was determining in 100 μm^2 regions

based on Hoechst staining (4 mice/genotype; 3–4 sections/mouse) as described for parvalbumin immunostaining.

3.2.7. Histological analyses

The overall cerebellar size was determined by using rehydrated paraffin sections of PN15 *wt*, *Npc1^{nmf164}* and *Npc1^{nmf164}* CD-treated mice. Sections were incubated with hematoxylin (Sigma-Aldrich, Milan, Italy) for 15 min and then washed in running hot water for 15 min. After a brief washing in dH₂O, sections were immersed in 95% ethanol for 30 s and then incubated with eosin Y (0.3% in ethanol 80%; Sigma-Aldrich) for 15 sec. Sections were dehydrated and mounted with Eukitt mounting medium (Electron Microscopy Sciences, Hatfield, PA, USA). Images were obtained using a Zeiss Axioplan microscope equipped with a Sony nex-3 N mirror-less camera (Sony Europe Limited, Milano, Italy).

The area of total cerebellum volume, was independently measured by two investigators on three consecutive mid-sagittal sections of at least five mice per group, using ImageJ NIH software version 1.47v (National Institutes of Health, Bethesda, MD). Images to be compared were carefully selected paying attention that they were the closest possible to the parasagittal position, as inferred by the deeper white matter tracts matching very well in each image. The region of interest (ROI) in each section was outlined using the “selection brush” or the “polygon tool”, obtaining similar results.

The number of BG, PC and Basket/Stellate interneurons was determined as previously described for parvalbumin immunostaining.

To determine the number of GNs, rehydrated paraffin sections of PN15 *wt*, *Npc1^{nmf164}* and *Npc1^{nmf164}* CD-treated mice were stained with 0.5 µg/mL Hoechst (Hoechst-33258, Invitrogen, Milan, Italy) for 4 min.

Sections were mounted with Prolong Gold Antifade Reagent and analyzed with an epifluorescence Zeiss microscope. The total number of cells was determined in 100 µm² regions (4 mice/genotype; 3–4 sections/mouse).

3.2.8. Behavioral assessment

Preweaning and adult behavioral performances were analyzed on the same cohorts of 10 *Npc1^{nmf164}* and 10 *wt* littermates, obtained from 5 litters made of at least 7 pups. Because a preliminary evaluation ruled out any gender effect on preweaning and adult behavioral performances, male and female mice were grouped together for analyses.

The effect of CD administration on behavioral performances of preweaning pups was assessed on a cohort of 10 *Npc1^{nmf164}* and 10 *wt* littermates (5 pups either PBS- or CD-injected/genotype), obtained from 5 litters made of at least 7 pups.

Preweaning behavior assessment

From postnatal day (PN) 3 to PN21, pups were separated from their dams daily between 9:00 a.m. and 3:00 p.m. for a maximum of 15 min, and tested for physical, postural, locomotor and complex motor behavior development in a warmed environment (30–32 °C) (Petrosini et al., 1990; Caporali et al., 2014). Behavioral assessment evaluated the development of physical parameters (body weight, eye opening, fur appearance, incisor eruption), locomotion (pivoting, crawling, quadrupedal locomotion), swimming performance (direction and limb use), reflex appearance (surface righting reflex, negative geotaxis, cliff avoidance) and complex motor behaviors (ascending a ladder, crossing a narrow bridge, suspension on a wire). Besides direct behavioral observations, videos were also recorded throughout the entire test cycle. To avoid the possibility of order effect(s), the test sequence was administered to each pup in random order for each test. The attribution of the dominant behavior to a specific category in each observation period was made blindly with regard to pup's genotype. Categorization was considered reliable only when judgments were consistent (inter-rater reliability > 0.9). The test batteries used for the assessment of physical and sensorimotor development were as follows:

(a) Physical development. The body weight was measured daily in the interval PN3-PN21 and eye opening, fur appearance and incisor eruption were evaluated by visual inspection.

(b) Development of quadrupedal locomotion. Fluent forward movements with all limbs supporting the whole body and the pelvis elevated were analyzed from PN3 to PN15 by using Ethovision XT software (Noldus, The Netherlands). The pup was placed on a board and video-recorded for 120 s to analyze the following locomotion categories: (i) *pivoting*, turning movements by broad swipes with forepaws, using only one hindlimb as a pivot and

having the pelvis anchored to the ground; (ii) *crawling*, dragging the body forward or pushing it backward by undulating movements of the trunk and often dragging the hindlimbs in an extended position with foot soles facing upward; (iii) *quadrupedal locomotion*, smooth and coordinated walking, in which the body is supported in sequence by different numbers of feet in combination, suitable for variegated velocities and without any directional bias. The developmental acquisition of the various locomotion categories was determined as dominant behavior according to the rating scale of **Table 2**.

SCORE	Quadrupedal locomotion	Swimming performance	
		direction	limb use
0	----	sinking	absent
1	pivoting	floating	only forelimbs
2	crawling	in circles	four limbs
3 ^a	quadrupedal locomotion	in a straight line	only hindlimbs

↓
 Maturation

Table 2. Rating scale of the development of quadrupedal locomotion and swimming performance.

(c) Development of swimming performance. The pup was gently released in a glass tank (cm 100 × 50 × 20) filled with warmed (35 °C) water and allowed to swim freely. The parameters swimming direction and limb use were evaluated and scored according to the rating scale of **Table 2**.

(d) Reflex appearance. (i) *Surface righting reflex*: the pup was placed gently on its back and the time to turn over on the belly was recorded (allotted time 30 s). (ii) *Negative geotaxis*: the pup was placed on an inclined (30°) plane with the head pointing downwards and the time to face up to the slope was recorded (allotted time 60 s). (iii) *Cliff avoidance*: the pup was placed on an edge with forepaws and nose just over the edge and the time to retract itself by backward and/or sideward movements was recorded (allotted time 60 s).

(e) Development of complex motor behaviors. Because the acquisition of complex motor abilities requires the complete maturation of basic reflexes such as the grasping response, which normally appears by the end of the first postnatal week (Heyser, 2004) the development of complex motor behaviors was scored from PN10 on:

(i) *Ascending a ladder*: the pup was placed on a steel ladder (cm 15 × 25, 20 rungs, 1 cm apart, inclination angle 25°) with top leaning against a platform holding littermates. The ability to ascend the ladder within 120 s was evaluated and the day of the first successful performance was recorded;

(ii) *Crossing a narrow bridge*: the pup was placed on the start platform connected by a plywood bridge (40 × 1 × 3 cm) to the goal platform holding littermates. The ability to traverse the bridge within 120 s was evaluated and the day of the first successful crossing was recorded;

(iii) *Suspension on a wire*: the pup was suspended by its forepaws on a wire (2 mm diameter and 50 cm long) extended horizontally between two poles (30 cm high). The suspension time and the first suspension with the 4 limbs (hind limb suspension) were recorded (allotted time 60 s).

Adult behaviour assessment

PN30, PN60 and PN90 *Npc1^{nmf164}* and *wt* littermates were subjected to two daily sessions (morning and afternoon) of the following consecutively administered tests assessing motor behavior (Võikar, 2002):

(i). *Vertical screen*: the mouse was placed on a horizontal wire screen (cm 15x25, wire diameter 2 mm, spaced at 1 cm). The screen was rapidly turned to vertical position with the mouse facing the floor at the lower edge. The latency to turn upward and to climb to the upper edge was measured during 60 s. This test was performed as the first one of the morning session and was not repeated in the afternoon of that day;

(ii). *Balance beam*: the mouse was placed perpendicularly at the center of a horizontal round beam (covered with paper tape, outer diameter 2 cm, length 1 m, divided into 10 sections and placed 50 cm above a padded surface). The retention time and the number of beam sections crossed during 180 s were recorded and the results of morning and afternoon trials were averaged;

(iii). *Coat hanger*: the mouse was suspended in the middle of the horizontal bar of a coat hanger (diameter 3 mm, length 35 cm, placed 30 cm above a padded surface) with its forepaws. The body position of the animal was observed for 60 s and scored as follows: 0, a fall within 10 s; 1, grasping the hanger with one limb; 2, grasping the hanger with two limbs; 3, grasping the hanger with three limbs; 4, grasping the hanger with four limbs; 5, actively escaping to the end of the bar. The values of morning and afternoon trials were averaged.

These tests were selected because they were similar to those we had exploited in behavioral analyses of preweaning pups in terms of functions evaluated and experimental setting.

3.3. Statistical analyses

Statistical analyses were performed with STATISTICA 8 (StatSoft) software. Data were first tested for normality (Wilk-Shapiro's test) and homoscedasticity (Levene's test), and then analyzed by unpaired two-tailed Student's t test or two-way ANOVAs for independent (genotype, treatment) and repeated (age) measures, followed by Bonferroni's post-hoc test. When data did not fully meet parametric assumptions, or were ordinal (locomotion and swimming measures), comparisons between groups were performed by Mann-Whitney's U test.

To control for alpha inflation, i.e. the proportion of type I errors among all rejected null hypotheses, the False Discovery Rate (FDR) was set to 0.05 and estimated through a bootstrap procedure (Storey, 2004). Differences were considered to be significant at the $p \leq 0.01$ level.

3.4. Results

3.4.1. The overall cerebellar size is reduced in *Npc1^{nmf164}* and is rescued by CD treatment

The size of the adult cerebellum mainly depends on granule neuron (GN) proliferation in the external granule layer (EGL) (Solecki et al., 2001).

In the mouse, GN proliferation lasts from embryonal day E18.5 up to PN16.5 and is regulated by the release of Sonic hedgehog (Shh) by Purkinje cells (PCs), which thereby determines both final cerebellar size and shape (Vaillant and Monard, 2009; Wallace, 1999; Wechsler-Reya and Scott, 1999).

Because of the covalent attachment of a cholesterol moiety to the C-terminus of the proteolytically-generated active Shh fragment (Repetto et al., 1990; Lanoue et al., 1997; Dehart et al., 1997), we hypothesized that impaired cholesterol availability associated to *Npc1*-deficiency might influence GN proliferation.

To address this issue, we measured the total cerebellar area of hematoxylin/eosin Y stained parasagittal sections of PN15 *wt*, *Npc1^{nmf164}* and *Npc1^{nmf164}* CD-treated mice.

This analysis showed that, similarly to *Npc1^{-/-}* mice (Nusca et al., 2014), also *Npc1^{nmf164}* mice display a 25-30% reduction in cerebellar size in comparison to *wild-type (wt)* age-matched mice.

Two consecutive subcutaneous injections of 2-hydroxypropyl- β -cyclodextrin (CD) to PN4 and PN7, largely rescues this phenotype (**Figure 1**).

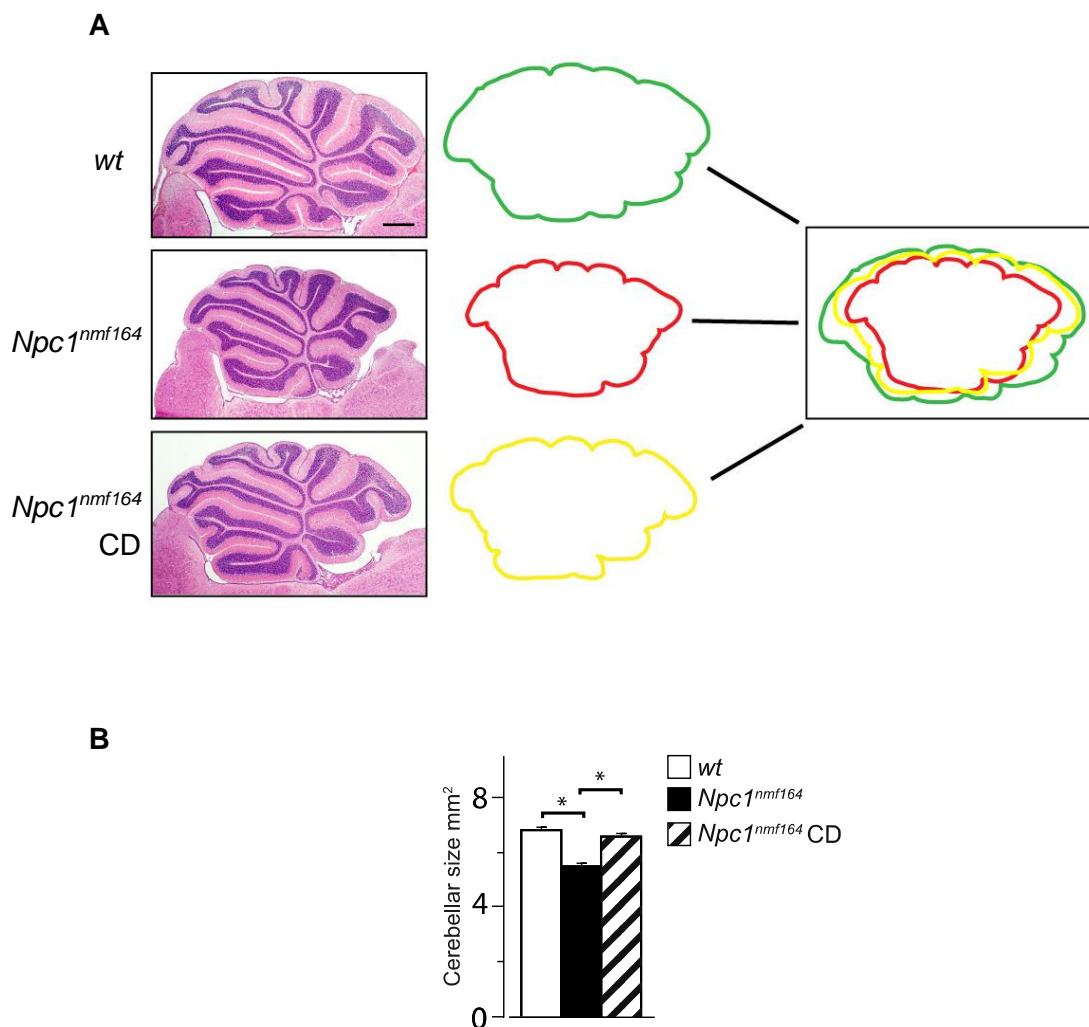


Figure 1. Cerebellum of PN15 *Npc1^{nmf164}* mice is reduced in size. (A) Hematoxylin/eosin Y stain of sagittal sections of cerebellar vermis of PN15 *wt*, *Npc1^{nmf164}* and *Npc1^{nmf164}* CD-treated mice. Representative sections encompassing sagittal midline of vermis are shown in the figure. Superimposition of total vermis tracings indicates an overall size reduction in *Npc1^{nmf164}* compared to *wt* mice that was largely rescued by CD treatment. Scale bars indicate 500 μ m. (B) Histograms indicate total areas (mean \pm SEM; 3 mice/group) measured on representative sections of *Npc1^{nmf164}* (empty bar), *Npc1^{nmf164}* (full bar) and *Npc1^{nmf164}* CD-treated mice (dashed bar). Asterisk indicates statistically significant differences (unpaired two-tailed Student's t test, * $p < 0.05$).

3.4.2. *Npc1^{nmf164}* mice display a reduced density of GNs in the external granule layer (EGL)

Since the time of birth, some GN precursors exit the cell cycle and begin to differentiate into mature GNs (Altman and Bayer, 1996).

Then, post-mitotic GNs migrate along Bergmann glia (BG) fibers and cross both molecular layer (ML) and Purkinje cell layer (PCL) to form the Internal granule layer (IGL) (Buffo and Rossi, 2013). This leads to the gradual thinning and disappearance of the EGL by the third post-natal week (Altman and Bayer, 1996).

We determined the EGL thickness in parasagittal sections obtained from cerebella of PN15 *wt*, *Npc1^{nmf164}* and *Npc1^{nmf164}* CD-treated mice. The EGL was visualized by staining GN nuclei with Hoechst-33258, while GN density was determined by counting cell nuclei in randomly selected regions of 100 μm^2 each. This analysis showed that the EGL thickness and GN densities of *Npc1^{nmf164}* mice were significantly reduced compared to *wt* mice. Indeed, only few scattered GNs, not even forming a single row of cells, were observed in both crowns than fissures of anterior and posterior lobules of *Npc1^{nmf164}* mice.

Two consecutive subcutaneous injections of CD performed at PN4 and PN7 doubled the number of GNs in the EGL of PN15 *Npc1^{nmf164}* mice, leading to a neuronal population even greater than that of *wt* mice (**Figure 2A,B**).

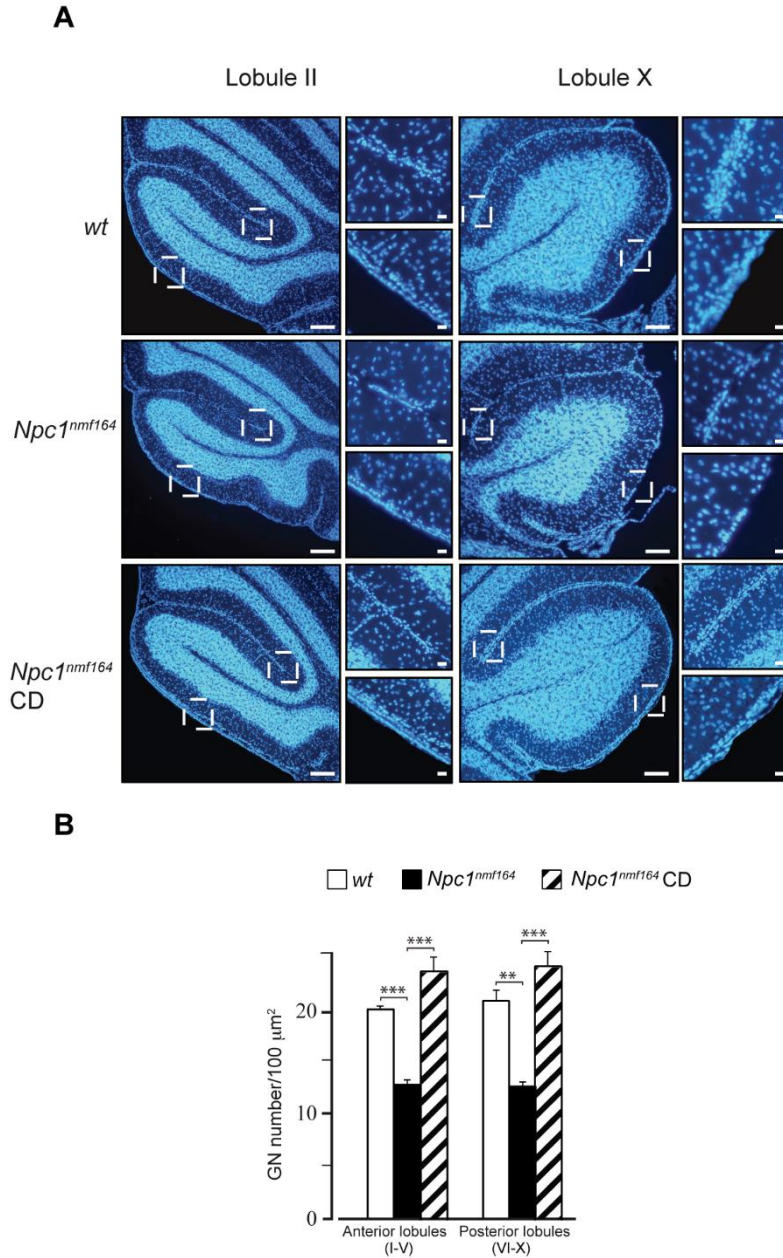


Figure 2. *Npc1^{nmf164}* mice display a reduced granule cells density in the outer cerebellar cortex layer at PN15, a phenotype widely rescued by the CD treatment. (A) A representative Hoechst-33258 stained sections of *wt*, *Npc1^{nmf164}* and *Npc1^{nmf164}* CD-treated mice are shown in figure. Higher magnification fields of EGL base or crown of lobules II and X on the right of low magnification fields show that the EGL of PN15 *Npc1^{nmf164}* mice is thinner than that of age-matched *wt* mice. CD treatment makes the EGL of *Npc1^{nmf164}* mice comparable with that of wild type mice. Scale bar indicate 250 μm (panels) and 50 μm (insets). **(B)** Histogram represent GN densities (mean \pm SEM of all sections examined; N = 4 mice/genotype; 3–4 sections/mouse) determined in 100 μm^2 regions of the crowns of *wt*, *Npc1^{nmf164}* and *Npc1^{nmf164}* CD-treated mice anterior (I-V) and posterior

(VI-X) lobules. Graphs show that CD treatment rescues the number of granule cells that can still be found in EGL of *Npc1^{nmf164}* mice at PN15. Asterisks indicate statistically significant differences (unpaired two-tailed Student's t test, ** p < 0.001; *** p < 0.0001).

3.4.3. The reduced density of GNs in the EGL is due to defective proliferation of precursors

The finding that *Npc1^{nmf164}* mice display a shorter lasting EGL compared to age matched *wt* suggested that the clock driving symmetric division of GN precursors could be dysregulated, leading these cells to prematurely exit from cell cycle.

This possibility was investigated by determining the number of cells incorporating BrdU 20 hours after a single BrdU injection of PN13 or PN15 *wt*, *Npc1^{nmf164}* and *Npc1^{nmf164}* CD-treated mice. This analysis showed that the number of BrdU-positive cells in both crowns and fissures of anterior cerebellar lobules was significantly reduced in *Npc1^{nmf164}*.

In posterior cerebellar lobules a reduction of BrdU-positive cells was only observed in fissures of PN15 *Npc1^{nmf164}* mice.

CD treatment led *Npc1^{nmf164}* mice to display a number of BrdU-positive cells similar to that of *wt* mice (**Figure 3A,B**).

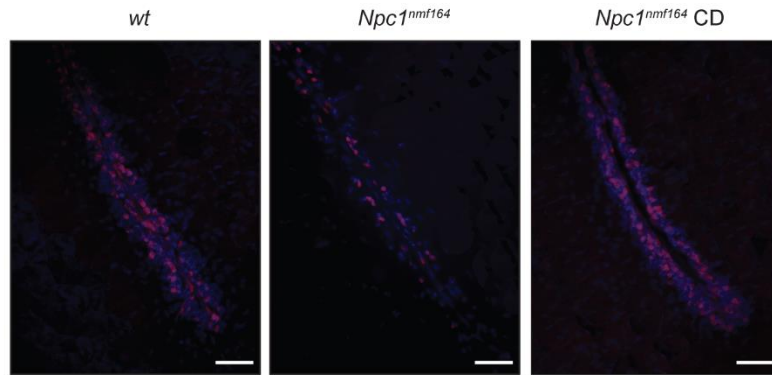
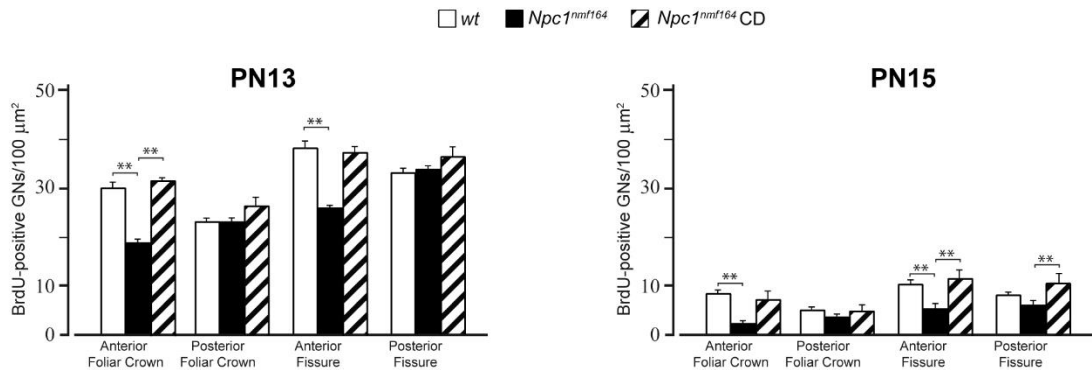
A**B**

Figure 3. *Npc1^{nmf164}* mice display reduced number of proliferating granule neurons that is rescued by CD treatment. (A) A representative field showing BrdU-positive cells (red) of fissure between lobules II and III of PN13 *wt*, *Npc1^{nmf164}* and *Npc1^{nmf164}* CD-treated mice. Scale bar indicates 50 μm. (B) Histograms represent the number of BrdU-positive cells (mean ± SEM; 4 mice/genotype; 3–4 sections/mouse) determined in 100 μm² regions corresponding to the bases and crowns of PN13 and PN15 *wt*, *Npc1^{nmf164}* and *Npc1^{nmf164}* CD-treated mice anterior (I–V) and posterior (VI–X) lobules. The number of BrdU immunopositive granule neurons is significantly reduced in cerebellum of *Npc1^{nmf164}* mice compared with age-matched *wt* mice, a phenomenon more pronounced in the anterior than in posterior folia. Graphs show that in the CD-treated *Npc1^{nmf164}* mice the number of proliferating granule neurons is comparable to the number present in wild type. Asterisks indicate statistically significant differences (unpaired two-tailed Student's t test, ** $p < 0.001$; *** $p < 0.0001$).

3.4.4. GN precursor proliferation defect results in a disorganized cellular architecture of the EGL

Since early postnatal development, the EGL splits into two layers, an outer layer (oEGL) containing mitotically-active p27Kip1-negative GNs progenitors and an inner layer (iEGL) containing p27Kip1-positive post-mitotic GNs that are differentiating and migrating toward their final destination in the IGL (Altman, 1972; Miyazawa et al., 2000).

To gain insights on GNs development in the EGL of *Npc1^{nmf164}* mice, we performed an immunohistochemistry analysis for p27Kip1 detection on cerebella slices of *wt*, *Npc1^{nmf164}* and *Npc1^{nmf164}* CD-treated mice at PN11. This analysis revealed that the stereotyped and ordered EGL architecture in the inner and outer sub-regions markedly differed between *wt* and *Npc1^{nmf164}* mice (**Figure 4**). Indeed, p27Kip1-immunopositive cells were scattered along the entire EGL and apparently represented the largest fraction of *Npc1^{nmf164}* mouse GNs, indicating that at PN11, the niche of mitotically active, p27Kip1-negative GNs (identifying the oEGL) is strongly reduced or even lost in *Npc1^{nmf164}* mice. CD treatment re-established the sharp boundary between the outer and inner EGLs (**Figure 4**).

A scheme representing the feature of GN proliferation in *wt*, *Npc1^{nmf164}* and *Npc1^{nmf164}* CD-treated mouse EGLs, based on the findings so far described, is shown in **Figure 5**.

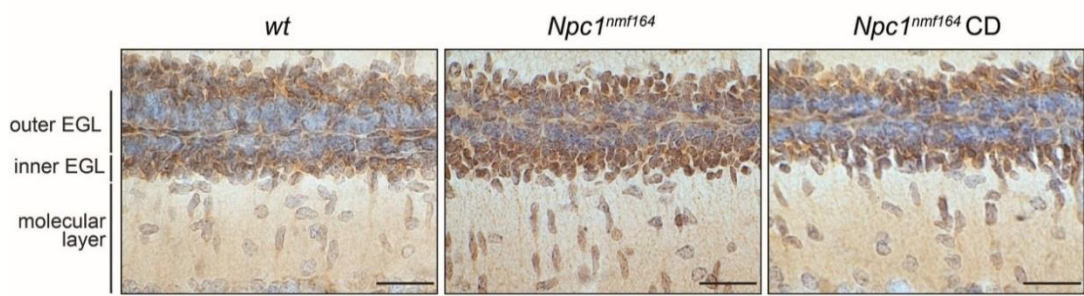


Figure 4. Cerebellar granule neurons of *Npc1^{nmf164}* mice exit the cell cycle earlier than those of *wt* mice. Cerebellar sections of PN11 *wt*, *Npc1^{nmf164}* and *Npc1^{nmf164}* CD-treated mice (3–4 mice/group; 3–4 sections/mouse) were immunostained with anti-p27Kip1 antibodies (brown). Nuclei were stained with methyl green. A representative field of fissure between lobules II and III is shown. Note the presence of scattered p27Kip1-positive GNs along the entire EGL of *Npc1^{nmf164}*. The CD treatment fully reestablished the p27Kip1 expression pattern in *Npc1^{nmf164}* mice. Scale bars indicate 50 μ m.

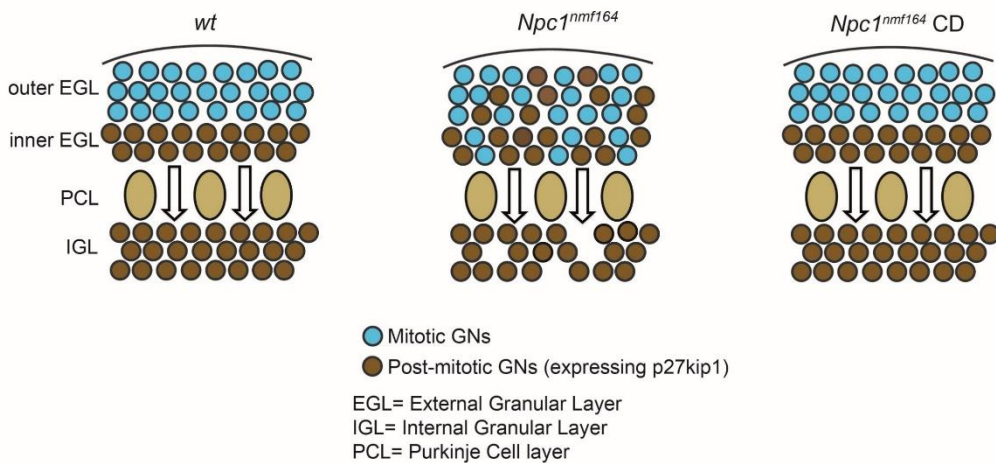


Figure 5. A model of defective GN proliferation in the *Npc1^{nmf164}* mice.

3.4.5. *Npc1^{nmf164}* mice display abnormal Bergmann glia morphogenesis and early astrocyte activation that are not rescued by the CD treatment

During the first weeks of postnatal development, BG radial shafts span the entire ML, providing the scaffold for GN migration (Gregory et al., 2004) and directing the distal growth of the PC dendritic tree (Lordkipanidze et al., 2005).

Further BG development favors PC dendritic arborization and synapse formation, leading to the complex reticular meshwork of the adult cerebellar cortex (Yamada and Watanabe, 2002).

In normal conditions, astrocyte play a key role in the formation, maintenance, function and pruning of synapses, as well as in regulating neurotransmitter uptake and maintaining the blood–brain barrier (Molofsky et al., 2012; Pekny et al., 2014).

CNS injury or neurodegeneration results in astrocyte activation, or reactive gliosis, in which both astrocyte cell body and processes become hypertrophic and modify their gene expression pattern, upregulating the intermediate filament Glial Fibrillary Acidic Protein (GFAP) (Sofroniew, 2009).

It has been shown that in *Npc1^{-/-}* mice there is an increase of activated astrocyte number starting from 7-8 week of age (German et al., 2002). Maue and coll. (2012) found a similar phenotype also in *Npc1^{nmf164}* but this analysis was performed only at the terminal stages of the disease (PN120) and not during cerebellar development (Maue et al., 2012).

To determine whether *Npc1*-deficiency affected BG morphology and caused the activation of astrocytes at early developmental stages, we assessed the expression and pattern of GFAP, by immunohistochemistry and Western blot analysis. While no significant difference was found between *Npc1^{nmf164}* and *wt* mice at PN11 (**Figure 6C**), BG of PN15 *Npc1^{nmf164}* mice had radial shafts, which were enlarged and irregular in caliber and displayed hypertrophic astrocytes in the IGL (**Figure 6A**). The overall increase in size of BG and astrocytes of *Npc1^{nmf164}* mice was accompanied by an abnormal increase in GFAP expression, as quantified by Western blot analysis (**Figure 6B**).

It is worth noting the presence of two GFAP protein bands having an apparent MW of 50 and 48 kDa, respectively, both more abundant in *Npc1^{nmf164}* mice compared to *wt* littermates (main effect of genotype: 48 kDa, $t_6 = 4.34$, $p = 0.005$; 50 kDa, $t_6 = 3.44$, $p = 0.01$).

The 48 kDa protein band is generated by calpain I proteolytic cleavage (Lee et al., 2000) and increases during neurodegenerative processes (Fujita et al., 1998).

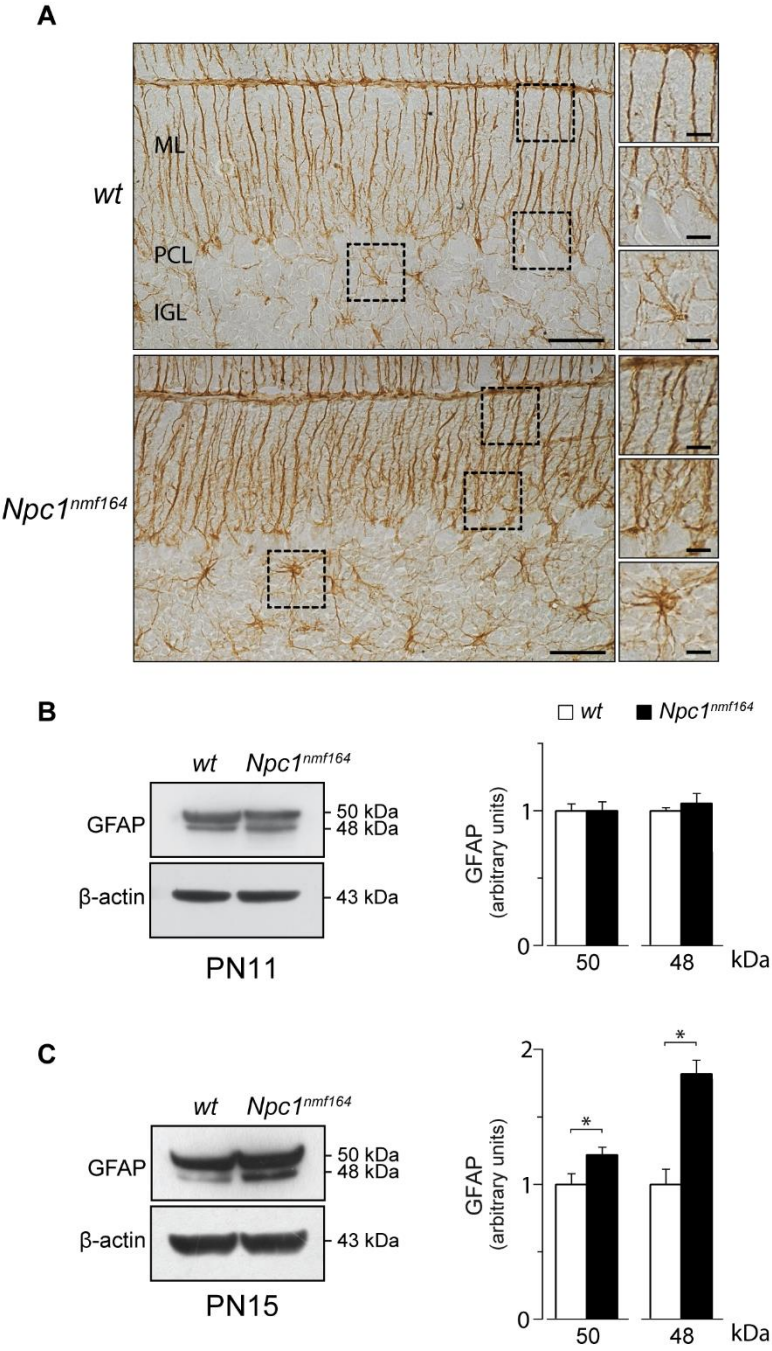


Figure 6. *Npc1^{nmf164}* mice display an abnormal Bergmann glia morphogenesis and an early astrocytes activation. (A) Immunostaining with antibodies directed to GFAP (brown) shows that BG of PN15 *Npc1^{nmf164}* mice have radial shafts that are enlarged and irregular in caliber, as well as hypertrophic astrocytes within the IGL, compared to *wt* littermates. Representative fields of parasagittal sections of *wt* and *Npc1^{nmf164}* mouse cerebella are shown in the Figure; scale bars: 50 μ m. Higher magnification fields are shown on the right; scale bars: 25 μ m. ML: Molecular Layer; PCL: Purkinje Cell Layer; IGL: Internal Granular Layer. Western blot analysis of GFAP protein expression in cerebella of PN11 (B) and PN15 (C) *wt* and *Npc1^{nmf164}* mice. Histograms indicate the abundance (mean \pm SEM) of each GFAP isoforms determined by densitometry of protein bands obtained in at least 3 independent experiments taking β -actin as internal reference. * $p \leq 0.01$

To evaluate the efficacy of CD treatment in rescuing this phenotype, we assessed the expression pattern of GFAP in PN15 *wt* and *Npc1^{nmf164}*, either sham- or CD-treated mouse cerebella by immunohistochemistry and Western blot analysis. This analysis showed that CD treatment didn't rescue defective BG morphology and astrocyte activation of *Npc1^{nmf164}* mice, as CD-treated *wt* mice display enlarged radial shaft and hypertrophic astrocytes similar to those of *Npc1^{nmf164}* (results of statistical analyses are shown in **Table 4**) (**Figure 7**).

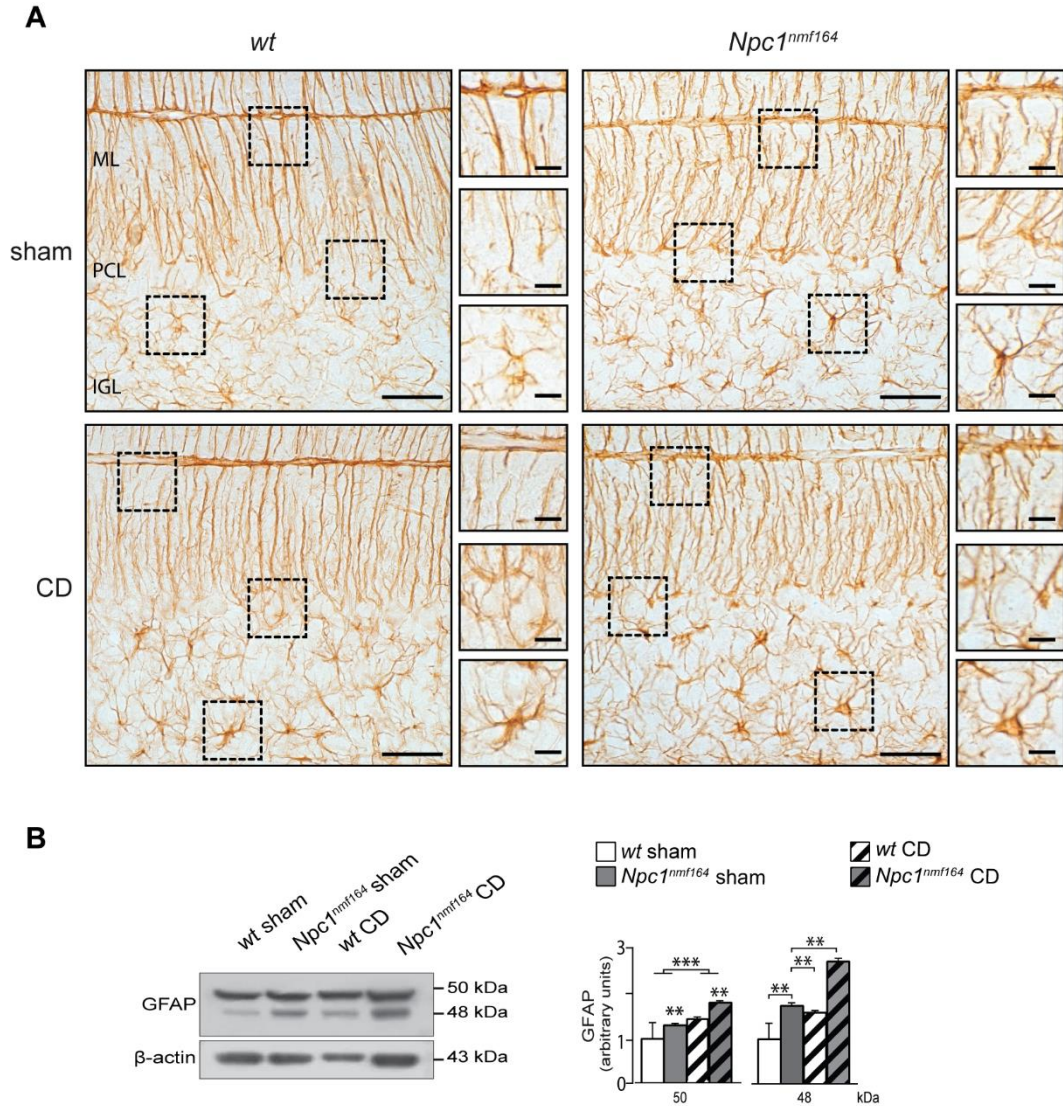


Figure 7. CD treatment does not rescue defective BG morphology and astrocyte activation. (A) Immunostaining with antibodies directed to GFAP (brown) of PN15 *wt* and *Npc1^{nmf164}*, either sham- or CD-treated mouse cerebella. Note that CD-treated *wt* mice display enlarged radial shaft and hypertrophic astrocytes similar to those of *Npc1^{nmf164}*. Representative fields of parasagittal sections are shown; scale bar indicate 50 μ m. Higher magnification fields are shown on the right; scale bars: 25 μ m. ML: Molecular Layer; PCL: Purkinje Cell Layer; IGL: Internal Granular Layer. (B) Western blot analysis of GFAP protein expression in cerebella of PN15 *wt* and *Npc1^{nmf164}* mice, either sham- or CD-treated. Histograms indicate the abundance (mean \pm SEM) of each protein determined by densitometry of protein bands of at least 3 independent experiments taking β -actin as internal reference. * $p \leq 0.01$, ** $p < 0.001$, *** $p < 0.0001$

3.4.6. Bergmann glia functions are defective in *Npc1^{nmf164}* mice

BG is normally provided with a large amount of **GLutamate ASpartate Transporter (GLAST)**, which is particularly abundant in the cell body and perisynaptic membranes, here preventing glutamate spillover between adjacent PCs (Takayasu et al., 2009).

We determined GLAST expression by immunostaining and Western blot analyses at PN11 and PN15. Although no difference were found at PN11, we observed a significant GLAST reduction in *Npc1^{nmf164}* compared to *wt* littermates at PN15 (main effect of genotype: $t_6 = 4.27$, $p = 0.005$) (**Figure 8A,C**).

Such GLAST reduction was particularly evident around PC soma, which are normally enwrapped by lamellar processes arising from BG cell bodies (Palay and Chan-Palay, 1974; Caviness et al., 1995; Yamada and Watanabe, 2002) and in the distal BG radial shaft close to the pial surface.

Because after the uptake into BG, glutamate is converted by the enzyme **Glutamine synthetase** into glutamine and recycled back to synapses for reconversion into active transmitter (Sofroniew and Vinters, 2010), we also determined Glutamine synthetase expression by immunostaining and Western blot analyses at PN11 and PN15.

Consistently with our findings with GLAST expression, we found a significant Glutamine synthetase reduction in *Npc1^{nmf164}* compared to *wt* littermates at PN15 (main effect of genotype: $t_6 = 4.79$, $p = 0.003$) but not at PN11 (**Figure 8B,D**).

The decrease in Glutamine synthetase was stronger at the level of BG soma and milder along BG radial shafts.

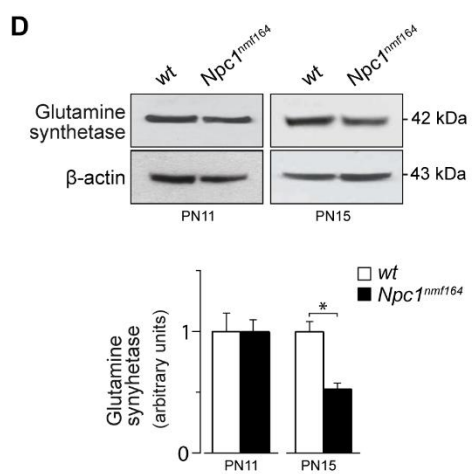
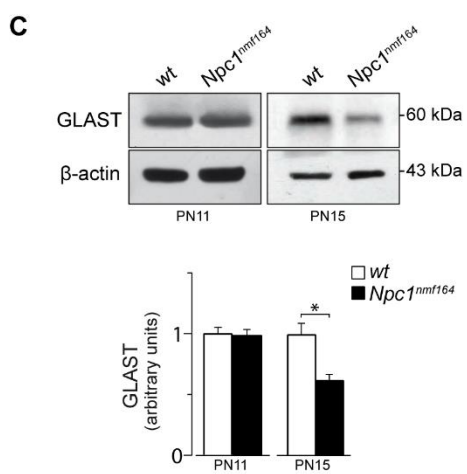
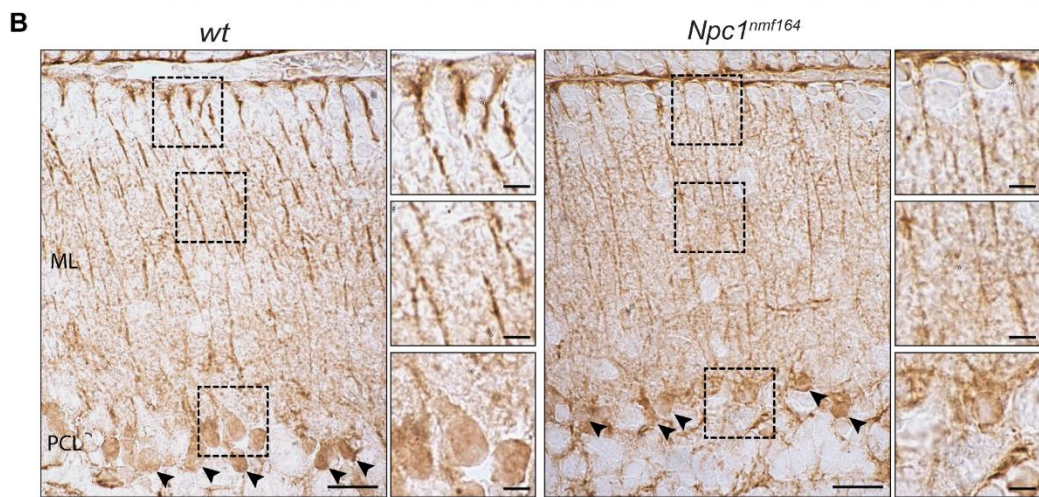
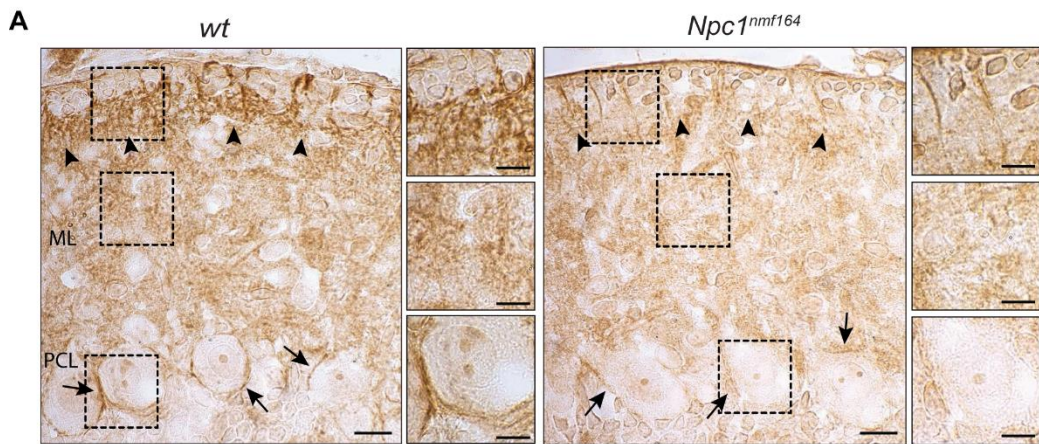


Figure 8. Bergmann glia function appears to be defective in *Npc1^{nmf164}* mice. (A) Immunostaining with antibodies directed to GLAST (brown) shows that PN15 *Npc1^{nmf164}* mice display a reduced expression of GLAST at the level of BG processes in the outer part of molecular layer (arrowheads) and around Purkinje cell soma (arrows) compared to *wt* littermates. Representative fields of parasagittal sections of *wt* and *Npc1^{nmf164}* mouse cerebella are shown in the Figure 36a; scale bars: 10 μ m. Higher magnification fields are shown on the right; scale bars: 5 μ m. **(B)** Immunostaining with antibodies directed to Glutamine synthetase (brown) shows that PN15 *Npc1^{nmf164}* mice display a reduced expression of Glutamine synthetase at the level of BG soma (arrowheads) and processes compared to *wt* littermates. Representative fields of parasagittal sections of *wt* and *Npc1^{nmf164}* mouse cerebella are shown in the Figure 36b; scale bars: 20 μ m. Higher magnification fields are shown on the right; scale bars: 5 μ m. ML: Molecular Layer; PCL: Purkinje Cell Layer. Western blot analyses of GLAST **(C)** and Glutamine synthetase **(D)** protein expression in cerebella of PN11 and PN15 *wt* and *Npc1^{nmf164}* mice. Histograms indicate GLAST **(C)** and Glutamine synthetase **(D)** abundance (mean \pm SEM) determined by densitometry of protein bands obtained in at least 3 independent experiments taking the β -actin as internal reference. * $p < 0.01$

CD treatment only rescued Glutamine synthetase deficiency (results of statistical analyses are shown in **Table 4**) (**Figure 9**).

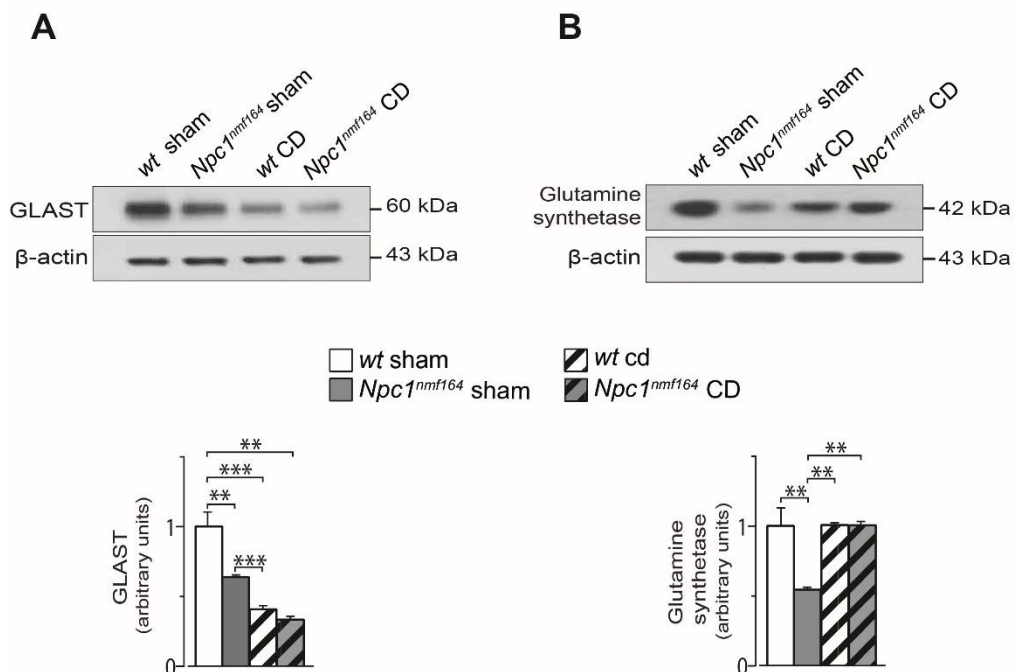


Figure 9. CD treatment partially rescue the defective Bergmann glia function of *Npc1^{nmf164}* mice. Western blot analysis of **(A)** GLAST and **(B)** Glutamine synthetase protein expression in cerebella of PN15 *wt* and *Npc1^{nmf164}* mice, either sham- or CD-treated. Histograms indicate the abundance (mean \pm SEM) of each protein determined by densitometry of protein bands of at least 3 independent experiments taking β -actin as internal reference. * $p \leq 0.01$, ** $p < 0.001$, *** $p < 0.0001$

3.4.7. The cerebellar cortex of PN15 *wt* and *Npc1^{nmf164}* mice displays similar densities of Bergmann glia, Purkinje cells and Basket/Stellate interneurons

The prominent neuropathological sign of NP-C disease is the massive loss of PCs (Higashi et al., 1993; Ong et al., 2001). In *Npc1^{nmf164}* mice PC degeneration and loss begins at PN30 and becomes very pronounced at PN60 leading to cerebellar ataxia (Maue et al., 2012).

It was estimated that in rodent cerebellum there are ~8 BG cells *per* PC and that each PC receives over 100.000 inputs from inhibitory interneurons enwrapped by BG processes (Ito et al., 2008; Reichenbanch et al., 2010). The inhibitory input that PCs receive from Basket/stellate interneurons (BCs/SCs) is essential to provide the appropriate motor output (Wulff et al., 2009).

Therefore, we decided to determine BG, PC and BC/SC densities in *Npc1^{nmf164}*. The number of BG, PCs and BCs/SCs was determined by counting cell nuclei in randomly selected regions of 0.04 mm² each in parasagittal cerebellar sections of PN15 *wt* and *Npc1^{nmf164}* mice stained with Hematoxylin/eosin Y (**Figure 10; right panel**) or processed for immunostaining with anti-parvalbumin antibody (**Figure 10; left panel**) to better identify GABAergic neurons/interneurons.

The number and localization of GABAergic interneurons, PC and BG appeared similar in *Npc1^{nmf164}* and *wt* mice (**see histograms in Figure 10**).

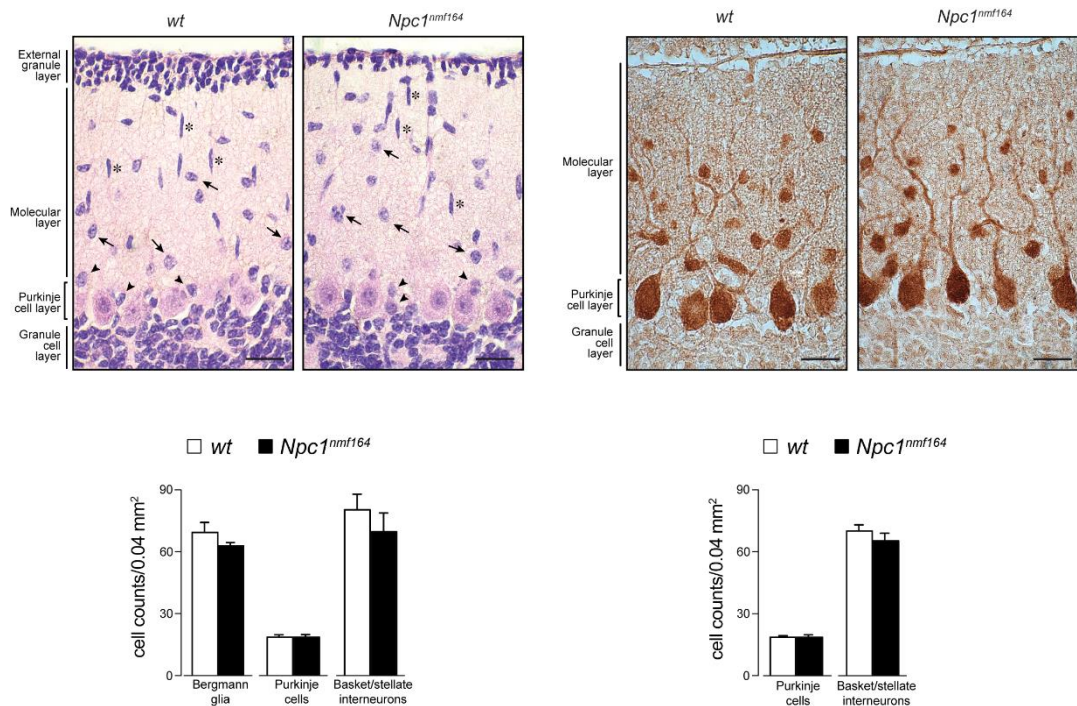


Figure 10. The cerebellar cortex of PN15 *wt* and *Npc1^{nmf164}* mice displays similar densities of Bergmann glia, Purkinje cells and basket/stellate interneurons. Hematoxylin/eosin Y staining (right panel; asterisks: migrating GNs; arrows: basket/stellate interneurons; arrowheads: Bergmann glia) and immunostaining with anti-parvalbumin antibody (left panel); Scale bar: 50 μ m. Histograms represent cell densities (mean \pm SEM of all sections examined; N = 3 mice/genotype; 3–4 sections/mouse) determined in 0.04 mm² regions randomly selected in each microscopic field of anterior (I-V) and posterior (VI-X) lobules of *wt* and *Npc1^{nmf164}* mouse cerebella, stained with Hematoxylin/eosin Y (right) or anti-parvalbumin antibody (left). Since any significant difference was found between counts of anterior and posterior lobules, values were averaged. Comparisons were performed by unpaired two-tailed Student's t test.

3.4.8. Purkinje cells of *Npc1^{nmf164}* mice display a reduced number of glutamatergic and GABAergic inputs which is rescued by the CD treatment

PCs display distinct anatomical and functional compartments, which receive at least two excitatory and two inhibitory inputs on different proximal and distal sub-compartments of cerebellar cortex (Palay and Chan-Palay, 1974) respectively, dividing the molecular layer into outer and inner parts.

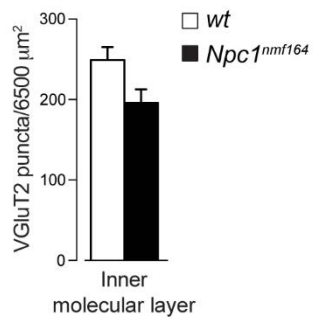
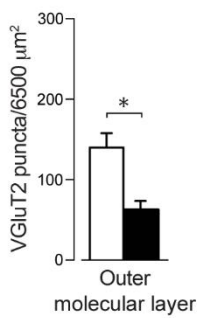
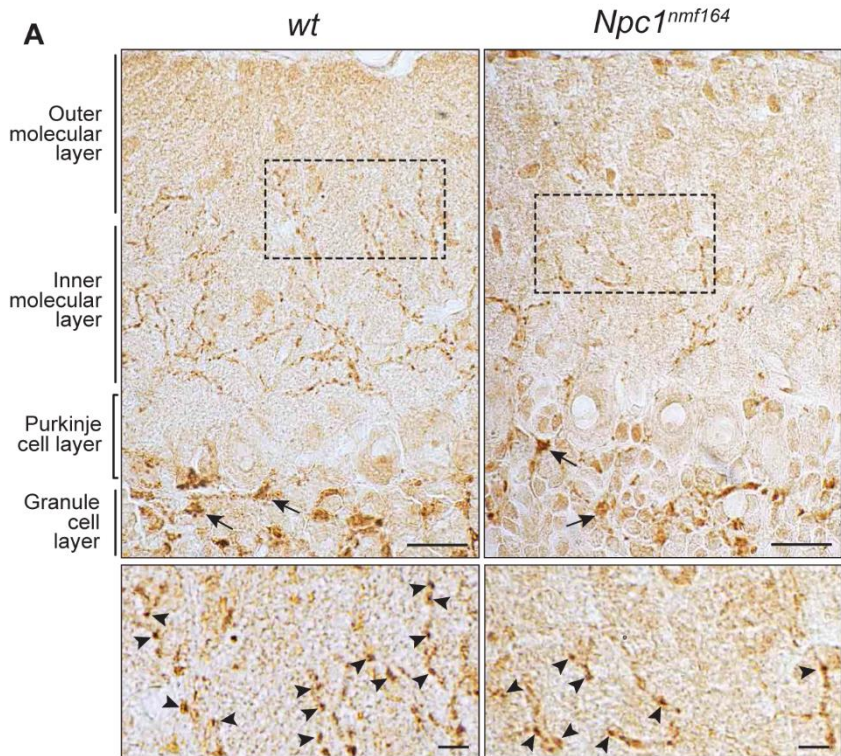
In fact, thin distal PC dendrite branchlets receive glutamatergic inputs from parallel fibers and GABAergic inputs from SCs (Ango et al., 2004), whereas the thick proximal PC dendritic shafts receive synapses mostly from GABAergic BCs and glutamatergic climbing fibers (Ichikawa et al., 2002).

We studied glutamatergic and GABAergic inputs to PCs by immunostaining histological sections of PN15 *Npc1^{nmf164}* and *wt* cerebella with antibodies directed to vesicular glutamate transporter subtype 2 (VGluT2, labeling glutamatergic terminals) and glutamic acid decarboxylase 65 (GAD65, labeling GABAergic terminals).

Compared to *wt* littermates, the ML of *Npc1^{nmf164}* mouse cerebella displayed a reduced number of VGluT2-positive puncta, which was particularly pronounced at the level of outer part of ML (main effect of genotype: $t_6 = 3.87$, $p = 0.008$), whereas differences at the level of inner molecular layer didn't reach statistical significance (main effect of genotype: $t_6 = 2.55$, $p = 0.04$) (**Figure 11A**).

As expected, VGluT2 immunostaining was also detected at the level of glomeruli, where glutamatergic afferent mossy fibers synapse with GN dendrites, with similar expression patterns in *wt* and *Npc1^{nmf164}* mice.

Finally, Western blot analysis revealed a significant reduction of VGluT2 protein levels in the cerebellum of PN15 *Npc1^{nmf164}* mice (main effect of genotype: $t_6 = 4.75$, $p = 0.003$) (**Figure 11B**)



B

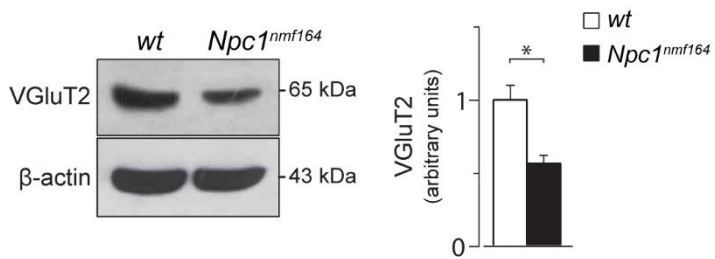


Figure 11. Purkinje cells of *Npc1^{nmf164}* mice display a reduced number of glutamatergic inputs. (A) Immunostaining with antibodies directed to VGluT2 (brown) shows that PN15 *Npc1^{nmf164}* mice display a reduced expression of VGluT2 in the outer part of molecular layer compared to *wt* littermates. Representative fields of parasagittal sections of lobule II of *wt* and *Npc1^{nmf164}* mouse cerebella are shown. Upper panels: arrows indicate VGluT2-positive synapses of internal granule layer glomeruli; scale bars: 20 μ m. Bottom panels: higher magnifications of selected areas. Arrowheads indicate typical VGluT2 positive puncta; scale bars: 5 μ m. Histograms indicate VGluT2-positive puncta densities in the outer and inner molecular layers (mean \pm SEM). (B) Western blot analysis of VGluT2 protein expression in cerebella of PN15 *wt* and *Npc1^{nmf164}* mice. Histograms indicate VGluT2 abundance (mean \pm SEM) determined by densitometry of protein bands obtained in at least 3 independent experiments taking the β -actin as internal reference. * $p < 0.01$

Although the number and localization of GABAergic interneurons along the ML appeared similar in *Npc1^{nmf164}* and *wt* mice (see Figure 10), the analysis of GAD65 expression patterns showed that GABAergic inputs were significantly reduced in *Npc1^{nmf164}* cerebella.

To investigate this issue, we arbitrarily divided the ML into outer and inner and determined the density of GAD65-positive puncta in both upper and lower ML and PCL, observing a significant reduction of puncta in molecular and PC layers of *Npc1^{nmf164}* vs *wt* mice (main effect of genotype: outer ML: $t_6 = 3.64$, $p = 0.01$; lower ML: $t_6 = 3.44$, $p = 0.01$; PCL: $t_6 = 3.58$, $p = 0.01$) (Figure 12A).

Reduced GAD65 expression was also confirmed by Western blot analysis (main effect of genotype: $t_6 = 3.71$, $p = 0.01$) (Figure 40b).

No difference in the expression level of GAD65 were found at PN11 between *wt* and *Npc1^{nmf164}* mice (Figure 12B).

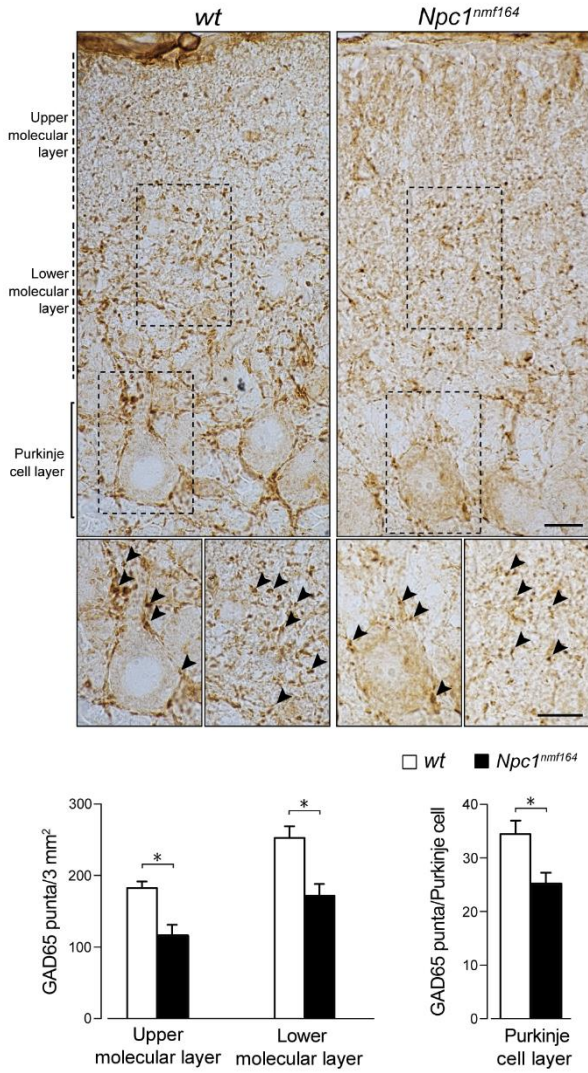
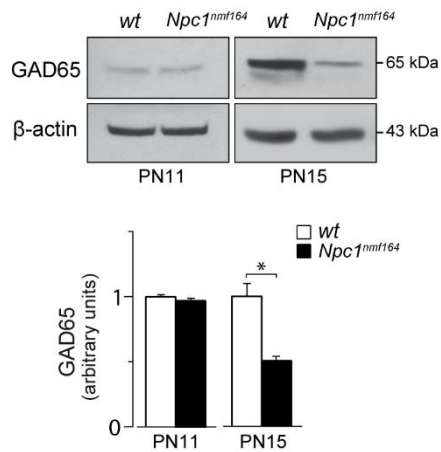
A**B**

Figure 12. Purkinje cells of *Npc1^{nmf164}* mice display a reduced number of GABAergic inputs. (A) Immunostaining with antibodies directed to GAD65 (brown) shows a reduced density of GAD65-positive puncta (arrowheads) around Purkinje cell soma and throughout the entire molecular layer of PN15 *Npc1^{nmf164}* mice compared to *wt* littermates. Representative fields of parasagittal sections of lobule II *wt* and *Npc1^{nmf164}* mice cerebella are shown in the Figure 40a; scale bars: 10 μ m. Higher magnifications are shown in bottom panel insets; Arrowheads indicate typical GAD65-positive puncta; scale bars: 10 μ m. Histograms indicate the density of GAD65-positive puncta in outer and inner molecular layers and Purkinje cell layer. **(B)** Western blot analysis of GAD65 protein expression in cerebella of PN11 and PN15 *wt* and *Npc1^{nmf164}* mice. Histograms indicate GAD65 abundance (mean \pm SEM) determined by densitometry of protein bands obtained in at least 3 independent experiments taking the β -actin as internal reference. * $p = 0.01$

To evaluate the efficacy of CD treatment in rescuing this phenotype, we assessed the expression pattern of GAD65 and VGluT2 in PN15 *wt* and *Npc1^{nmf164}*, either sham- or CD-treated mouse cerebella by Western blot analysis. This analysis showed that CD treatment fully rescue these deficits (**Figure 13A,B**) (results of statistical analyses are shown in **Table 4**). The efficacy of CD in restoring the normal VGluT2 expression pattern were also confirmed by immunohistochemistry. This analysis revealed that *Npc1^{nmf164}* display an abundance and distribution of VgluT2-puncta similar to that of *wt* mice (**Figure 13C,D**).

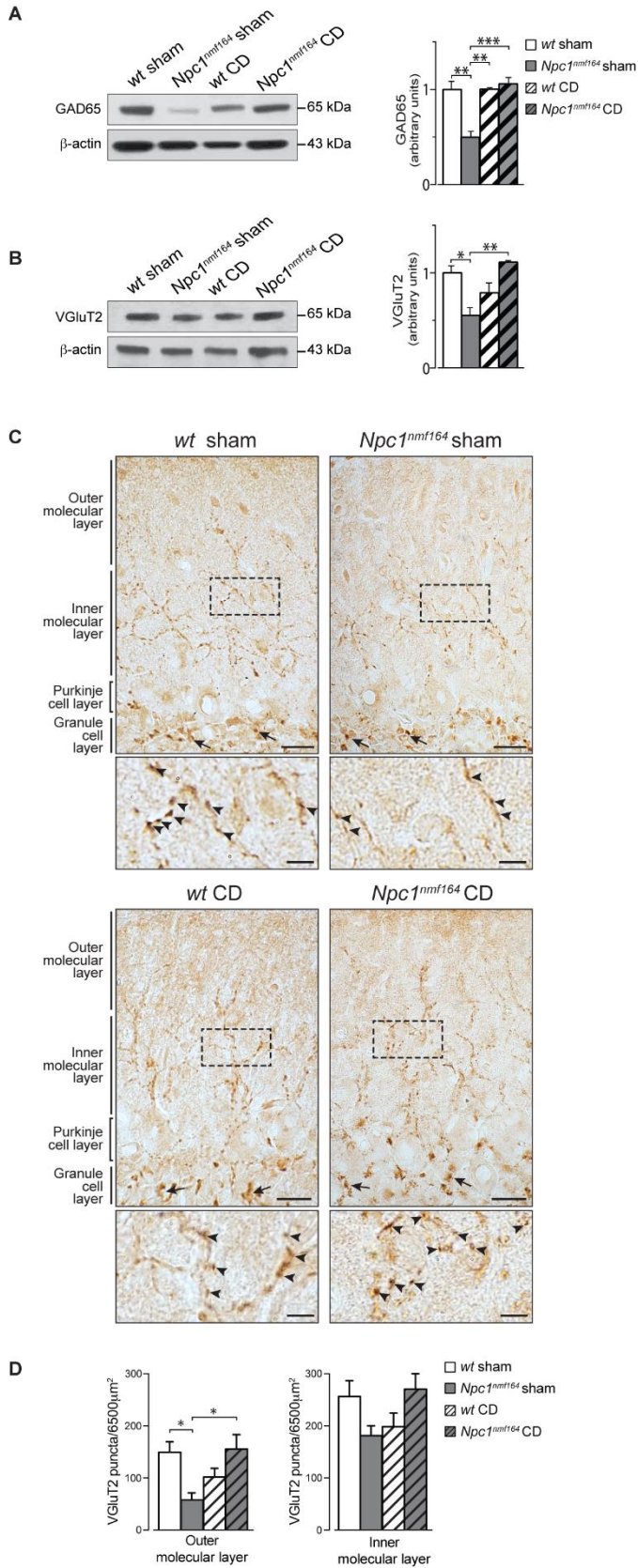


Figure 13. CD treatment fully rescued the reduced number of GABAergic/glutamatergic inputs. Western blot analyses of GAD65 (A) and VGluT2 (B) protein expression in cerebella of PN15 *wt* and *Npc1^{nmf164}* mice either sham- or CD-treated. Histograms indicate the abundance (mean \pm SEM) of each protein determined by densitometry of protein bands of at least 3 independent experiments taking β -actin as internal reference. * $p \leq 0.01$, ** $p < 0.001$, *** $p < 0.0001$ (C) Immunostaining with antibodies directed to VGluT2 (brown) of PN15 *wt* and *Npc1^{nmf164}*, either sham- or CD-treated mouse cerebella. Representative fields of parasagittal sections are shown in the figure. Upper panels, arrows indicate VGluT2-positive synapses of internal granule layer glomeruli; scale bars: 20 μ m. Bottom panels, higher magnifications of selected areas. Arrowheads indicate VGluT2 positive puncta; scale bars: 5 μ m. (D) Histograms indicate VGluT2-positive puncta densities in the outer and inner molecular layers (mean \pm SEM of all sections examined; $N=4$ mice/genotype/treatment; 3–4 sections/mouse) of *wt* and *Npc1^{nmf164}* mice, either sham- or CD-treated. Asterisks indicate statistically significant differences (two-way ANOVA, * $p < 0.01$).

3.4.9. *Npc1^{nmf164}* mice display defective myelin maturation

It was recently shown that the selective ablation of *Npc1* expression in oligodendrocytes results in defective myelin formation in the forebrain and corpus callosum of PN16 mice (Yu and Lieberman, 2013) indicating that these cells need exogenous cholesterol uptake at least during early postnatal life. This finding is in agreement with previous observations showing the expression of low-/very low-density lipoprotein receptors by oligodendrocytes (Zhao et al., 2007) and the dependence on glia-derived cholesterol of *Npc1*-deficient brains (Borbon et al., 2012; Zhang et al., 2008).

Moreover, dysmyelination and myelin loss were previously reported in prefrontal cortex, corpus callosum and hippocampus of *Npc1^{-/-}* mice (Takikita et al., 2004) and found to be associated with defective genetic control of oligodendrocyte differentiation (Yan et al., 2011).

To investigate whether/how *Npc1*-deficiency also affected myelin formation during cerebellum development, we determined the expression of myelin basic protein (MBP), a well-established marker of mature myelin (Baumann et al., 2001) in PN11 and PN15 cerebella of *Npc1^{nmf164}* and *wt* mice.

As shown by Western blot analysis (**Figure 14A**) the level of MBP isoforms was significantly reduced with respect to *wt* at either PN11 (main effect of genotype: 17.2 kDa: $t_6 = 4.21$, $p = 0.006$; 18.5 kDa: $t_6 = 4.38$, $p = 0.005$; 21.5 kDa: $t_6 = 4.03$, $p = 0.007$) and PN15 (main effect of genotype: 17.2 kDa: $t_6 = 4.76$, $p = 0.003$; 18.5 kDa: $t_6 = 3.51$, $p = 0.01$; 21.5 kDa: $t_6 = 21.86$, $p = 0.000001$).

Various MBP isoforms are generated by alternative splicing and exert specific functions in different intracellular compartments. Namely, the 17.2 and 21.5 kDa isoforms are highly expressed in the cell body and nucleus of developing oligodendrocytes, playing a regulatory role in the genetic program of oligodendrocyte differentiation (Pedraza et al., 1997). In contrast, the 18.5 kDa isoform localizes at the plasma membrane and actively participates in membrane compaction typical of mature myelin (Harauz and Boggs, 2013). Immunohistochemistry of PN15 cerebellar sections fully confirmed the impairment of myelin formation in *Npc1^{nmf164}* mice, showing a significant reduction of MBP immunostaining at the level of PC axons and white matter (**Figure 14B**).

To further characterize this defect, similar analyses were also performed on cerebral cortex and corpus callosum, i.e. brain areas in which individual oligodendrocytes are more easily detected (**Figure 14C**).

Based on these analyses, the dysmyelination of *Npc1^{nmf164}* mice appeared to be associated with poor oligodendrocyte differentiation, as indicated by the reduced length of the processes that typically radiate from oligodendrocyte soma. Accordingly, the MBP immunostaining of cerebral cortex and corpus callosum was strongly reduced, in agreement with previous observations (Takikita et al., 2004).

CD administration to *Npc1^{nmf164}* mice fully rescued the decrease of MBP, restoring protein levels similar to those of sham *wt* mouse cerebella (results of statistical analyses are shown in **Table 4**) (**Figure 14D**).

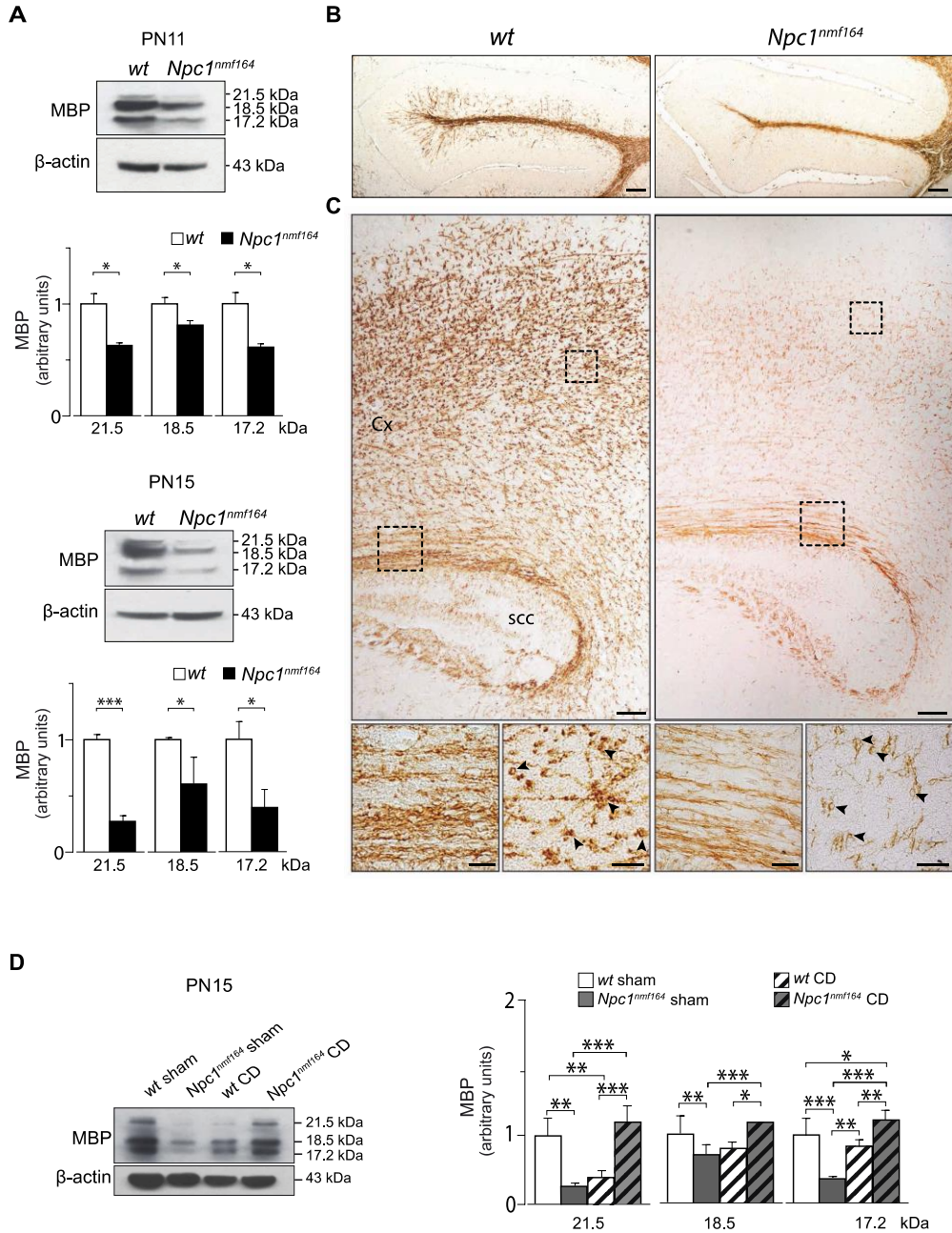


Figure 14. Oligodendrocyte maturation is impaired in *Npc1^{nmf164}* mice. (A) Western blot analysis of MBP protein expression in cerebella of PN11 and PN15 *wt* and *Npc1^{nmf164}* mice. Histograms indicate the abundance (mean \pm SEM) of each isoform determined by densitometry of protein bands obtained in at least 3 independent experiments taking β -actin as internal reference. * $p \leq 0.01$, * $p < 0.0001$. (B) Immunostaining with antibodies directed to MBP (brown) shows that PN15 *Npc1^{nmf164}***

mouse cerebella display a reduction of MBP expression at the level of PC axons and white matter compared to *wt* littermates. Representative fields of parasagittal sections of lobule III of PN15 *wt* and *Npc1^{nmf164}* mouse cerebella are shown in the Figure; scale bars: 100 μ m. **(C)** Immunostaining with antibodies directed to MBP (brown) showing that PN15 *Npc1^{nmf164}* mice display a poorer oligodendrocyte differentiation as indicated by the reduced length of MBP-positive processes that typically radiate from oligodendrocyte soma (arrowheads), compared to *wt* littermates. Representative fields of parasagittal sections of PN15 *wt* and *Npc1^{nmf164}* mouse cerebral cortex (Cx) and splenium of corpus callosum (scc) are shown in the Figure; scale bars: 100 μ m. Higher magnifications are shown in panel C (bottom); scale bars: 20 μ m. **(D)** Western blot analysis of MBP protein expression in cerebella of PN15 *wt* and *Npc1^{nmf164}* mice either sham- or CD-treated. Histograms indicate the abundance (mean \pm SEM) of each protein determined by densitometry of protein bands of at least 3 independent experiments taking β -actin as internal reference. * $p \leq 0.01$, ** $p < 0.001$, *** $p < 0.0001$

3.4.10. *Npc1^{nmf164}* mice display normal levels of activated microglia but a reduced microglia-mediated phagocytosis

Microglia plays a crucial role in the regulation of brain development and homeostasis secreting several signaling molecules, such as cytokines, neurotransmitters (e.g. glutamate) and trophic factors (e.g. BDNF) that promote neurogenesis, neuronal growth/survival, oligodendrogenesis, synaptic activity and functional plasticity (Tay et al., 2016).

During development, activated microglia phagocytose apoptotic neurons, as well as pathogens to promote tissue repair/remodeling (Minghetti and Levi, 1998; Goldmann and Prinz, 2013) and mediates synaptic pruning to increase the efficiency of neuronal transmissions (Marin-Teva et al., 2004; Peri and Nüsslein-Volhard, 2008; Paolicelli et al., 2011; Swinnen et al., 2013).

We studied the microglia activation assessing by Western blot analysis the expression levels of CD11b at PN15, finding no significant differences between *wt* and *Npc1^{nmf164}* littermates. The treatment with CD didn't vary the expression level of this protein in both genotypes (results of statistical analysis are shown in **Table 4**) (**Figure 15A**).

We also evaluated the ability of activated microglia to phagocytose cell debris determining CD68 expression by Western blot analysis at PN15, observing a significant CD68 reduction in *Npc1^{nmf164}* compared to *wt* littermates. Treatment with CD fully rescued this phenotype (results of statistical analysis are shown in **Table 4**) (**Figure 15B**).

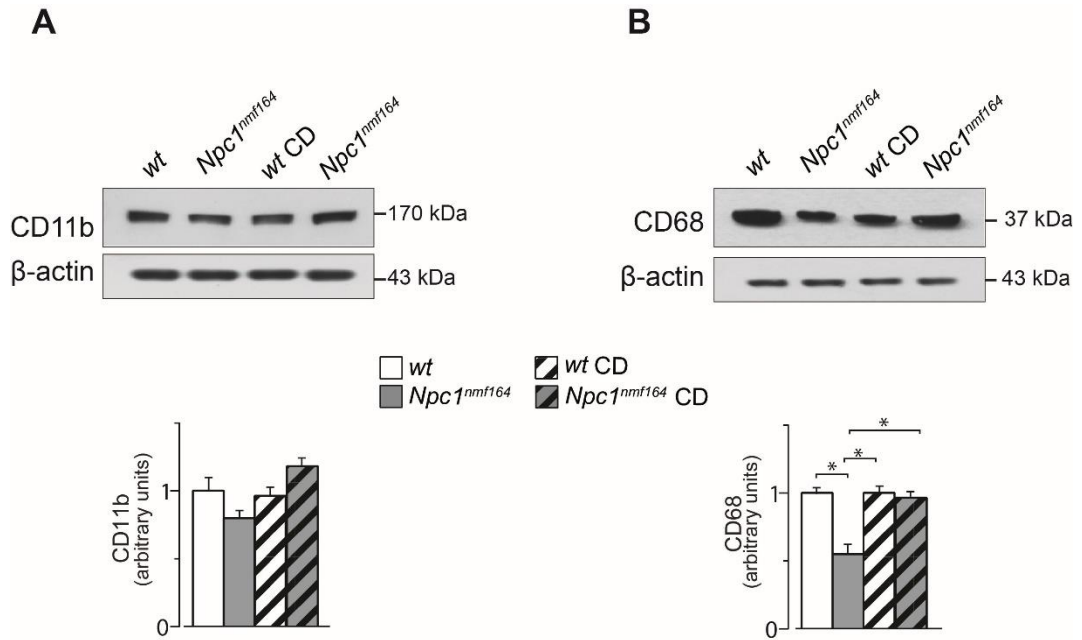


Figure 15. *Npc1^{nmf164}* mice display a reduced microglia-mediated phagocytosis. Western blot analyses of CD11b (A) and CD68 (B) protein expression in cerebella of PN15 *wt* and *Npc1^{nmf164}* mice either untreated or CD-treated. Histograms indicate the abundance (mean \pm SEM) of each protein determined by densitometry of protein bands of at least 3 independent experiments taking β -actin as internal reference. * $p \leq 0.01$, ** $p < 0.001$, *** $p < 0.0001$

3.4.11. *Npc1^{nmf164}* mice display an abnormal BDNF signaling pathway

Among signaling pathways controlling cerebellar development, BDNF, by binding the lipid raft-associated TrkB receptor, acts as a chemokinetic factor to induce GNs migration and as chemodynamic factor to guide GNs along BGs fibers (Borghesani et al., 2002). Also, BDNF is required for the development of dendritic spines and arborization of PCs and axonal growth of GNs, to modulate the dendritic morphology of BCs/SCs and to regulate the cholesterol metabolism for synapses formation (Morrison and Mason, 1998 Suzuki et al., 2007; Mertz et al., 2000).

Mature-BDNF is synthesized from pro-BDNF, which in turn can act as a signaling molecule by binding P75^{NTR} receptors (Barker, 2009).

However, during neurodevelopment pro-BDNF mediates opposite effects compared to BDNF, by promoting apoptosis and negatively regulating neurite growth, dendritic spine formation and GNs migration (Lu, 2005; Khoshimizu et al., 2009).

In addition, there is an intermediate isoform, truncated-BDNF, but at present its functional role remains unknown (Carlino et al., 2013).

It has been shown that Shh signaling promotes the expression of BDNF through a post-transcriptional mechanism (Bond et al., 2013), suggesting that both pro-BDNF and BDNF signaling pathway could be altered in *Npc1^{nmf164}* mice.

To investigate this issue, we determined the expression levels of pro-BDNF, truncated-BDNF, mature-BDNF, TrkB and P75^{NTR} by Western blot analyses in cerebella of PN11 mice, observing a significant reduction of all proteins examined in *Npc1^{nmf164}* compared to *wt* littermates (results of statistical analyses are shown in Table 4) (**Figure 16**).

CD treatment re-stored expression levels similar to those of *wt* for mature-BDNF, truncated-BDNF, mature-BDNF and P75^{NTR} but not for TrkB (**Figure 16**).

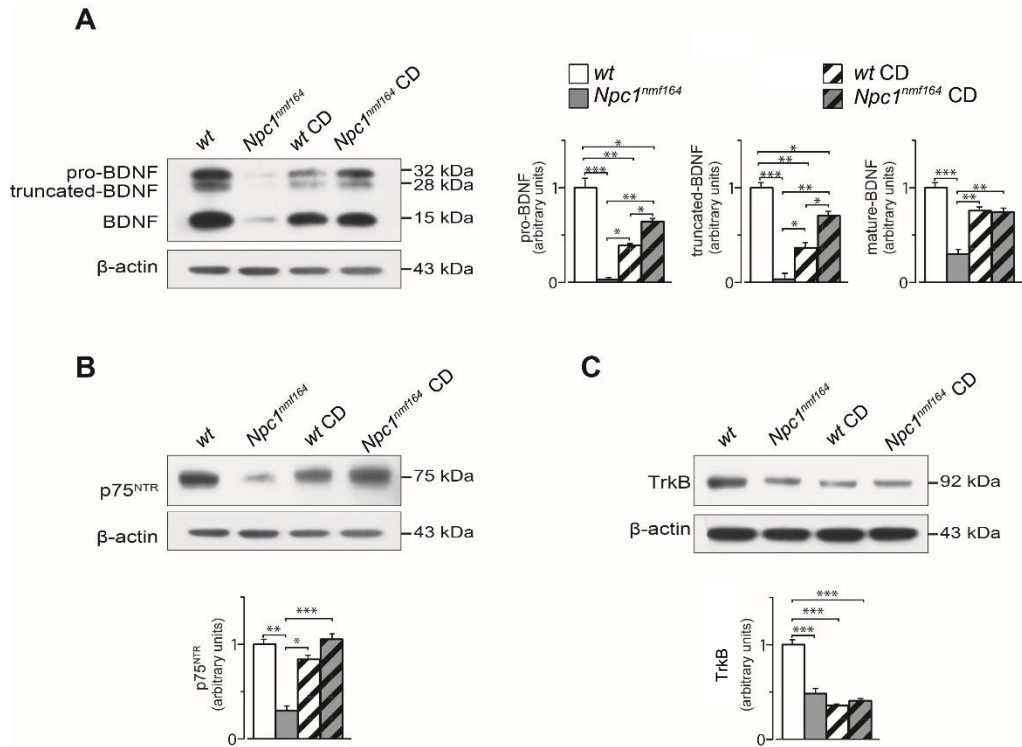


Figure 16. *Npc1^{nmf164}* mice display an abnormal BDNF signaling pathway. Western blot analyses of pro-BDNF, truncated BDNF, mature BDNF (A) TrkB (B) and P75^{NTR} (C) protein expression in cerebella of PN11 *wt* and *Npc1^{nmf164}* mice either untreated or CD-treated. Histograms indicate the abundance (mean \pm SEM) of each protein determined by densitometry of protein bands of at least 3 independent experiments taking β -actin as internal reference. * $p \leq 0.01$, ** $p < 0.001$, *** $p < 0.0001$

3.4.12. *Npc1^{nmf164}* mice show a delay in the acquisition of complex motor skills requiring fine motor coordination and balance

Because sensorimotor reflexes and motor skills normally appear with a definite timing during the first 3 weeks after birth, they represent a useful tool to assess early postnatal neural development (de Souza et al., 2004).

We therefore evaluated the acquisition of several developmental milestones in the physical and sensorimotor development of *Npc1^{nmf164}* mice from PN3 until weaning (PN21). Body weight, fur appearance, incisor eruption and eye opening were recorded as indexes of physical growth and development, observing no difference between *Npc1^{nmf164}* and *wt* littermates (**Figure 17A**). All pups similarly increased their body weight in the interval PN3-PN21 (main effect of genotype: $F_{1,18} = 0.80$, $p = 0.78$; main effect of age: $F_{18,324} = 364.14$, $p < 0.00001$; interaction between genotype and age: $F_{18,324} = 0.47$, $p = 0.97$), and showed dorsal and ventral fur appearance after PN5 (main effect of genotype: $Z = -1.30$, $p = 0.47$), incisor eruption after PN7 (main effect of genotype: $Z = 0.32$, $p = 0.80$), and eye opening after PN14 (main effect of genotype: $Z = -1.58$, $p = 0.14$).

To analyze the locomotor development we determined the appearance of the dominant locomotor categories pivoting (turning with circular motions), crawling (moving forward/pushing backward the body) and quadrupedal locomotion (showing fluent and swift forward movements), observing no difference between *Npc1^{nmf164}* and *wt* littermates (**Figure 17B, Table 5**). Namely, pups showed pivoting from PN3 to PN9, crawling at PN10-11 and quadrupedal locomotion since PN12.

We also determined the development of swimming abilities and observed no effect of genotype: all pups floated with asynchronous limb movements at PN4, swam in circles at PN5, swam in a straight line at PN12 and displayed the adult swimming pattern (paddling only the hindlimbs) after PN14 (**Figure 17C,D, Table 5**).

We then recorded the appearance of reflexes as surface righting reflex, negative geotaxis and cliff avoidance, which involve vestibular, tactile and proprioceptive systems (Altman and Sudarshan, 1975).

Negative geotaxis and cliff avoidance are more representative of sensory ability, whereas the surface righting reflex is more representative of motor ability (Heyser, 2004). *Npc1^{nmf164}* mice displayed a timing of reflex appearance that matched that of *wt* littermates (**Figure 17E**), exhibiting similar appearance of surface righting reflex (main effect of genotype: $Z = -1.70$, $p = 0.10$) and negative geotaxis since PN4 (main effect of genotype:

Z = 0.38, p = 0.74), as well as cliff avoidance since PN7 (main effect of genotype: Z = 0.20, p = 0.85).

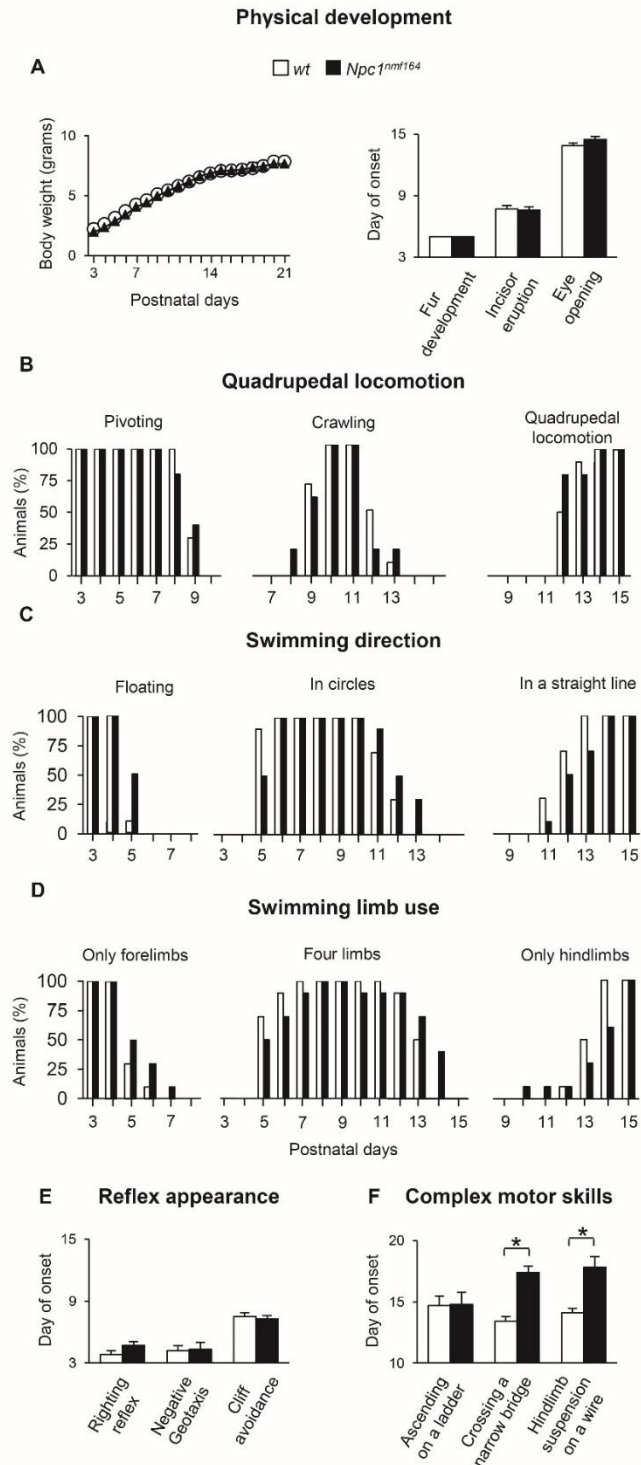


Figure 17. *Npc1^{nmf164}* pups show a delay in the acquisition of complex motor skills requiring fine motor coordination and balance. (A) Line graph indicates body weight values of experimental group mice of increasing age. Histograms indicate the day of onset of physical development landmarks. **(B-D)** Histograms indicate the fraction of: pups engaged in pivoting, crawling or quadrupedal locomotion **(B)**; pups floating, swimming in circles or in a straight line **(C)**; pups paddling with only forelimbs, four limbs or only hindlimbs **(D)** in the PN3-PN15 time interval. **(E-F)** Histograms indicate the day of onset of sensorimotor reflexes **(E)** and complex motor skills **(F)**. Note that *Npc1*-deficiency delays the acquisition of complex motor behaviors requiring fine motor coordination and balance, whereas it does not influence physical and sensorimotor development. **(A, E, F)** Data are expressed as mean \pm SEM. **(B-D)** Data are expressed as percentages of animals displaying the behavior. * $p \leq 0.01$

Age ^b	Quadrupedal locomotion	Swimming performance	
		<i>direction</i>	<i>limb usage</i>
PN3	Z = 1.00; p = 0.74	Z = 0.00; p = 1.00	Z = 0.00; p = 1.00
PN4	Z = -1.00; p = 0.74	Z = 0.00; p = 1.00	Z = 0.00; p = 1.00
PN5	Z = 1.00; p = 0.74	Z = 1.90; p = 0.14	Z = 0.89; p = 0.48
PN6	Z = -1.00; p = 0.74	Z = 0.00; p = 1.00	Z = 1.09; p = 0.48
PN7	Z = -0.61; p = 0.74	Z = 0.00; p = 1.00	Z = 1.00; p = 0.74
PN8	Z = 0.97; p = 0.53	Z = 0.00; p = 1.00	Z = 0.00; p = 1.00
PN9	Z = -0.59; p = 0.63	Z = 0.00; p = 1.00	Z = 0.00; p = 1.00
PN10	Z = 0.00; p = 1.00	Z = 0.00; p = 1.00	Z = -1.00; p = 0.74
PN11	Z = -1.09; p = 0.48	Z = -1.09; p = 0.48	Z = -1.00; p = 0.74
PN12	Z = 1.37; p = 0.28	Z = 0.89; p = 0.48	Z = 0.00; p = 1.03
PN13	Z = -1.13; p = 0.44	Z = 1.83; p = 0.28	Z = 0.89; p = 0.48
PN14	Z = -1.45; p = 0.48	Z = 0.00; p = 1.00	Z = 2.18; p = 0.14
PN15	Z = 0.00; p = 1.00	Z = 0.00; p = 1.00	Z = 1.00; p = 0.74

Table 5. Statistical analysis outputs of quadrupedal locomotion and swimming performance development in *Npc1^{nmf164}* and *wt* littermates^a

^a Experimental groups were compared at increasing postnatal days by Mann-Whitney U test

^b PN: postnatal day

In the mouse, complex motor abilities requiring fine limb coordination, balance and muscle strength are normally acquired by the end of the second postnatal week.

Three tasks (ascending a ladder, crossing a narrow bridge and suspension on a wire) allowed us to differentiate the contribution of motor coordination and balance from that of grip and muscle strength. *Npc1^{nmf164}* pups acquired these abilities with a significant delay compared to *wt* littermates (**Figure 17F**).

Indeed, whereas *wt* pups crossed the narrow bridge in its entire length and hanged on the wire with four limbs after PN14, *Npc1^{nmf164}* mice crossed the bridge only at PN17 (main effect of genotype: $Z = -2.54$, $p = 0.01$) and developed the four-limb hanging ability at PN18 (main effect of genotype: $Z = -2.98$, $p = 0.004$). In contrast, grip ability and muscle strength developed similarly in *Npc1^{nmf164}* and *wt* littermates, as shown by their similar ability to ascend the ladder after PN15 (main effect of genotype: $Z = 0.27$, $p = 0.80$) and to hang on the wire for a longer time with increasing age (main effect of genotype: $F_{1,18} = 1.09$, $p = 0.31$; main effect of age: $F_{10,180} = 3.23$, $p = 0.0008$; interaction between genotype and age: $F_{10,180} = 0.20$, $p = 0.99$).

The possibility of evaluating the efficacy of CD to rescue the developmental delay in motor skills acquisition of *Npc1^{nmf164}* and *wt* littermates was hampered by the hyperactivity of mouse pups elicited by the injection *per se*. Both CD-treated and sham group pups, regardless of genotype resisted our attempts to perform motor behavior assessments.

3.4.13. Motor deficits of *Npc1^{nmf164}* mice become more severe in the adulthood

To fully characterize motor phenotype in adults, PN30, PN60 and PN90 *Npc1^{nmf164}* and *wt* littermates were subjected to a battery of tests including Vertical screen, Balance beam, and Coat hanger.

The Vertical screen test (similar to the ascending on a ladder) investigates the climbing response that requires good grip and muscle strength (**Figure 18A**). In this test *Npc1^{nmf164}* mice reached the upper edge of the screen more slowly than *wt* littermates, even if both genotypes turned upwards with similar time (turning upward: main effect of genotype: $F_{1,18} = 0.12$, $p = 0.73$; main effect of age: $F_{2,36} = 1.91$, $p = 0.16$; interaction between genotype and age: $F_{2,36} = 1.52$, $P = 0.23$); (climbing to the upper edge: main effect of genotype: $F_{1,18} = 11.31$, $p = 0.004$; main effect of age: $F_{2,36} = 0.59$, $p = 0.57$; interaction between genotype and age: $F_{2,36} = 2.63$, $p = 0.09$).

The Balance beam test (similar to crossing a narrow bridge) measures fine motor coordination and balance (**Figure 18B**). When placed on an elevated round beam, *Npc1^{nmf164}* mice crossed significantly fewer beam sections than *wt* mice did and significantly fewer sections as days went by (main effect of genotype: $F_{1,18} = 34.92$, $p = 0.00001$; main effect of age: $F_{2,36} = 5.08$, $p = 0.01$; interaction between genotype and age: $F_{2,36} = 4.09$, $p = 0.03$). Moreover, *Npc1^{nmf164}* mice did not differ from *wt* until PN90 in terms of retention time (main effect of genotype: $F_{1,18} = 54.28$, $p < 0.00001$; main effect of age: $F_{2,36} = 6.48$, $p = 0.004$; interaction between genotype and age: $F_{2,36} = 6.01$, $p = 0.006$).

The Coat hanger test (similar to suspending on a wire) further characterizes motor coordination by providing an “agility score” (**Figure 18C**). *Npc1^{nmf164}* mice obtained scores lower than those of *wt* mice when suspended on the coat hanger. In fact, while *wt* mice rapidly escaped to the bar end, *Npc1^{nmf164}* mice did not progress to the end of the bar although they were able to grasp the bar with four limbs (main effect of genotype: $F_{1,18} = 18.81$, $p = 0.0004$; main effect of age: $F_{2,36} = 3.80$, $p = 0.03$; interaction between genotype and age: $F_{2,36} = 2.30$, $p = 0.11$).

The possibility that body weight influenced motor behavior was routinely checked before all behavioral evaluations (**Figure 18D**). Body weight of *Npc1^{nmf164}* and *wt* mice did not differ at PN30 and PN60, while it significantly decreased in PN90 *Npc1^{nmf164}* mice, as previously described (Maue et al., 2012) (main effect of genotype: $F_{1,18} = 13.35$, $p = 0.002$; main effect

of age: $F_{2,36} = 125.40$, $p < 0.00001$; interaction between genotype and age: $F_{2,36} = 22.26$, $p < 0.00001$).

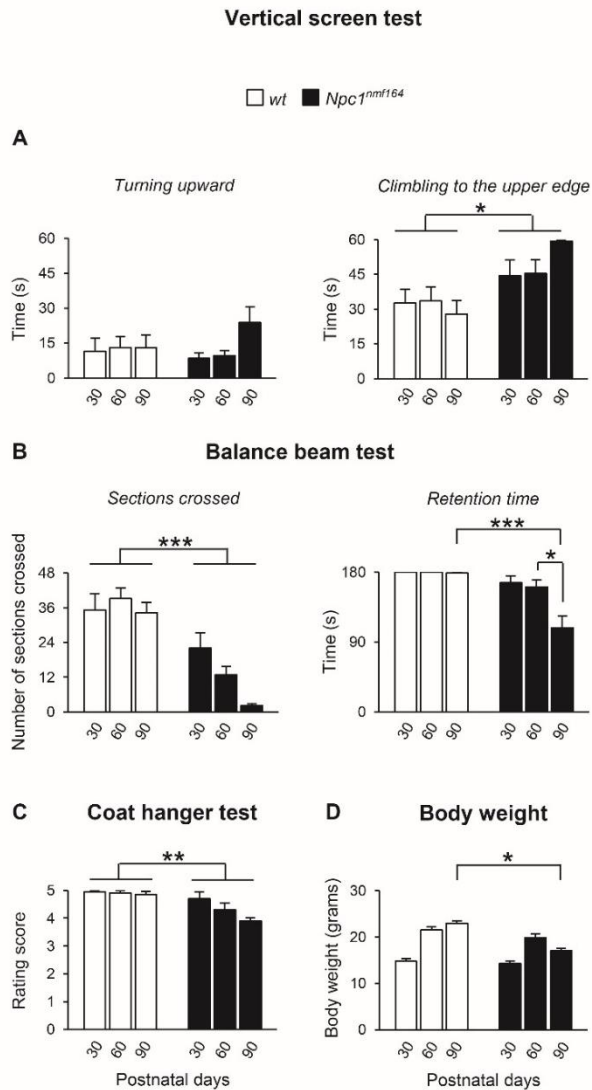


Figure 18. *Npc1^{nmf164}* adult mice display motor deficits after PN30. (A-D) Histograms indicate: latency values to turn upward and climb to the upper edge in the Vertical screen test (A); number of sections crossed and retention time values in the Balance beam test (B); rating score values in the Coat hanger test (C); body weight values (D) of experimental group mice of increasing age. All data are expressed as mean \pm SEM. * $p < 0.01$, ** $p < 0.001$, *** $p < 0.0001$

		Genotype ^a	Treatment ^b	Genotype x treatment
GFAP	50 kDa	$F_{(1,12)}=29.35, p=0.0001$	$F_{(1,12)}=52.17, p<0.0001$	$F_{(1,12)}=0.70, p=0.42$
	48 kDa	$F_{(1,12)}=199.21, p<0.0001$	$F_{(1,12)}=152.93, p<0.0001$	$F_{(1,12)}=8.78, p=0.01$
GLAST	60 kDa	$F_{(1,12)}=22.77, p=0.0005$	$F_{(1,12)}=95.83, p<0.0001$	$F_{(1,12)}=9.63, p=0.01$
Glutamine Synthetase	42 kDa	$F_{(1,12)}=12.85, p=0.004$	$F_{(1,12)}=12.51, p=0.004$	$F_{(1,12)}=11.48, p=0.005$
VGluT2	65 kDa	$F_{(1,12)}=0.83, p=0.38$	$F_{(1,12)}=5.47, p=0.04$	$F_{(1,12)}=26.21, p=0.0003$
GAD65	65 kDa	$F_{(1,12)}=13.53, p=0.003$	$F_{(1,12)}=22.02, p=0.0005$	$F_{(1,12)}=21.89, p=0.0005$
MBP	21.5 kDa	$F_{(1,12)}=0.14, p=0.71$	$F_{(1,12)}=3.37, p=0.09$	$F_{(1,12)}=74.51, p<0.0001$
	18.5 kDa	$F_{(1,12)}=0.04, p=0.84$	$F_{(1,12)}=5.60, p=0.04$	$F_{(1,12)}=24.13, p=0.0004$
	17.2 kDa	$F_{(1,12)}=1.55, p=0.24$	$F_{(1,12)}=47.36, p<0.0001$	$F_{(1,12)}=92.86, p<0.0001$
CD11b	170 kDa	$F_{(1,20)}=2.47, p=0.01$	$F_{(1,20)}=3.54, p=0.01$	$F_{(1,12)}=5.69, p=0.01$
CD68	37 kDa	$F_{(1,20)}=17.78, p<0.01$	$F_{(1,20)}=19.89, p<0.01$	$F_{(1,20)}=21.86, p<0.01$
pro-BDNF	32 kDa	$F_{(1,20)}=129.04, p<0.0001$	$F_{(1,20)}=0.73, p=0.40$	$F_{(1,20)}=393.79, p<0.0001$
truncated-BDNF	28 kDa	$F_{(1,20)}=103.62, p<0.0001$	$F_{(1,20)}=0.02, p=0.006$	$F_{(1,20)}=533.19, p<0.0001$
mature-BDNF	15 kDa	$F_{(1,20)}=90.850, p<0.0001$	$F_{(1,20)}=13.81, p=0.001$	$F_{(1,20)}=84.11, p<0.0001$
TrkB	92 kDa	$F_{(1,20)}=87.85, p<0.0001$	$F_{(1,20)}=83.85, p<0.0001$	$F_{(1,20)}=12.85, p=0.001$
p75 ^{NTR}	75 kDa	$F_{(1,20)}=17.038, p=0.002$	$F_{(1,20)}=84.55, p<0.0001$	$F_{(1,20)}=150.76, p<0.0001$

Table 4. Statistical analysis outputs on WB assays of *wt* and *Npc1^{nmf164}* littermates either sham- or CD-treated.

^a differences were analyzed by two-way ANOVAs

^b *wt* and *Npc1^{nmf164}* littermates received subcutaneous injections of plain PBS or CD at PN4 and PN7.

Discussion and conclusions

This study disclosed several developmental anomalies that impinge on the functionality of Purkinje cells (PCs), suggesting the possibility that the selective vulnerability of these cells represents the final outcome of defective differentiation of glial and neuronal cells forming the ordered pattern of cell-to-cell interaction and synaptic connectivity of cerebellar cortex (Llinas et al., 2004).

According to evidence recently obtained by our group, showing that both Sonic Hedgehog (Shh) availability and reception are severely impaired by *Npc1*-deficiency (Nusca et al., 2014; Canterini et al., *manuscript in preparation*) it is likely that abnormal cerebellar morphogenesis is a consequence of an impairment of Shh signaling. This possibility is strengthened by the finding that the C-terminus of proteolytically-generated active Shh fragment is modified by the covalent attachment of a cholesterol moiety (Repetto et al., 1990; Lanoue et al., 1997; Dehart et al., 1997). Moreover, cholesterol availability influences the function of lipid rafts that play a key role in signal transduction (Crane and Tamm, 2004).

Effect of altered Shh signaling on cerebellar morphogenesis

Our findings indicate that altered Shh signaling causes a poorer morphological differentiation of Bergmann glia (BG) as indicated by thicker radial shafts and a less elaborate reticular pattern of lateral processes. This could compromise the cerebellar function since the BG processes organize the compartmentalization pattern of synaptic inputs that reach PCs (Palay and Chan-Palay, 1974) playing a prominent role in the differential guidance and targeting of basket and stellate cell axons (Ango et al., 2004) and regulate cerebellar synaptic activity (Buffo and Rossi, 2013) by almost completely enwrapping the synapses that parallel and climbing fibers establish with PCs (Yamada and Watanabe, 2002; Palay and Chan-Palay, 1974). In particular, the glutamate transporter GLAST finely regulates PC firing at BG perisynaptic processes by preventing glutamate

spillover between adjacent PCs (Takayasu et al., 2009) and maintaining the one-to-one functional relationship between climbing fibers and PCs that is crucial for cerebellar control of motor function (Watase et al., 1998; Chen et al., 1995; Offermanns et al., 1997). Because the glutamate recovered by GLAST is metabolized to glutamine by Glutamine synthetase (Bak et al., 2006) the reduced expression of GLAST and Glutamine synthetase in *Npc1^{nmf164}* mice is in line with the proposal that GLAST is a limiting factor in glutamate synthesis (Martinez et al., 2014).

Also, GFAP plays a key role in astrocyte-neuron interactions, by modulating the trafficking and function of astrocytic and neuronal glutamate transporters, as well as glutamine production (Middeldorp and Hol, 2011). All together these findings suggest that the abnormal morphological differentiation of BG affects the functional specialization of their processes, as also indicated by the reduced expression of GLAST and Glutamine synthetase. In addition to BG, a decrease of GLAST and Glutamine synthetase expression is likely to occur in astrocytes, the functional impairment of which is indicated by astrogliosis displayed by *Npc1^{nmf164}* cerebella.

Npc1 is also abundant in the recycling endosomes of presynaptic terminals. In fact, *Npc1*-deficiency results in morphological, biochemical and functional modification of both excitatory and inhibitory presynaptic terminals and synaptic vesicle turnover (Karten et al., 2006). This may explain the reduction of both excitatory and inhibitory inputs received by PCs, as indicated by the significant reduction of VGLUT2 and GAD65 puncta. This imbalance of synaptic inputs associated with *Npc1*-deficiency is in agreement with previous findings showing a decrease of synaptic inputs to PCs in co-cultures of *Npc1*-deficient neurons and glial cells (Buard and Pfrieger, 2014).

The lower number of granule neurons (GNs) that are generated in the cerebellum of *Npc1^{nmf164}* mice likely contributes to the reduction in glutamatergic inputs, as indicated by our finding that VGLUT2 puncta reduction is prominent in the outer molecular layer, which is mostly made of GN axons. On the other hand, the GN reduction may also impinge on the full differentiation of basket/stellate interneurons, which, among other intrinsic genetic programs and extracellular cues, depends on connectivity with GN axons (Rakic, 1972; Cameron et al., 2009). Along the same line, the lower number of GNs may also be responsible for the abnormal differentiation of BG processes in *Npc1^{nmf164}* mice, because the glutamate released by parallel fibers modulates the degree of BG perisynaptic envelopment acting through calcium-permeable AMPA receptors (Buffo and Rossi, 2013).

Defective oligodendrocyte maturation likely underlines the overall reduction in MBP we have observed in *Npc1^{nmf164}* cerebellum, in line with previous studies showing dysmyelination in both NPC patients and *Npc1^{-/-}* mice (Takikita et al., 2004; Walterfang et al., 2010). Moreover, the decreased MBP expression not only affected the 18.5 kDa (specific to mature oligodendrocytes), but also the 17.5 kDa and 21.5 kDa isoforms (specific to developing oligodendrocytes), indicating that oligodendrocyte differentiation *per se* is also impaired in *Npc1*-deficient mice. Although *Npc1* deletion in neurons triggers the block of oligodendrocyte maturation and thus leads to a subsequent failure of myelin formation (Yu and Lieberman, 2013) the exogenous cholesterol uptake by oligodendrocytes coupled to *Npc1*-mediated intracellular trafficking is also relevant for the formation of myelin sheaths (Zhao et al., 2007; Yan et al., 2011).

Microglia involvement

It is worth noting that in *Npc1^{-/-}* mice astrocytosis is consistently accompanied by microglia activation (Maue et al., 2012; German et al., 2002; Baudry et al., 2003) and the down regulation of GLAST has been found to correlate with the release of inflammatory cytokines by activated microglia (Tilleux and Hermans, 2008). Interestingly, we have not found significant differences in the expression levels of CD11b, a well-established marker of microglia activation (Perego et al., 2011), whereas we have found reduced expression levels of the lysosomal/endosomal-associated membrane glycoprotein CD68 which represents a useful marker of microglia-mediated active phagocytosis (Perego et al., 2011). This observation suggests that in *Npc1^{nmf164}* mice activated microglia fails to destroy pathogens and apoptotic neurons as well as to phagocyte synaptic elements during synaptic pruning, which in turn may cause inflammation and defective synapse formation and maturation. However, further investigations are needed to explore these issues.

Effect of altered BDNF signaling on cerebellar morphogenesis

Among signaling pathways controlling cerebellar development, Brain-Derived Neurotrophic Factor (BDNF), by binding the lipid raft-associated tropomyosin receptor kinase B (TrkB) exerts a crucial for proper proliferation and differentiation of various neuronal and glial cell, likely influencing the overall pattern of synaptic connectivity of the cerebellar cortex (Saab et al., 2003; Borghesani et al., 2002; Merz et al., 2000; Kokubo et al., 2009).

Also, BDNF elicits neuronal *de novo* synthesis of cholesterol stimulating the transcription of several enzymes involved in the cholesterol biosynthetic pathway (Suzuki et al., 2007). The BDNF-dependent cholesterol biosynthesis plays a critical role for the development of synapses and lipid rafts (Suzuki et al., 2007). The BDNF reduced availability may also alter the composition of lipid rafts observed in both NPC1-patient and mice (Kuech et al., 2014; Vainio et al., 2005), which in turn may explain the reduced TrkB expression that we have observed. Because Shh signaling promotes the expression of BDNF through a post-transcriptional mechanism (Bond et al., 2013), BDNF-deficiency may also depend on the reduced availability of Shh. According to this hypothesis we have observed a downregulation of the expression levels of BDNF precursor protein, namely pro-BDNF, and its high-affinity receptor p75^{NTR}. Further investigations are needed to quantify the pro-BDNF transcripts and highlight if the reduction of BDNF protein occurs in neuronal or glial, as it is synthesized and released by PCs, GNs, BG, intraparenchymal astrocytes, oligodendrocytes and microglia (Marini et al., 1998; Jean et al., 2008; Poblete-Naredo et al., 2011; Coull et al., 2005). Our findings indicate that the expression of BDNF and TrkB is downregulated in in the cerebellum of *Npc1^{nmf164}* mice, as early as at PN11. These findings pinpoint BDNF dysregulation, among others molecular mechanisms, as a possible candidate responsible for abnormal cerebellum morphogenesis, opening novel perspectives for NP-C1 disease therapies.

Motor behavior anomalies

These overall disturbances of cerebellar morphogenesis cause in *Npc1^{nmf164}* mice a delay in the acquisition of complex motor skills, that require fine motor coordination and balance, in spite of a normal physical and postural development. The presence of a developmental delay instead of a more severe deficit of these abilities is likely explained by the greater plasticity of developing cerebellum and/or the availability of cholesterol of neuronal origin before the full shift to astrocyte-derived cholesterol, which compensates the deficit of Npc1 function.

The normal appearance of sensorimotor reflexes and locomotion development of *Npc1^{nmf164}* pups within the first two postnatal weeks indicate that vestibular, tactile, and proprioceptive systems; descending motor pathways; and brain stem-spinal networks (Altman and Sudarshan, 1975; Clarac et al., 2004) are not apparently affected by Npc1-deficiency. Conversely, the domain of complex motor abilities is damaged by Npc1-deficiency because they are also prematurely lost in the adulthood. In fact, motor

coordination and balance are more severely impaired than grip capacity and muscle strength as early as at PN30 and these motor defects thereafter translate to severe ataxia, because of the massive PC degeneration (Maue et al., 2012; Vöikar et al., 2002).

The acquisition of complex motor abilities depends on proper sequencing and coordination of motor outputs. These are prominent properties of cerebellar circuitry (Dehorter et al., 2012) consisting of several functional modules that allow the real-time control of movements and the long-term changes underlying motor learning, by finely regulated signal generation and flow that ultimately converge on PCs. The inhibitory activity of PCs is dynamically orchestrated at the level of both dendritic shafts and cell body by a number of excitatory and inhibitory neurons, while PCs in turn modulate the excitability of deep cerebellar nuclei. Therefore, an altered pattern of synaptic inputs to PCs may affect the timing of their firing and finally result in behavior abnormalities. For example, it was recently demonstrated that an altered GN development results in impaired motor coordination (Ceccarelli et al., 2015; Prestori et al., 2008).

Similar features were also reported as a consequence of a defective development of BG processes (Müller Smith et al., 2012; Watase et al., 1998) likely because correct BG development is crucial for cerebellar cytoarchitecture and function processes (Müller Smith et al., 2012). Conversely, a precocious BG and PC maturation is associated with an earlier acquisition of motor abilities in young and improved motor learning and coordination in adult mice (Marazziti et al., 2013).

In light of these findings, it is possible that the developmental delay in the acquisition of complex motor skills we have observed in *Npc1^{nmi164}* pups results from a derangement of synaptic inputs to PCs.

Efficacy of CD treatment

Present findings also demonstrate that early postnatal CD treatment effectively re-wires developmental trajectories, by partly rescuing the defective cerebellar morphogenesis and thus explaining the well-established beneficial effect a single CD administration to PN7 *Npc1^{-/-}* mice has in rescuing lysosomal cholesterol accumulation and slowing down the appearance of ataxic symptoms (Camargo et al., 2001; Raminez et al., 2010; Vite et al., 2015; Davidson et al., 2009; Liu et al., 2008). In fact, this treatment is particularly timely because cerebellar morphogenesis maximizes the need for cholesterol, making the exogenous LDL-uptaken cholesterol a rate-limiting factor for neurons (Fiorenza et al., 2013;

Zhang and Liu, 2015). Noteworthy, CD administration didn't rescue either GFAP hyper- or GLAST hypo-expression of *Npc1^{nmf164}* mice, although it fully rescued Glutamine synthetase levels in these mice. Because Glutamine synthetase is mainly expressed by astrocytes, this observation rules out the possibility that astrocytes are not influenced by CD, making this issue worthy of further investigation, also in light of the ability of CD administration to influence GFAP and GLAST expression of *wt* mice.

Conclusions

In conclusion, we have demonstrated that the downregulation in both synthesis and release of Shh by PCs causes an abnormal GNs proliferation, as well as a number of glial cell differentiation anomalies, derangement of synaptic input to PCs and a down-regulation of BDNF expression that in turn, may correlate with the delay of complex motor skills acquisition of *Npc1^{nmf164}* mice. In this contest, microglia fail to perform active phagocytosis.

We believe that these findings are relevant because: i) delineate a novel perspective to explain the selective Purkinje cell vulnerability in NPC1 mouse models and patients; and, ii) emphasize the need of early diagnosis to secure the best treatment efficacy in patients.

References

- ❖ Abbott NJ, Patabendige AA, Dolman DE, Yusof SR, Begley DJ. Structure and function of the blood–brain barrier. *Neurobiology of Disease* (2010) 37:13–25.
- ❖ Abel LA, Walterfang M, Fietz M, Bowman EA, Velakoulis D. Saccades in adult Niemann–Pick disease type C reflect frontal, brainstem, and biochemical deficits. *Neurology* (2009) 72:1083-1086.
- ❖ Abi-Mosleh L, Infante RE, Radhakrishnan A, Goldstein JL, Brown MS. Cyclodextrin overcomes deficient lysosome-to-endoplasmic reticulum transport of cholesterol in Niemann-Pick type C cells. *PNAS USA* (2009) 106:19316–19321.
- ❖ Aerts JM, Groener JE, Kuiper S, Donker-Koopman WE, Strijland A, Ottenhoff R, van Roomen C, Mirzaian M, Wijburg FA, Linthorst GE, Vedder AC, Rombach SM, Cox-Brinkman J, Somerharju P, Boot RG, Hollak CE, Brady RO, Poorthuis BG. Elevated globotriaosylsphingosine is a hallmark of Fabry disease. *PNAS USA* (2008) 105:2812–2817.
- ❖ Albanese A, Bhatia K, Bressman SB, DeLong MR, Fahn S, Fung VS, Hallett M, Jankovic J, Jinnah HA, Klein C, Lang AE, Mink JW, Teller JK. Phenomenology and classification of dystonia: a consensus update. *Movement Disorders* (2013) 28(7):863-873.
- ❖ Alobaidy H. Recent Advances in the Diagnosis and Treatment of Niemann-Pick Disease Type C in Children: A Guide to Early Diagnosis for the General Pediatrician. *International Journal of Pediatrics* (2015):816593.
- ❖ Altman J, Bayer SA. Development of the Cerebellar System in Relation to its Evolution, Structure and Functions. CRC press, New York. (1996).
- ❖ Altman J, Bayer SA. Time of origin and distribution of a new cell type in the rat cerebellar cortex. *Exp Brain Res.* (1977) 29:265–274.
- ❖ Altman J, Sudarshan K. Postnatal development of locomotion in the laboratory rat. *Animimal Behaviour* (1975) 23:896–920.
- ❖ Altman J. Postnatal development of the cerebellar cortex in the rat. I. The external germinal layer and the transitional molecular layer. *Journal of Comparative Neurology* (1972) 145:353–397.
- ❖ Alvelius G, Hjalmanson O, Griffiths WJ, Björkhem I, Sjövall J. Identification of unusual 7-oxygenated bile acid sulfates in a patient with Niemann-Pick disease, type C. *Journal of Lipid Research* (2001) 42:1571–1577.
- ❖ Andersen BB, Korbo L, Pakkenberg B. A quantitative study of the human cerebellum with unbiased stereological techniques. *Journal of Comparative Neurology* (1992) 326: 549–560.

- ❖ Ango F, di Cristo G, Higashiyama H, Bennett V, Wu P, Huang ZJ. Ankyrin-based subcellular gradient of neurofascin, an immunoglobulin family protein, directs GABAergic innervation at purkinje axon initial segment. *Cell* (2004) 119:257–272.
- ❖ Ango F, Wu C, Van der Want JJ, Wu P, Schachner M, Huang ZJ. Bergmann glia and the recognition molecule CHL1 organize GABAergic axons and direct innervation of Purkinje cell dendrites. *PLoS Biology* (2008) 6:e103.
- ❖ Bak LK, Schousboe A, Waagepetersen HS. The glutamate/GABA-glutamine cycle: aspects of transport, neurotransmitter homeostasis and ammonia transfer. *Journal of Neurochemistry* (2006) 98:641–53.
- ❖ Balakrishnan S, Bellamy TC. Depression of parallel and climbing fiber transmission to Bergmann glia is input specific and correlates with increased precision of synaptic transmission. *Glia* (2009) 57:393–401.
- ❖ Balakrishnan S, Dobson KL, Jackson C, Bellamy TC. Ectopic release of glutamate contributes to spillover at parallel fibre synapses in the cerebellum. *The Journal of Physiology* (2014) 592:1493–1503
- ❖ Barker PA. Whither proBDNF? *Nature Neuroscience* (2009) (2):105-106.
- ❖ Barmack NH, Yakhnitsa V. Functions of interneurons in mouse cerebellum. *Journal of Neuroscience* (2008) 28:1140–1152.
- ❖ Barmack NH, Yakhnitsa V. Functions of interneurons in mouse cerebellum. *Journal of Neuroscience* (2008) 28:1140–1152.
- ❖ Barres BA. The mystery and magic of glia: a perspective on their roles in health and disease. *Neuron* (2008) 60:430–440.
- ❖ Baudry M, Yao Y, Simmons D, Liu J, Bi X. Postnatal development of inflammation in a murine model of Niemann-Pick type C disease: immunohistochemical observations of microglia and astroglia. *Experimental Neurology* (2003) 84:887–903.
- ❖ Bauer P, Knoblich R, Bauer C, Finckh U, Hufen A, Kropp J, Braun S, Kustermann-Kuhn B, Schmidt D, Harzer K, Rolfs A. NPC1: Complete genomic sequence, mutation analysis, and characterization of haplotypes. *Human Mutation* (2002) 19:30-38.
- ❖ Baumann N, Pham-Dinh D. Biology of oligodendrocyte and myelin in the mammalian central nervous system. *Physiological Reviews* (2001) 81:871–927.
- ❖ Beffert U, Danik M, Krzywkowski P, Ramassamy C., Berrada F, Poirier J. The neurobiology of apolipoproteins and their receptors in the CNS and Alzheimer's disease. *Brain Research Reviews* (1998) 27:119-142.
- ❖ Benarroch EE. Brain cholesterol metabolism and neurologic disease. *Neurology* (2008) 71:1368–1373.
- ❖ Bergles DE, Dzubay JA, Jahr CE. Glutamate transporter currents in Bergmann glial cells follow the time course of extrasynaptic glutamate. *PNAS USA* (1997) 94:14821–14825.
- ❖ Bjurulf B, Spetalen S, Erichsen A, Vanier MT, Strom EH, Stromme P. Niemann–Pick disease type C2 presenting as fatal pulmonary alveolar lipoproteinosis: morphological findings in lung and nervous tissue. *Medical Science Monitor* (2008) 14:71-75.
- ❖ Blank T, Prinz M. Microglia as modulators of cognition and neuropsychiatric disorders. *Glia* (2013) 61:62–70.
- ❖ Boenzi S, Deodato F, Taurisano R, Martinelli D, Verrigni D, Carrozzo R, Bertini E, Pastore A, Dionisi-Vici C, Johnson DW, A new simple and rapid LC-ESI-MS/MS method for quantification of plasma oxysterols as dimethylaminobutyrate esters. Its

- successful use for the diagnosis of Niemann-Pick type C disease. *Clinica Chimica Acta* (2014) 437:93–100.
- ❖ Boggs JM. Myelin basic protein: a multifunctional protein. *Cellular and Molecular Life Sciences* (2006) 63:1945–1961.
 - ❖ Borbon I, Totenhagen J, Fiorenza MT, Canterini S, Ke W, Trouard T, Erickson RP. Niemann-Pick C1 mice, a model of “juvenile Alzheimer’s disease”, with normal gene expression in neurons and fibrillary astrocytes show long term survival and delayed neurodegeneration. *Journal of Alzheimer’s Disease* (2012) 30:875–887.
 - ❖ Borghesani PR, Peyrin JM, Klein R, Rubin J, Carter AR, Schwartz PM, Luster A, Corfas G, Segal RA. BDNF stimulates migration of cerebellar granule cells. *Development* (2002) 129:1435–1442.
 - ❖ Bouslama-Oueghlani L, Wehrle R, Doulazmi M, Chen XR, Jaudon F, Lemaigre-Dubreuil Y, Rivals I, Sotelo C, Dusart I. Purkinje cell maturation participates in the control of oligodendrocyte differentiation: role of sonic hedgehog and vitronectin. *PLoS One* (2012) 7(11):e49015.
 - ❖ Brady RO, Kanfer JN, Mock MB, Fredrickson DS. The metabolism of sphingomyelin II. Evidence of an enzymatic deficiency in Niemann-Pick disease. *PNAS USA* (1966) 366-369.
 - ❖ Bremova T, Malinova V, Amraoui Y, Mengel E, Reinke J, Kolnikova M, Kolníková M, Strupp M. Acetyl-DL-leucine in Niemann-Pick type C: a case series. *Neurology* (2015) 85:1368–1375.
 - ❖ Buard I, Pfrieger FW. Relevance of neuronal and glial NPC1 for synaptic input to cerebellar Purkinje cells. *Molecular and Cellular Neuroscience* (2014) 61:65–71.
 - ❖ Buckner RL. The cerebellum and cognitive function: 25 years of insight from anatomy and neuroimaging. *Neuron* (2013) 80:807–815.
 - ❖ Buffo A, Rossi F. Origin, lineage and function of cerebellar glia. *Progress in Neurobiology* (2013) 109:42–63.
 - ❖ Bushong EA, Martone ME, Jones YZ, Ellisman MH: Protoplasmic astrocytes in CA1 stratum radiatum occupy separate anatomical domains. *Journal of Neuroscience* (2002) 22:183–192.
 - ❖ Bustamante A, Dominguez C, Rodriguez-Sureda V, Vilches A, Penalba A, Giralt D, Garcia Berrocoso T, Llombart V, Flores A, Rubiera M, Molina C, Alvarez-Sabin J, Montaner J. Prognostic value of plasma chitotriosidase activity in acute stroke patients. *Internal Journal of Stroke* (2014) 9:910–916.
 - ❖ Cajal R.Y.S. *Histologie du Système Nerveux de l’Homme et des Vertébrés*. Maloine, Paris, France (1909, 1911).
 - ❖ Camargo F, Erickson RP, Garver WS, Hossain GS, Carbone PN, Heidenreich RA, Blanchard J. Cyclodextrins in the treatment of a mouse model of Niemann-Pick C disease. *Life Science* (2001) 70:131–42.
 - ❖ Cameron DB, Kasai K, Jiang Y, Hu T, Saeki Y, Komuro H. Four distinct phases of basket/stellate cell migration after entering their final destination (the molecular layer) in the developing cerebellum. *Developmental Biology* (2009) 332: 309-324.
 - ❖ Caporali P, Cutuli D, Gelfo F, Laricchiuta D, Foti F, De Bartolo P, Mancini L, Angelucci F, Petrosini L. Pre-reproductive maternal enrichment influences offspring developmental trajectories: motor behavior and neurotrophin expression. *Frontiers in Behavioral Neuroscience* (2014) 8:195.
 - ❖ Carletti B, Rossi F. Neurogenesis in the cerebellum. *Neuroscientist* (2008) 14:91–100.

- ❖ Carstea ED, Morris JA, Coleman KG, Loftus SK, Zhang D, Cummings C, Gu J, Rosenfeld MA, Pavan WJ, Krizman DB, Nagle J, Polymeropoulos MH, Sturley SL, Ioannou Ya, Higgins ME, Comly M, Cooney A, Brown A, Kanetski CR, Blanchette Makie EJ, Dwyer NK, Neufeld EB, Chang TY, Liscum L, Strauss JF 3rd, Ohono K, Zeigler M, Carmi R, Sokol J, Markie D, O'Neill RR, van Diggelen OP, Elleder M, Patterson MC, Brady Ro, Vanier MT, Pantchev PG, Tagle DA. Niemann-Pick C1 disease gene: homology to mediators of cholesterol homeostasis. *Science* (1997) 277:228-231.
- ❖ Caviness Jr VS, Takahashi T, Nowakowski RS. Numbers, time and neocortical neurogenesis: a general developmental and evolutionary model. *Trends in Neurosciences* (1995) 18:379–83.
- ❖ Ceccarelli M, Micheli L, D'Andrea G, De Bardi M, Scheijen B, Ciotti M, Leonardi L, Luvisetto S, Tirone F. Altered cerebellum development and impaired motor coordination in mice lacking the Btg1 gene: Involvement of cyclin D1. *Developmental Biology* (2015) 408:109–125.
- ❖ Cerminara NL, Lang EJ, Sillitoe RV, Apps R. Redefining the cerebellar cortex as an assembly of non-uniform Purkinje cell microcircuits. *Nature Reviews Neuroscience* (2015) 16: 79–93.
- ❖ Chamoun Z, Mann RK, Nellen D, von Kessler DP, Bellotto M, Beachy PA, Basler K. Skinny hedgehog, an acyltransferase required for palmitoylation and activity of the hedgehog signal. *Science* (2001) 293(5537):2080–2084.
- ❖ Chen C, Kano M, Abeliovich A, Chen L, Bao S, Kim JJ, Hashimoto K, Thompson RF, Tonegawa S. Impaired motor coordination correlates with persistent multiple climbing fiber innervation in PKC gamma mutant mice. *Cell* (1995) 83:1233–1242.
- ❖ Chikh K, Vey S, Simonot C, Vanier MT, Millat G. Niemann-Pick type C disease: importance of N-glycosylation sites for function and cellular location of the NPC2 protein. *Molecular Genetics and Metabolism* (2004) 83(3):220-230.
- ❖ Christopherson KS, Ullian EM, Stokes CC, Mallowney CE, Hell JW, Agah A, Lawler J, Moshier DF, Bornstein P, Barres BA. Thrombospondins are astrocyte-secreted proteins that promote CNS synaptogenesis. *Cell* (2005) 120:421–433.
- ❖ Chuang WL, Pacheco J, Cooper S, McGovern MM, Cox GF, Keutzer J, Zhang XK, Lyso-sphingomyelin is elevated in dried blood spots of Niemann-Pick B patients. *Molecular Genetics and Metabolism* (2014) 111(2):209-211.
- ❖ Chuang WL, Pacheco J, Zhang XK, Martin MM, Biski CK, Keutzer JM, Wenger DA, Caggana M, Orsini JJ Jr., Determination of psychosine concentration in dried blood spots from newborns that were identified via newborn screening to be at risk for Krabbe disease. *Clinica Chimica Acta* (2013) 419:73–76.
- ❖ Clarac F, Brocard F, Vinay L. The maturation of locomotor networks. *Progress in Brain Research* (2004) 143:57–66.
- ❖ Clark BA, Barbour B. Currents evoked in Bergmann glial cells by parallel fibre stimulation in rat cerebellar slices. *The Journal of Physiology* (1997) 502:(2)335–350.
- ❖ Cluzeau CV, Watkins-Chow DE, Fu R, Borate B, Yanjanin N, Dail MK, Davidson CD, Walkley SU, Ory DS, Wassif CA, Pavan WJ, Porter FD, 2012. Microarray expression analysis and identification of serum biomarkers for Niemann-Pick disease, type C1. *Human Molecular Genetics* (2012) 21(16):3632-3646.
- ❖ Cohen MM Jr. The hedgehog signaling network. *American Journal of Medical Genetics* (2004) 123A(1):5–28.

- ❖ Collin L, Doretto S, Malerba M, Ruat M, Borrelli E. Oligodendrocyte ablation affects the coordinated interaction between granule and Purkinje neurons during cerebellum development. *Experimental Cell Research* (2007) 313:2946–2957.
- ❖ Consalez GG, Hawkes R. The compartmental restriction of cerebellar interneurons. *Frontiers in Neural Circuits* (2012) 6:123.
- ❖ Corrales JD, Rocco GL, Blaess S, Guo Q, Joyner AL. Spatial pattern of sonic hedgehog signaling through Gli genes during cerebellum development. *Development* (2004) 131(22):5581-5590.
- ❖ Crane JM, Tamm LK. Role of Cholesterol in the Formation and Nature of Lipid Rafts in Planar and Spherical Model Membranes. *Biophysical Journal* (2004) 86(5): 2965–2979.
- ❖ Crocker AC, Farber S. Niemann-Pick disease: a review of eighteen patients. *Medicine (Baltimore)* (1958) 37:1-95.
- ❖ Crocker AC. The cerebral defect in Tay-Sachs disease and Niemann-Pick disease. *Journal of Neurochemistry* (1961) 7:69-80.
- ❖ Crook J, Hendrickson A, Robinson FR. Co-localization of glycine and gaba immunoreactivity in interneurons in Macaca monkey cerebellar cortex. *Neuroscience* (2006) 141:1951–1959.
- ❖ Cuadros MA, Moujahid A, Quesada A, Navascués J. Development of microglia in the quail optic tectum. *Journal of Comparative Neurology* (1994) 348:207-224
- ❖ Cuadros MA, Rodríguez-Ruiz J, Calvente R, Almendros A, Marín-Teva JL, Navascués J. Microglia development in the quail cerebellum. *Journal of Comparative Neurology* (1997) 389:390-401.
- ❖ Cunha C, Brambilla R, Thomas KL. A simple role for BDNF in learning and memory? *Frontiers in Molecular Neuroscience* (2010) 3:1.
- ❖ D'Angelo E, Casali S. Seeking a unified framework for cerebellar function and dysfunction: from circuit operations to cognition. *Frontiers in Neural Circuits* (2013) 6:1–23.
- ❖ Davidson CD, Ali NF, Micsenyi MC, Stephney G, Renault S, Dobrenis K, Ory DS, Vanier MT, Walkley SU. Chronic cyclodextrin treatment of murine Niemann-Pick C disease ameliorates neuronal cholesterol and glycosphingolipid storage and disease progression. *PLOS One* (2009) 4:e6951.
- ❖ Davies JP, Levy B, Ioannou YA. Evidence for a Niemann-pick C (NPC) gene family: identification and characterization of NPC1L1. *Genomics* (2000) 65(2):137-145.
- ❖ Davis ME, Brewster ME. Cyclodextrin-based pharmaceuticals: past, present and future. *Nature Reviews Drug Discovery* (2004) 3:1023–1035.
- ❖ De Luca A, Cerrato V, Fuca E, Parmigiani E, Buffo A, Leto K. Sonic hedgehog patterning during cerebellar development. *Cellular and Molecular Life Sciences* (2016) 73:291–303.
- ❖ de Souza SL, Nogueira MI, de Jesus Deiró TC, de Castro FM, da Silva CM, da Silva MC, de Lirac LO, Azmitiab EC, de Castroc RM. Differential effects on somatic and reflex development by chronic clomipramine treatment. *Physiology & Behavior* (2004) 82:375–379.
- ❖ De Zeeuw CI, Hoogland TM. Reappraisal of Bergmann glial cells as modulators of cerebellar circuit function. *Frontiers in Cellular Neuroscience* (2015) 9:246.
- ❖ Dehart DB, Lanoue L, Tint GS, Sulik KK. Pathogenesis of malformations in a rodent model for Smith-Lemli-Opitz Syndrome. *American Journal of Medical Genetics* (1997) 68: 328-337.

- ❖ Dehorter N, Vinay L, Hammond C, Ben-Ari Y. Timing of developmental sequences in different brain structures: physiological and pathological implications. *European Journal of Neuroscience* (2012) 35:1846–1856.
- ❖ Dieudonné S, Dumoulin A. Serotonin-driven long-range inhibitory connections in the cerebellar cortex. *Journal of Neuroscience* (2000) 20:1837–48
- ❖ Dieudonné S. Submillisecond kinetics and low efficacy of parallel fibre-Golgi cell synaptic currents in the rat cerebellum. *The Journal of Physiology* (1999) 510(3):845–866
- ❖ Doretto S, Malerba M, Ramos M, Ikrar T, Kinoshita C, De Mei C, Tirota E, Xu X, Borrelli E. Oligodendrocytes as regulators of neuronal networks during early postnatal development. *PLOS One* (2011) 6:e19849.
- ❖ Dumoulin A, Triller A, Dieudonne S. IPSC kinetics at identified GABAergic and mixed GABAergic and glycinergic synapses onto cerebellar Golgi cells. *Journal of Neuroscience* (2001) 21:6045–6057.
- ❖ Dvorakova L, Sikora J, Hrebicek M, Hulkova H, Bouckova M, Stolnaja L, Elleder M. Subclinical course of adult visceral Niemann–Pick type C1 disease. A rare or underdiagnosed disorder? *Journal of Inherited Metabolic Disease* (2006) 29:591–597.
- ❖ Eccles JC, Ito M, Szentágothai J. The Cerebellum as a Neuronal Machine. *Springer-Verlag, Berlin* (1967).
- ❖ Echelard Y, Epstein DJ, St-Jacques B, Shen L, Mohler J, McMahon JA, McMahon AP. Sonic hedgehog, a member of a family of putative signaling molecules, is implicated in the regulation of CNS polarity. *Cell* (1993) 75(7):1417–1430.
- ❖ Elmonem MA, Amin HS, El-Essawy RA, Mehaney DA, Nabil M, Kamel LN, Farid IM. Association of chitotriosidase enzyme activity and genotype with the risk of nephropathy in type 2 diabetes. *Clinical Biochemistry* (2016) 49:444–448.
- ❖ Erbel-Sieler C, Dudley C, Zhou Y, Wu X, Estill SJ, Han T, Diaz-Arrastia R, Brunskill EW, Potter SS, McKnight SL. Behavioral and regulatory abnormalities in mice deficient in the NPAS1 and NPAS3 transcription factors. *PNAS USA* (2004) 101:13648–13653.
- ❖ Erickson RP. Current controversies in Niemann-Pick C1 disease: steroids or gangliosides; neurons or neurons and glia. *Journal of Applied Genetics* (2013) 54(2):215–224.
- ❖ Fauquier T, Romero E, Picou F, Chatonnet F, Nguyen XN, Quignodon L, Flamant F. Severe impairment of cerebellum development in mice expressing a dominant-negative mutation inactivating thyroid hormone receptor alpha1 isoform. *Developmental Biology* (2011) 356:350–358.
- ❖ Finckbone V, Oomman SS, Strahlendorf HK, Strahlendorf JC. Regional differences in the temporal expression of non-apoptotic caspase-3-positive Bergmann glial cells in the developing rat cerebellum. *Frontiers in Neuroanatomy* (2009) 3:3.
- ❖ Fiorenza MT, Dardis A, Canterini S, Erickson RP. Cholesterol metabolism-associated molecules in late onset Alzheimer's disease. *Journal of Biological Regulators & Homeostatic Agents* (2013) 27:23–35.
- ❖ Fox CA, Barnard JW. A quantitative study of the Purkinje cell dendritic branchlets and their relationship to afferent fibres. *Journal of Anatomy* (1957) 91:299–313.
- ❖ Friedland N, Liou HL, Lobel P, Stock AM. Structure of a cholesterol-binding protein deficient in Niemann-Pick type C2 disease. *PNAS USA* (2003) 100(5):2512–2517.

- ❖ Fuccillo M, Joyner AL, Fishell G. Morphogen to mitogen: the multiple roles of hedgehog signaling in vertebrate neural development. *Nature Reviews Neuroscience* (2006) 7(10):772–783.
- ❖ Fujita K, Yamauchi M, Matsui T, Titani K, Takahashi H, Kato T, Isomura G, Ando M, Nagata Y. Increase of glial fibrillary acidic protein fragments in the spinal cord of motor neuron degeneration mutant mouse. *Brain Research* (1998) 785:31–40.
- ❖ García-Robles AA, Company-Albir MJ, Megías-Vericat JE, Fernández-Megía MJ, Pérez-Miralles FC, López-Briz E, Alcalá-Vicente C, Galeano I, Casanova B, Poveda JL. Use of 2 hydroxypropyl-beta-cyclodextrin therapy in two adult Niemann Pick Type C patients. *Journal of the Neurological Sciences* (2016) 366:65–67.
- ❖ Garver WS, Francis GA, Jelinek D, Shepherd G, Flynn J, Castro G, Walsh C, Coppock DL, Pettit KM, Heidenreich RA, Meaney. The National Niemann–Pick C1 disease database: report of clinical features and health problems. *American Journal of Medical Genetics* (2007) 143:1204–1211.
- ❖ German DC, Liang CL, Song T, Yazdani U, Xie C, Dietschy JM. Neurodegeneration in the Niemann-Pick C mouse: glial involvement. *Neuroscience* (2002) 109:437–50.
- ❖ Ginhoux F, Prinz M. Origin of microglia: current concepts and past controversies. *Cold Spring Harbor Perspectives in Biology* (2015) 7:a020537.
- ❖ Ginhoux, F, Greter M, Leboeuf M, Nandi S, See P, Gokhan S, Mehler MF, Conway SJ, Ng LG, Stanley ER, Samokhvalov IM, Merad M. Fate mapping analysis reveals that adult microglia derive from primitive macrophages. *Science* (2010) 330:841–845.
- ❖ Goldmann T, Wieghofer P, Müller PF, Wolf Y, Varol D, Yona S, Brendecke SM, Kierdorf K, Staszewski O, Datta M, Luedde T, Heikenwalder M, Jung S, Prinz M. A new type of microglia gene targeting shows TAK1 to be pivotal in CNS autoimmune inflammation. *Nature Neuroscience* (2013) 16(11):1618–1626.
- ❖ Gordon GR, Mulligan SJ, MacVicar BA. Astrocyte control of the cerebrovasculature. *Glia* (2007) 55:1214–1221.
- ❖ Greer WL, Donson MJ, Girouard GD, Byers DM, Riddell DC, Neumann PE. Mutations in NPC1 highlight a conserved NPC1-specific cysteine-rich domain. *American Journal of Human Genetics* (1999) 65:1252–1260.
- ❖ Griese M, Brasch F, Aldana VR, Cabrera M, Goelnitz U, Ikonen E, Karam BJ, Liebisch G, Linder MD, Lohse P, Meyer W, Schmitz G, Pamir A, Ripper J, Rolfs A, Schams A, Lezana FJ. Respiratory disease in Niemann–Pick type C2 is caused by pulmonary alveolar proteinosis. *Clinical Genetics* (2010) 77:119–130.
- ❖ Griffin LD, Gong W, Verot L, Mellon SH. Niemann-Pick type C disease involves disrupted neurosteroidogenesis and responds to allopregnanolone. *Nature Medicine* (2004) 10:704–711.
- ❖ Grimes JM, Ricci LA, Melloni RH., Jr Glutamic acid decarboxylase (GAD65) immunoreactivity in brains of aggressive, adolescent anabolic steroid-treated hamsters. *Hormones and Behavior* (2003) 44:271–80.
- ❖ Grosche J, Matyash V, Moller T, Verkhratsky A, Reichenbach A, Kettenmann H. Microdomains for neuron–glia interaction: parallel fiber signaling to Bergmann glial cells. *Nature Neuroscience* (1999) 2:139–143.
- ❖ Guijarro P, Simo S, Pascual M, Abasolo I, Del Rio JA, Soriano E. Netrin1 exerts a chemorepulsive effect on migrating cerebellar interneurons in a Dccindependent way. *Molecular and Cellular Neuroscience* (2006) 33:389–400.

- ❖ Halassa MM, Fellin T, Haydon PG. The tripartite synapse: roles for gliotransmission in health and disease. *Trends in Molecular Medicine* (2007) 13:54–63.
- ❖ Hallonet ME, Le Douarin NM. Tracing neuroepithelial cells of the mesencephalic and metencephalic alar plates during cerebellar ontogeny in quail chick chimaeras. *Europe Journal of Neuroscience* (1993) 5:1145–1155.
- ❖ Harauz G, Boggs JM. Myelin management by the 18.5-kDa and 21.5-kDa classic myelin basic protein isoforms. *Journal of Neurochemistry* (2013) 125:334–361.
- ❖ Hastings C, Request for intrathecal delivery of HPBCD for Niemann Pick Type C patients, Caroline Hastings, M.D. Principal Investigator Department of Pediatric Hematology Oncology Children's Hospital & Research Center Oakland Submission. Date to FDA: August 13 (2010). <http://addiandcassi.com/wordpress/wp-content/uploads/HempelCyclodextrin-Intrathecal-FDA-Filing-2010-Aug.pdf>
- ❖ Hatten ME. Central nervous system neuronal migration. *Annual Review of Neuroscience* (1999) 22:511–539.
- ❖ Henderson LP, Lin L, Prasad A, Paul CA, Chang TY, Maue RA. Embryonic striatal neurons from Niemann-Pick type C mice exhibit defects in cholesterol metabolism and neurotrophin responsiveness. *The Journal of Biological Chemistry* (2000) 275:20179–20187.
- ❖ Herz J. Alipoprotein E receptors in the nervous system. *Current Opinion in Lipidology* (2009) 20:190-196.
- ❖ Heyser CJ. Assessment of developmental milestones in rodents. *Current Protocols in Neuroscience* (2004) Chapter 8: Unit 8.18.
- ❖ Higgins JJ, Patterson MC, Dambrosia JM. A clinical staging classification for type C Niemann–Pick disease. *Neurology* (1992) 42:2286–2290.
- ❖ Hoeffel G, Wang Y, Greter M, See P, Teo P, Malleret B, Leboeuf M, Low D, Oller G, Almeida F, Choy SH, Grisotto M, Renia L, Conway SJ, Stanley ER, Chan JK, Ng LG, Samokhvalov IM, Merad M, Ginhoux F. Adult Langerhans cells derive predominantly from embryonic fetal liver monocytes with a minor contribution of yolk sac-derived macrophages. *The Journal of Experimental Medicine* (2012) 209:1167–1181.
- ❖ Hoogland TM, Kuhn B. Recent developments in the understanding of astrocyte function in the cerebellum in vivo. *Cerebellum* (2010) 9:264–271.
- ❖ Hughes V. Microglia: the constant gardeners. *Nature* (2012) 485:570–572.
- ❖ Hulette CM, Earl NL, Anthony DC, Crain BJ. Adult onset Niemann–Pick disease type C presenting with dementia and absent organomegaly. *Clinical Neuropathology* (1992) 11:293-297.
- ❖ Iadecola C, Nedergaard M. Glial regulation of the cerebral microvasculature. *Nature Neuroscience* (2007) 10:1369–1376.
- ❖ Ichikawa R, Miyazaki T, Kano M, Hashikawa T, Tatsumi H, Sakimura K, Mishina M, et al. Distal extension of climbing fiber territory and multiple innervation caused by aberrant wiring to adjacent spiny branchlets in cerebellar Purkinje cells lacking glutamate receptor delta 2. *Journal of Neuroscience* (2002) 22:8487–8503.
- ❖ Iino M, Goto K, Kakegawa W, Okado H, Sudo M, Ishiuchi S, Miwa A, Takayasu Y, Saito I, Tsuzuki K, Ozawa S. Glia-synapse interaction through Ca²⁺-permeable AMPA receptors in Bergmann glia. *Science* (2001) 292: 926–929.
- ❖ Ikonen E. Mechanisms for cellular cholesterol transport: defects and human disease. *Physiological Reviews* (2006) 86(4):1237-61.

- ❖ Imrie J, Dasgupta S, Besley GT, Harris C, Heptinstall L, Knight S, Vanier MT, Fensom AH, Ward C, Jacklin E, Whitehouse C, Wraith JE. The natural history of Niemann–Pick disease type C. *UK. Journal of Inherited Metabolic Disease* (2007) 30:51-59.
- ❖ Imrie J, Vijayaraghaven S, Whitehouse C, Harris S, Heptinstall L, Church H, Cooper A, Besley GT, Wraith JE. Niemann–Pick disease type C in adults. *Journal of Inherited Metabolic Disease* (2002) 25:491-500.
- ❖ Infante RE, Wang ML, Radhakrishnan A, Kwon HJ, Brown MS, Goldstein JL. NPC2 facilitates bidirectional transfer of cholesterol between NPC1 and lipid bilayers, a step in cholesterol egress from lysosomes. *PNAS USA* (2008) 105:15287-15292.
- ❖ Ioannou YA, Yiannis A. Guilty until proven innocent: the case of NPC1 and cholesterol. *Trends in Biochemical Sciences* (2005) 30(9):498–505.
- ❖ Ito I, Ong RCY, Raman B, Stopfer M. Sparse odor representation and olfactory learning. *Nature Neuroscience* (2008) (10):1177-1184.
- ❖ Ito M. Cerebellar circuitry as a neuronal machine. *Progress in Neurobiology* (2006) 78:272–303.
- ❖ Iturriaga C, Pineda M, Fernández-Valero EM, Vanier MT, Coll MJ. Niemann-Pick C disease in Spain: clinical spectrum and development of a disability scale. *Journal of Neurological Sciences* (2006) 249(1):1-6.
- ❖ Jakoby P, Schmidt E, Ruminot I, Gutiérrez R, Barros LF, Deitmer JW. Higher transport and metabolism of glucose in astrocytes compared with neurons: a multiphoton study of hippocampal and cerebellar tissue slices. *Cerebral Cortex* (2014) 24:222–231.
- ❖ Jan MM, Camfield PR. Nova Scotia Niemann–Pick disease (type D): clinical study of 20 cases. *Journal of Child Neurology* (1998) 13:75-78.
- ❖ Jiang X, Sidhu R, Mydock-McGrane L, Hsu FF, Covey DF, Scherrer DE, Earley B, Gale SE, Farhat NY, Porter FD, Dietzen DJ, Orsini JJ, Berry-Kravis E, Zhang X, Reunert J, Marquardt T, Runz H, Giugliani R, Schaffer JE, Ory DS. Development of a bile acid-based newborn screen for Niemann-Pick disease type C. *Science Translational Medicine* (2016) 8:337-363.
- ❖ Jiang X, Sidhu R, Porter FD, Yanjanin NM, Speak AO, te Vruchte DT, Platt FM, Fujiwara H, Scherrer DE, Zhang J, Dietzen DJ, Schaffer JE, Ory DS. A sensitive and specific LC-MS/MS method for rapid diagnosis of Niemann-Pick C1 disease from human plasma. *Journal of Lipid Research* (2011) 52:1435–1445.
- ❖ Jordan FL, Thomas WE. Brain macrophages: questions of origin and interrelationship. *Brain Research Reviews* (1988) 13:165-178.
- ❖ Kapfhammer JP, Schwab ME. Inverse patterns of myelination and GAP-43 expression in the adult CNS: neurite growth inhibitors as regulators of neuronal plasticity? *Journal of Comparative Neurology* (1994) 340:194–206.
- ❖ Karten B, Campenot RB, Vance DE, Vance JE. Expression of ABCG1, but not ABCA1, correlates with cholesterol release by cerebellar astroglia. *Journal of Biological Chemistry* (2001) 281: 4049-4057.
- ❖ Karten B, Campenot RB, Vance DE, Vance JE. The Niemann-Pick C1 protein in recycling endosomes of presynaptic nerve terminals. *Journal of Biological Chemistry* (2006) 47:504–514.
- ❖ Kelly DA, Portmann B, Mowat AP, Sherlock S, Lake BD. Niemann–Pick disease type C: diagnosis and outcome in children, with particular reference to liver disease. *Journal of Pediatrics* (1993) 123:242-247.

- ❖ Kierdorf K, Erny D, Goldmann T, Sander V, Schulz C, Perdiguero EG, Wieghofer P, Heinrich A, Riemke P, Hölscher C, Müller DN, Luckow B, Brocker T, Debowski K, Fritz G, Opendakker G, Diefenbach A, Biber K, Heikenwalder M, Geissmann F, Rosenbauer F, Prinz M. Microglia emerge from erythromyeloid precursors via Pu.1- and Irf8-dependent pathways. *Nature Neuroscience* (2013) 16:273–280.
- ❖ Kim SJ, Lee BH, Lee YS, Kang KS. Defective cholesterol traffic and neuronal differentiation in neural stem cells of Niemann-Pick Type C disease improved by valproic acid, a histone deacetylase inhibitor. *Biochemical and Biophysical Research Communications* (2007) 360:593–599.
- ❖ Kita Y, Kawakami K, Takahashi Y, Murakami F. Development of cerebellar neurons and glia revealed by in utero electroporation: golgi-like labeling of cerebellar neurons and glia. *PLOS One* (2013) 8:e70091.
- ❖ Klarner B, Klunemann HH, Lurding R, Aslanidis C, Rupprecht R. Neuropsychological profile of adult patients with Niemann–Pick C1 (NPC1) mutations. *Journal of Inherited Metabolic Disease* (2007) 30:60–67.
- ❖ Klinke G, Rohrbach M, Giugliani R, Burda P, Baumgartner MR, Tran C, Gautschi M, Mathis D, Hersberger M. LC-MS/MS based assay and reference intervals in children and adolescents for oxysterols as a biomarker for Niemann-Pick A/B disease. *20th ESGLD Workshop, Abstracts, Unpublished results, Naples, Italy, (2015), pp. 92.*
- ❖ Klünemann HH, Elleder M, Kaminski WE, Snow K, Peyser JM, O'Brien JF, Munoz D, Schmitz G, Klein HE, Pendlebury WW. Frontal lobe atrophy due to a mutation in the cholesterol binding protein HE1/NPC2. *Annals of Neurology* (2002) 52:743–749
- ❖ Koppel I, Aid-Pavlidis T, Jaanson K, Sepp M, Pruunsild P, Palm K, Timmusk T. Tissue-specific and neural activity-regulated expression of human BDNF gene in BAC transgenic mice. *BMC Neuroscience* (2009) 25:10:68.
- ❖ Korbo L, Andersen BB, Ladefoged O, Møller A. Total numbers of various cell types in rat cerebellar cortex estimated using an unbiased stereological method. *Brain Research* (1993) 609:262–268.
- ❖ Koshimizu H, Kiyosue K, Hara T, Hazama S, Suzuki S, Uegaki K, Nagappan G, Zaitsev E, Hirokawa T, Tatsu Y, Ogura A, Lu B, Kojima M. Multiple functions of precursor BDNF to CNS neurons: negative regulation of neurite growth, spine formation and cell survival. *Molecular Brain* (2009) 2:27.
- ❖ Kosters A, Jirsa M, Groen AK. Genetic background of cholesterol gallstone disease. *Biochimica et Biophysica Acta* (2003) 1637(1):1–19.
- ❖ Kuchar L, Asfaw B, Poupetova H, Lugowska A, Ledvinova J. Elevated plasma lysosphingomyelin as a biomarker for Niemann-Pick A/B disease. *20th ESGLD Workshop, Abstracts, Unpublished results, Naples, Italy, 2015, pp. 92.*
- ❖ Lachmann RH, Platt FM. Substrate reduction therapy for glycosphingolipid storage disorders. *Expert Opinion on Investigational Drugs* (2001)10(3):455–466.
- ❖ Lachmann RH, te Vruchte D, Lloyd-Evans E, Reinkensmeier G, Sillence DJ, Fernandez-Guillen L, Dwek RA, Butters TD, Cox TM, Platt FM. Treatment with miglustat reverses the lipid-trafficking defect in Niemann-Pick disease type C. *Neurobiology of Disease* (2004) 16(3):654–658.
- ❖ Lainé J, Axelrad H. Morphology of the Golgi-impregnated Lugaro cell in the rat cerebellar cortex: a reappraisal with a description of its axon. *Journal of Comparative Neurology* (1996) 375:618–640.
- ❖ Lainé J, Axelrad H. The candelabrum cell: a new interneuron in the cerebellar cortex. *Journal of Comparative Neurology* (1994) 339:159–173.
- ❖ Lanoue L, Dehart DB, Hinsdale ME, Maeda N, Tint GS, Sulik KK. Limb, genital, CNS, and facial malformations result from gene/environment-induced cholesterol

- deficiency: further evidence for a link to sonic hedgehog. *American Journal of Medical Genetics* (1997) 73:24–31.
- ❖ Larsen LB, Ravn P, Boisen A, Berglund L, Petersen TE. Primary structure of EPV20, a secretory glycoprotein containing a previously uncharacterized type of domain. *European Journal of Biochemistry* (1997) 243(1-2):437-441.
 - ❖ Lawson LJ, Perry VH, Dri P, Gordon S. Heterogeneity in the distribution and morphology of microglia in the normal adult mouse brain. *Neuroscience* (1990) 39:151–170.
 - ❖ Lee JJ, Ekker SC, von Kessler DP, Porter JA, Sun BI, Beachy PA. Autoproteolysis in hedgehog protein biogenesis. *Science* (1994) 266(5190):1528–1537.
 - ❖ Lee YB, Du S, Rhim H, Lee EB, Markelonis GJ, Oh TH. Rapid increase in immunoreactivity to GFAP in astrocytes in vitro induced by acidic pH is mediated by calcium influx and calpain I. *Brain Research* (2000) 864:220–229.
 - ❖ Lengyel D, Weissert M, Schmid L, Gottlob I. Eye movement abnormalities as a sign for the diagnosis in Niemann–Pick disease type C. *Klinische Monatsblätter für Augenheilkunde* (1999) 214:50-52.
 - ❖ Lin CY, Louis ED, Faust PL, Koeppen AH, Vonsattel JP, Kuo SH. Abnormal climbing fibre-Purkinje cell synaptic connections in the essential tremor cerebellum. *Brain* (2014) 137:3149–3159.
 - ❖ Lin SC, Huck JH, Roberts JD, Macklin WB, Somogyi P, Bergles DE. Climbing fiber innervation of NG2-expressing glia in the mammalian cerebellum. *Neuron* (2005) 46:773–785.
 - ❖ Liscum L, Munn NJ. Intracellular cholesterol transport. *Biochimica et Biophysica Acta* (1999) 1438:19–37.
 - ❖ Liscum L. Niemann–Pick Type C Mutations Cause Lipid Traffic jam. *Traffic* (2000) 1(3):218–225.
 - ❖ Liu B, Li H, Repa JJ, Turley SD, Dietschy JM. Genetic variations and treatments that affect the lifespan of the NPC1 mouse. *Journal of Lipid Research* (2008) 49:663–669.
 - ❖ Liu B, Ramirez CM, Miller AM, Repa JJ, Turley SD, Dietschy JM. Cyclodextrin overcomes the transport defect in nearly every organ of NPC1 mice leading to excretion of sequestered cholesterol as bile acid. *Journal of Lipid Research* (2010) 51:933–944.
 - ❖ Liu B. Therapeutic potential of cyclodextrins in the treatment of Niemann–Pick type C disease. *Clinical Lipidology* (2012) 7(3): 289–301.
 - ❖ Liu N, Tengstrand EA, Chourb L, Hsieh FY. Di-22:6-bis(monoacylglycerol)phosphate: a clinical biomarker of drug-induced phospholipidosis for drug development and safety assessment. *Toxicology and Applied Pharmacology* (2014) 279:467–476.
 - ❖ Liu Y, Zhou J. Oligodendrocytes in neurodegenerative diseases. *Frontiers of Biology* (2013) 8(2):127-133.
 - ❖ Llinas RR, Walton KD, Lang EJ. Cerebellum. In: Shepherd GM, editor. The synaptic organization of the brain. *New York: Oxford UP* (2004) pp. 271–310.
 - ❖ Lloyd-Evans E, Morgan AJ, He X, Smith DA, Elliot-Smith E, Sillence DJ, Churchill GC, Schuchman EH, Galione A, Platt FM. Niemann Pick disease C1 is a sphingosine storage disease that cause dysregulation of lysosomal calcium. *Nature Medicine* (2008) 14:1247-1255.

- ❖ Loftus SK, Morris JA, Carstea ED, Gu JZ, Cummings C, Brown A, Ellison J, Ohno K, Rosenfeld MA, Tagle DA, Pentchev PG, Pavan WJ. Murine model of Niemann-Pick C disease: mutation in cholesterol homeostasis gene. *Science* (1997) 277:232-235.
- ❖ Lordkipanidze T, Dunaevsky A. Purkinje cell dendrites grow in alignment mammalian central nervous system. *Physiological Reviews* (2001) 81:871–927.
- ❖ Lordkipanidze, T., Dunaevsky, A. Purkinje cell dendrites grow in alignment with Bergmann glia. *Glia* (2005) 51:229–234.
- ❖ Lowenthal AC, Cummings JF, Wenger DA, Thrall MA, Wood PA, de Lahunta A. Feline sphingomyelinosis resembling Niemann-Pick disease type C. *Acta Neuropathologica* (1990) 81:189-197.
- ❖ Lu DY, Che JY, Lu TR, Ding J. Ebola Origin and Therapies. *Metabolomics* (2015) 5:e138.
- ❖ Lyseng-Williamson KA. Miglustat: a review of its use in Niemann-Pick disease type C. *Drugs* (2014) 74(1):61-74.
- ❖ Maalouf K, Das AM, Naim HY. Niemann-Pick type C: restoration of lipid rafts and other biochemical anomalies by Nbutyl-deoxinojirimycin. *Journal of Inherited Metabolic Disease* (2011) 34(3):S193.
- ❖ Maarup T, Chen A, Porter F, Farhat N, Ory D, Sidhu R, Jiang X, Dickson PI. Intrathecal 2-hydroxypropyl-beta-cyclodextrin in a single patient with Niemann-Pick C1. *Molecular Genetics and Metabolism* (2015) 116: 75–79.
- ❖ Macías-Vidal J, Rodríguez-Pascau L, Sánchez-Ollé G, Lluch M, Vilageliu L, Grinberg D, Coll MJ; Spanish NPC Working Group. Molecular analysis of 30 Niemann-Pick type C patients from Spain. *Clin. Genet.* (2011) 80:39–49.
- ❖ Maeda N, Ichihara-Tanaka K, Kimura T, Kadomatsu K, Muramatsu T, Noda M. A receptor-like protein-tyrosine phosphatase PTPz/RPTPb binds a heparin-binding growth factor midkine. *The Journal of Biological Chemistry* (1999) 274, 12474–12479.
- ❖ Maeda N, Matsui F, Oohira A. A chondroitin sulfate proteoglycan that is developmentally regulated in the cerebellar mossy fiber system. *Developmental Biology* (1992) 151:564–574.
- ❖ Maeda N, Nishiwaki T, Shintani T, Hamanaka H, Noda M. 6B4 proteoglycan/phosphacan, an extracellular variant of receptor-like protein-tyrosine phosphatase z/RPTPb, binds pleiotrophin/heparin-binding growth-associated molecule (HB-GAM). *The Journal of Biological Chemistry* (1996) 271:21446–21452.
- ❖ Maekawa M, Misawa Y, Sotoura A, Yamaguchi H, Togawa M, Ohno K, Nittono H, Kakiyama G, Lida T, Hofmann AF, Goto J, Shimada M, Mano N. LC/ESI-MS/MS analysis of urinary 3β-sulfooxy-7β-N-acetylglucosaminyl-5-cholen-24-oic acid and its amides: new biomarkers for the detection of Niemann-Pick type C disease. *Steroids* (2013) 78:967–972.
- ❖ Mangin JM, Gallo V. The curious case of NG2 cells: transient trend or game changer? *ASN Neuro* (2011) 3:e00052.
- ❖ Marazziti D, Di Pietro C, Golini E, Mandillo S, La Sala G, Matteoni R, Tocchini-Valentini GP. Precocious cerebellum development and improved motor functions in mice lacking the astrocyte cilium-, patched 1-associated Gpr3711 receptor. *PNAS USA* (2013) 110:16486–16491.

- ❖ Maricich SM, Herrup K. Pax-2 expression defines a subset of GABAergic interneurons and their precursors in the developing murine cerebellum. *Journal of Neurobiology* (1999) 41:281–294.
- ❖ Marini AM, Rabin SJ, Lipsky RH, Mocchetti I. Activity-dependent release of brain-derived neurotrophic factor underlies the neuroprotective effect of N-methyl-D-aspartate. *Journal of Biological Chemistry* (1998) 273(45):29394-29399.
- ❖ Marin-Teva JL, Dusart I, Colin C, Gervais A, van Rooijen N, and Mallat M. Microglia promote the death of developing Purkinje cells. *Neuron* (2004) 41:535–547.
- ❖ Martínez D, García L, Aguilera J, Ortega A. An acute glutamate exposure induces long-term down regulation of GLAST/EAAT1 uptake activity in cultured Bergmann glia cells. *Neurochemical Research* (2014) 39:142–149.
- ❖ Mathis C, Collin L, Borrelli E. Oligodendrocyte ablation impairs cerebellum development. *Development* (2003) 130:4709–4718.
- ❖ Matsumoto K, Wanaka A, Mori T, Taguchi A, Ishi N, Muramatsu H, Muramatsu T, Tohyama M. Localization of pleiotrophin and midkine in the postnatal developing cerebellum. *Neuroscience Letters* (1994) 178:216–220.
- ❖ Matsuo M, Togawa M, Hirabaru K, Mochinaga S, Narita A, Adachi M, Egashira M, Irie T, Ohno K. Effects of cyclodextrin in two patients with Niemann-Pick Type C disease. *Molecular Genetics and Metabolism* (2013) 108(1):76-81.
- ❖ Matsuo M, Shraishic K, Wadad K, Ishitsukac Y, Doia H, Maedab M, Mizoguchia T, Etoa J, Mochinagab S, Arimac H, Iriec T. Effects of intracerebroventricular administration of 2-hydroxypropyl-β-cyclodextrin in a patient with Niemann–Pick Type C disease. *Molecular Genetics and Metabolism Reports* (1):391–400.
- ❖ Maue RA, Burgess RW, Wang B, Wooley CM, Seburn KL, Vanier MT, Rogers MA, Chang CC, Chang TY, Harris BT, Graber DJ, Penatti CA, Porter DM, Szwergold BS, Henderson LP, Totenhagen JW, Trouard TP, Borbon IA, Erickson RP. A novel mouse model of Niemann-Pick type C disease carrying a D1005G-Npc1 mutation comparable to commonly observed human mutations. *Human Molecular Genetics* (2012) 21:730–750.
- ❖ Maxfield FR, Menon AK. Intracellular sterol transport and distribution. *Current Opinion in Cell Biology* (2006) 18:379–385.
- ❖ Mazzacuva F, Mills P, Mills K, Camuzeaux S, Gissen P, Nicoli ER, Wassif C, Te Vruchte D, Porter FD, Maekawa M, Mano N, Iida T, Platt F, Clayton PT. Identification of novel bile acids as biomarkers for the early diagnosis of Niemann-Pick C disease. *FEBS Letters* (2016) 590(11):1651-62.
- ❖ Meikle PJ, Hopwood JJ, Clague AE, Carey WF. Prevalence of lysosomal storage disorders. *JAMA* (1999) 281: 249-254.
- ❖ Meiner V, Shpitzen S, Mandel H, Klar A, Ben-Neriah Z, Zlotogora J, Sagi M, Lossos A, Bargal R, Sury V, Carmi R, Leitersdorf E, Zeigler M. Clinical-biochemical correlation in molecularly characterized patients with Niemann-Pick type C. *Genetics in Medicine* (2001) 3:343-348.
- ❖ Mengel E, Klünemann HH, Lourenço CM, Hendriksz CJ, Sedel F, Walterfang M, Kolb SA. Niemann-Pick disease type C symptomatology: an expert-based clinical description. *Orphanet Journal of Rare Disease* (2013) 8:166.
- ❖ Mertz K, Koscheck T, Schilling K. Brain-derived neurotrophic factor modulates dendritic morphology of cerebellar basket and stellate cells: an in vitro study. *Neuroscience* (2000) 97(2):303-310.

- ❖ Miale IL, Sidman RL. An autoradiographic analysis of histogenesis in the mouse cerebellum. *Experimental Neurology* (1961) 4:277–296.
- ❖ Middeldorp J, Hol EM. GFAP in health and disease. *Progress in Neurobiology* (2011) 93:421–443.
- ❖ Millat G, Bailo N, Molinero S, Rodriguez C, Chikh K, Vanier MT. Niemann-Pick C disease: use of denaturing high performance liquid chromatography for the detection of NPC1 and NPC2 genetic variations and impact on management of patients and families. *Molecular Genetics and Metabolism* (2005) 86:220-232.
- ❖ Millat G, Bailo N, Molinero S, Rodriguez C, Chikh K, Vanier MT. Niemann-Pick C disease: use of denaturing high performance liquid chromatography for the detection of NPC1 and NPC2 genetic variations and impact on management of patients and families. *Molecular Genetics and Metabolism* (2005) 86:220-232.
- ❖ Millat G, Marçais C, Rafi MA, Yamamoto T, Morris JA, Pentchev PG, Ohno K, Wenger DA, Vanier MT. Niemann-Pick C1 disease: the I1061T substitution is a frequent mutant allele in patients of Western European descent and correlates with a classic juvenile phenotype. *American Journal of Human Genetics* (1999) 65(5):1321-1329.
- ❖ Millat G, Marçais C, Rafi MA, Yamamoto T, Morris JA, Pentchev PG, Ohno K, Wenger DA, Vanier MT. Niemann-Pick C1 disease: the I1061T substitution is a frequent mutant allele in patients of Western European descent and correlates with a classic juvenile phenotype. *Am J Hum Genet.* (1999) 65(5):1321-1329.
- ❖ Millat G, Marçais C, Tomasetto C, Chikh K, Fensom AH, Harzer K, Wenger DA, Ohno K, Vanier MT. Niemann-Pick C1 disease: correlations between NPC1 mutations, levels of NPC1 protein, and phenotypes emphasize the functional significance of the putative sterol-sensing domain and of the cysteine-rich luminal loop. *American Journal of Human Genetics* (2001a) 68:1373-1385.
- ❖ Miller WL, Strauss JF 3rd. Molecular pathology and mechanism of action of the steroidogenic acute regulatory protein, StAR. *The Journal of Steroid Biochemistry and Molecular Biology* (1999) 69(1-6):131-141.
- ❖ Minghetti L, Levi G. Microglia as effector cells in brain damage and repair: focus on prostanoids and nitric oxide. *Progress in Neurobiology* (1998) 54:99–125.
- ❖ Miyake T, Fujiwara T, Fukunaga T, Takemura K, Kitamura T. Glial cell lineage in vivo in the mouse cerebellum. *Development Growth and Differentiation* (1995) 37:273–285.
- ❖ Miyata T, Ono Y, Okamoto M, Masaoka M, Sakakibara A, Kawaguchi A, Hashimoto M, Ogawa M. Migration, early axonogenesis, and Reelin dependent layer-forming behavior of early/posterior-born Purkinje cells in the developing mouse lateral cerebellum. *Neural Development* (2010) 5:23.
- ❖ Miyawaki S, Mitsouka S, Sakiyama T, Kitagawa T. Sphingomyelinosis, a new mutation in the mouse. A model of Niemann-Pick disease in humans. *Journal of Heredity* (1982) 73:257-263.
- ❖ Molofsky AV, Krencik R, Ullian EM, Tsai HH, Deneen B, Richardson WD, Barres BA, Rowitch DH. Astrocytes and disease: a neurodevelopmental perspective. *Genes & Development* (2012) 26(9):891-907.
- ❖ Monsivais P, Clark BA, Roth A, Häusser M. Determinants of action potential propagation in cerebellar Purkinje cell axons. *J Neurosci* (2005) 25: 464–472.
- ❖ Mori T, Tanaka K, Buffo A, Wurst W, Kuhn R, Gotz M. Inducible gene deletion in astroglia and radial glia—a valuable tool for functional and lineage analysis. *Glia* (2006) 54:21–34.

- ❖ Morrison ME, Mason CA. Granule neuron regulation of Purkinje cell development: striking a balance between neurotrophin and glutamate signaling. *Journal of Neuroscience* (1998) 18(10):3563-3573.
- ❖ Motta M, Tatti M, Furlan F, Celato A, Di Fruscio G, Polo G, Manara R, Nigro V, Tartaglia M, Burlina A, Salvioli R. Clinical, biochemical and molecular characterization of prosaposin deficiency. *Clinical Genetics* (2016) 90(3):220-229.
- ❖ Mugnaini E, Floris A. The unipolar brush cell: a neglected neuron of the mammalian cerebellar cortex. *Journal of Comparative Neurology* (1994) 339:174–180.
- ❖ Müller Smith K, Williamson TL, Schwartz ML, Vaccarino FM. Impaired motor coordination and disrupted cerebellar architecture in Fgfr1 and Fgfr2 double knockout mice. *Brain Research* (2012) 1460:12–24.
- ❖ Munkacsı AB, Chen FW, Brinkman MA, Higaki K, Gutiérrez GD, Chaudhari J, Layer JV, Tong A, Bard M, Boone C, Ioannou YA, Sturley SL. An “exacerbate-reverse” strategy in yeast identifies histone deacetylase inhibition as a correction for cholesterol and sphingolipid transport defects in human Niemann-Pick Type C disease. *Journal of Biological Chemistry* (2011) 286:23842–23851.
- ❖ Nagappan G, Lu B. Activity-dependent modulation of the BDNF receptor TrkB: mechanisms and implications. *Trends in Neurosciences* (2005) 28:464–471.
- ❖ Nakagawa S, Watanabe M, Isobe T, Kondo H, Inoue Y. Cytological compartmentalization in the staggerer cerebellum, as revealed by calbindin immunohistochemistry for Purkinje cells. *Journal of Comparative Neurology* (1998) 395:112–120.
- ❖ Naureckiene S, Sleat DE, Lackland H, Fensom A, Vanier MT, Wattiaux R, Jadot M, Lobel P. Identification of HE1 as the second gene of Niemann-Pick C disease. *Science* (2000) 290:2298-2301.
- ❖ Navascués J, Cuadros MA, Almendros A. Development of microglia: Evidence from studies in the avian central nervous system. In: *Topical Issues in Microglia Research* (1996) 43-64.
- ❖ Nery S, Wichterle H, Fishell G. Sonic hedgehog contributes to oligodendrocyte specification in the mammalian forebrain. *Development* (2001) 128(4):527-540.
- ❖ Neufeld EB, Cooney AM, Pitha J, Dawidowicz EA, Dwyer NK, Pentchev PG, Blanchette-Mackie EJ. Intracellular trafficking of cholesterol monitored with a cyclodextrin. *The Journal of Biological Chemistry* (1996) 271(35):21604-21613.
- ❖ Niemann A. Ein unbekanntes Krankheitsbild. *Jahrb Kinderheilkd* (1914) 79: 1–3.
- ❖ Nishiyama A, Komitova M, Suzuki R, Zhu X. Polydendrocytes (NG2 cells): multifunctional cells with lineage plasticity. *Nature Reviews Neuroscience* (2009) 10:9–22.
- ❖ Nunzi MG, Birnstiel S, Bhattacharyya BJ, Slater NT, Mugnaini E. Unipolar brush cells form a glutamatergic projection system within the mouse cerebellar cortex. *Journal of Comparative Neurology* (2001) 434:329–341.
- ❖ Offermanns S, Hashimoto K, Watanabe M, Sun W, Kurihara H, Thompson RF, Inoue Y, Masanobu, Kano M, Simon MI. Impaired motor coordination and persistent multiple climbing fiber innervation of cerebellar Purkinje cells in mice lacking Galphaq. *PNAS USA* (1997) 94:14089–14094.
- ❖ Ogata K, Kosaka T. Structural and quantitative analysis of astrocytes in the mouse hippocampus. *Neuroscience* (2002) 113:221– 233.

- ❖ Ozbay T, Merrill AH Jr, Sewer MB. ACTH regulates steroidogenic gene expression and cortisol biosynthesis in the human adrenal cortex via sphingolipid metabolism. *Endocrine Research* (2004) 30:787–794.
- ❖ Pajares S, Arias A, Garcia-Villoria J, Macias-Vidal J, Ros E, de las Heras J, Giros M, Coll MJ, Ribes A. Cholestane-3 β ,5 α ,6 β -triol: high levels in Niemann-Pick type C, cerebrotendinous xanthomatosis, and lysosomal acid lipase deficiency. *Journal of Lipid Research* (2015) 56:1926–1935.
- ❖ Palay SL, Chan-Palay V. Cerebellar cortex: cytology and organization. *Berlin-Heidelberg-New York: Springer* (1974).
- ❖ Palkovits M, Magyar P, Szentágothai J. Quantitative histological analysis of the cerebellar cortex in the cat. II. Cell numbers and densities in the granular layer. *Brain Research* (1971) 32:15–30.
- ❖ Palladino G, Loizzo S, Fortuna A, Canterini S, Palombi F, Erickson RP, Mangia F, Fiorenza MT. Visual evoked potentials of Niemann-Pick type C1 mice reveal an impairment of the visual pathway that is rescued by 2-hydroxypropyl- β -cyclodextrin. *Orphanet Journal of Rare Disease* (2015) 10:133.
- ❖ Pandi S, Chandran V, Deshpande A, Kurien A. Niemann-Pick disease type C or Gaucher's disease type 3? A clinical conundrum. *BMJ Case Report* (2014) pii: bcr2014203713.
- ❖ Paolicelli RC, Bolasco G, Pagani F, Maggi L, Scianni M, Panzanelli P, Giustetto M, Ferreira TA, Guiducci E, Dumas L, Ragozzino D, Gross CT. Synaptic pruning by microglia is necessary for normal brain development. *Science* (2011) 333: 1456–1458.
- ❖ Papandreou A, Gissen P. Diagnostic workup and management of patients with suspected Niemann-Pick type C disease. *Therapeutic Advances in Neurological Disorders* (2016) 9(3):216–229.
- ❖ Park WD, O'Brien JF, Lundquist PA, Kraft DL, Vockley CW, Karnes PS, Patterson MC, Snow K. Identification of 58 novel mutations in Niemann-Pick disease type C: correlation with biochemical phenotype and importance of PTC1-like domains in NPC1. *Hum Mutat.* (2003) 22(4):313-25.
- ❖ Patterson MC, Platt F. Therapy of Niemann-Pick disease, type C. *Biochimica et Biophysica Acta* (2004) 1685:77–82.
- ❖ Patterson MC, Vanier MT, Suzuki K, Morris JA, Carstea E, Neufeld EB, Blanchette-Mackie JE, Pentchev P. Niemann-Pick disease type C: a lipid trafficking disorder. The Metabolic and Molecular Bases of Inherited Disease. *Clinical Genetics* (2001) 64: 269-281.
- ❖ Pedraza L, Fidler L, Staugaitis SM, Colman DR. The active transport of myelin basic protein into the nucleus suggests a regulatory role in myelination. *Neuron* (1997) 18:579–589.
- ❖ Pekny M, Wilhelmsson U, Pekna M. The dual role of astrocyte activation and reactive gliosis. *Neuroscience Letters* (2014) 565: 30–38.
- ❖ Pentchev PG, Boothe AD, Kruth HS, Weintraub H, Stivers J, Brady RO. A genetic storage disorder in BALB/C mice with a metabolic block in esterification of exogenous cholesterol. *Journal of Biological Chemistry* (1984) 259:5784-5791.
- ❖ Pentchev PG, Comly ME, Kruth HS, Tokoro T, Butler J, Sokol J, Filling-Katz M, Quirk JM, Marshall DC, Patel S. Group C Niemann-Pick disease: faulty regulation of low-density lipoprotein uptake and cholesterol storage in cultured fibroblasts. *The FASEB Journal* (1987) 1(1):40-45.

- ❖ Pentchev PG, Comly ME, Kruth HS, Tokoro T, Butler J, Sokol J, Filling-Katz M, Quirk JM, Marshall DC, Patel S. Group C Niemann-Pick disease: faulty regulation of low-density lipoprotein uptake and cholesterol storage in cultured fibroblasts. *The FASEB Journal* (1987) 1(1):40-45.
- ❖ Pentchev PG, Tagle DA. Niemann-Pick C1 disease gene: homology to mediators of cholesterol homeostasis. *Science* (1996) 277:228-231.
- ❖ Pentchev PG, Tagle DA. Niemann-Pick C1 disease gene: homology to mediators of cholesterol homeostasis. *Science* (1996) 277:228-231.
- ❖ Pepinsky RB, Zeng C, Wen D, Rayhorn P, Baker DP, Williams KP, Bixler SA, Ambrose CM, Garber EA, Miatkowski K, Taylor FR, Wang EA, Galdes A. Identification of a palmitic acid-modified form of human sonic hedgehog. *Journal of Biological Chemistry* (1998) 273(22):14037–14045.
- ❖ Perdiguero EG, Klapproth K, Schulz C, Busch K, Azzoni E, Crozet L, Garner H, Trouillet C, de Bruijn MF, Geissmann F, Rodewald HR. Tissue-resident macrophages originate from yolk-sac-derived erythro-myeloid progenitors. *Nature* (2015) 518:547–551.
- ❖ Perego C, Fumagalli S, De Simoni MG. Temporal pattern of expression and colocalization of microglia/macrophage phenotype markers following brain ischemic injury in mice. *Journal of Neuroinflammation* (2011) 8:174.
- ❖ Peri F, Nüsslein-Volhard C. Live imaging of neuronal degradation by microglia reveals a role for v0-ATPase a1 in phagosomal fusion in vivo. *Cell* (2008) 133:916–927.
- ❖ Perry VH. A revised view of the central nervous system microenvironment and major histocompatibility complex class II antigen presentation. *Journal of Neuroimmunology* (1998) 90:113–121.
- ❖ Peters A, Palay SL, Webster HF. The fine structure of the nervous system. *New York: Oxford UP* (1991).
- ❖ Petrosini L, Molinari M, Gremoli T. Hemispherectomy and motor behaviour in rats. I. Development of motor function after neonatal lesion. *Experimental Brain Research* (1990) 82:472–482.
- ❖ Pick L. Über die kipoidzellige Splenohepatomegalie typus Niemann-Pick als Stoffwechselerkrankung. *Medizinische Klinik* (1927) 23: 1483–1486.
- ❖ Picou F, Fauquier T, Chatonnet F, Flamant F. A bimodal influence of thyroid hormone on cerebellum oligodendrocyte differentiation. *Molecular Endocrinology* (2012) 26:608–618.
- ❖ Pinto R, Caseiro C, Lemos M, Lopes L, Fontes A, Ribeiro H, Pinto E, Silva E, Rocha S, Marcao A, Ribeiro I, Lacerda L, Ribeiro G, Amaral O. Prevalence of lysosomal storage diseases in Portugal. *European Journal of Human Genetics* (2004) 12:87-92.
- ❖ Pinto R, Caseiro C, Lemos M, Lopes L, Fontes A, Ribeiro H, Pinto E, Silva E, Rocha S, Marcao A, Ribeiro I, Lacerda L, Ribeiro G, Amaral O. Prevalence of lysosomal storage diseases in Portugal. *European Journal of Human Genetics* (2004) 12:87-92.
- ❖ Pipalia NH, Cosner CC, Huang A, Chatterjee A, Bourbon P, Farley N, Helquist P, Wiest O, Maxfield FR. Histone deacetylase inhibitor treatment dramatically reduces cholesterol accumulation in Niemann-Pick Type C1 mutant human fibroblasts. *PNAS USA* (2011) 108:5620–5625.

- ❖ Piraud M, Pettazzoni M, Pagan C, Cheillan D, Froissart R, Saban C. Measurement of lysosphingolipids and their isoforms by LC-MS/MS in plasma, urine and amniotic fluid: application to screening of sphingolipidoses. *20th ESGLD Workshop, Abstracts, Unpublished results, Naples, Italy, 2015*, pp. 111.
- ❖ Platt FM, Neises GR, Karlsson GB, Dwek RA, Butters TD. N-Butyldeoxygalactonojirimycin inhibits glycolipid biosynthesis but does not affect N-linked oligosaccharide processing. *Journal of Biological Chemistry* (1994) 269(43):27108–27114.
- ❖ Poblete-Naredo I, Guillem AM, Juárez C, Zepeda RC, Ramírez L, Caba M, Hernández-Kelly LC, Aguilera J, López-Bayghen E, Ortega A. Brain-derived neurotrophic factor and its receptors in Bergmann glia cells. *Neurochemistry International* (2011) 59(8):1133-1144.
- ❖ Porter FD, Scherrer DE, Lanier MH, Langmade SG, Molugu V, Gale SE, Olzeski D, Sidhu R, Dietzen DJ, R. Fu, Wassif CA, Yanjanin NM, Marso SP, House J, Vite C, Schaffer JE, Ory DS. Cholesterol oxidation products are sensitive and specific blood-based biomarkers for Niemann-Pick C1 disease. *Science Translational Medicine* (2010) 2:56ra81.
- ❖ Porter JA, Young KE, Beachy PA. Cholesterol modification of hedgehog signaling proteins in animal development. *Science* (1996) 274(5285):255–259.
- ❖ Prestori F, Rossi P, Bearzatto B, Lainé J, Necchi D, Diwakar S, Schiffmann SN, Axelrad H, D'Angelo E. Altered neuron excitability and synaptic plasticity in the cerebellar granular layer of juvenile prion protein knock-out mice with impaired motor control. *Journal of Neuroscience* (2008) 28:7091–7103.
- ❖ Rakic P, Sidman, RL. Histogenesis of cortical layers in human cerebellum, particularly the lamina dissecans. *Journal of Comparative Neurology* (1970) 139:473–500.
- ❖ Rakic P. Extrinsic cytological determinants of basket and stellate cell dendritic pattern in the cerebellar molecular layer. *Journal of Comparative Neurology* (1972) 146:335–354.
- ❖ Rakic P. Neuron-glia relationship during granule cell migration in developing cerebellar cortex. A Golgi and electronmicroscopic study in Macacus Rhesus. *Journal of Comparative Neurology* (1971) 141:283–312.
- ❖ Ramirez CM, Liu B, Taylor AM, Repa JJ, Burns DK, Weinberg AG, Turley SD, Dietschy JM. Weekly cyclodextrin administration normalizes cholesterol metabolism in nearly every organ of the Niemann-Pick type C1 mouse and markedly prolongs life. *Pediatric Research* (2010) 68:309–315.
- ❖ Raymond KM, Turgeon C, Ory D, Lourenço C, Giugliani R, Rinaldo P, Gavrillov D, Oglesbee D, Tortorelli S, Matern D, Combined analysis of plasma oxysterol and lysosphingomyelin, for Niemann-Pick types A, B and C diagnosis. *Journal of Inherited Metabolic Disease* (2015) 38(1):S36.
- ❖ Reichenbach A, Derouiche A, Kirchhoff F. Morphology and dynamics of perisynaptic glia. *Brain Research Reviews* (2010) 63:11–25.
- ❖ Reid PC, Sakashita N, Sugii S, Ohno-Iwashita Y, Shimada Y, Hickey WF, Chang TY. A novel cholesterol stain reveals early neuronal cholesterol accumulation in the Niemann-Pick type C1 mouse brain. *Journal of Lipid Research* (2004) 45:582–591.
- ❖ Repetto M, Maziere JC, Citadelle D, Dupus R, Meier M, Biade S, Quiec D, Roux C. Teratogenic effect of the cholesterol synthesis inhibitor AY 9944 on rat embryos in vitro. *Teratology* (1990) 42:611- 618.

- ❖ Reunert J, Fobker M, Kannenberg F, Du Chesne I, Plate M, Wellhausen J, Rust S, Marquardt T. Rapid diagnosis of 83 patients with Niemann Pick type C disease and related cholesterol transport disorders by cholestantriol screening. *EBioMedicine* (2016) 4:170–175.
- ❖ Reynolds R, Wilkin GP. Development of macroglial cells in rat cerebellum. II. An in situ immunohistochemical study of oligodendroglial lineage from precursor to mature myelinating cell. *Development* (1988) 102:409–425.
- ❖ Reynolds R, Wilkin GP. Development of macroglial cells in rat cerebellum. II. An in situ immunohistochemical study of oligodendroglial lineage from precursor to mature myelinating cell. *Development* (1988) 102:409–425.
- ❖ Ribas GS, Pires R, Coelho JC, Rodrigues D, Mescka CP, Vanzin CS, Biancini GB, Negretto G, Wayhs CA, Wajner M, Vargas CR. Oxidative stress in Niemann-Pick type C patients: a protective role of N-butyl-deoxyojirimycin therapy. *International Journal of Developmental Neuroscience* (2012) 30(6):439–44.
- ❖ Rico B, B Xu, Reichardt LF. TrkB receptor signaling is required for establishment of GABAergic synapses in the cerebellum. *Nature Neuroscience* (2002) 5:225–233.
- ❖ Ries M, Schaefer E, Luhrs T, Mani L, Kuhn J, Vanier MT, Krummenauer F, Gal A, Beck M, Mengel E. Critical assessment of chitotriosidase analysis in the rational laboratory diagnosis of children with Gaucher disease and Niemann-Pick disease type A/B and C. *Journal of Inherited Metabolic Disease* (2006) 29:647–652.
- ❖ Romanello M, Zampieri S, Bortolotti N, Deroma L, Sechi A, Fiumara A, Parini R, Borroni B, Brancati F, Bruni A, Russo CV, Bordugo A, Bembì B, Dardis A. Comprehensive evaluation of plasma 7-ketocholesterol and cholestan-3 β ,5 α ,6 β -triol in an Italian cohort of patients affected by Niemann-Pick disease due to NPC1 and SMPD1 mutations. *Clinica Chimica Acta* (2016) 455:39–45.
- ❖ Rosenbaum AI, Maxfield FR. Niemann-Pick type C disease: molecular mechanisms and potential therapeutic approaches. *Journal of Neurochemistry* (2011) 116(5):789–795.
- ❖ Rosenbaum AI, Rujoi M, Huang AY, Du H, Grabowski GA, Maxfield FR. Chemical screen to reduce sterol accumulation in Niemann-Pick C disease cells identifies novel lysosomal acid lipase inhibitors. *Biochimica et Biophysica Acta* (2009) 1791:1155–1165.
- ❖ Rosenbaum AI, Zhang G, Warren JD, Maxfield FR. Endocytosis of beta-cyclodextrins is responsible for cholesterol reduction in Niemann-Pick type C mutant cells. *PNAS USA* (2010b) 107:5477–5482.
- ❖ Rossi F, Corvetti L, Gianola S. The strange case of Purkinje axon regeneration and plasticity. *Cerebellum* (2006) 5:163–173.
- ❖ Runz H, Dolle D, Schlitter AM, Zschocke J. NPC-db, a Niemann-Pick type C disease gene variation database. *Human Mutations* (2008) 29:345–350.
- ❖ Saab AS, Neumeyer A, Jahn HM, Cupido A, Simek AAM, Boele HJ, Scheller A, Le Meur K, Gotz M, Monyer H, Sprengel R, Rubio ME, Deitmer JW, De Zeeuw CI, Kirchhoff F. Bergmann glial AMPA receptors are required for fine motor coordination. *Science* (2012) 337:749–753.
- ❖ Sahin M, Hockfield S. Molecular identification of the Lugaro cell in the cat cerebellar cortex. *Journal of Comparative Neurology* (1990) 301:575–584.

- ❖ Sarna JR, Larouche M, Marzban H, Sillitoe RV, Rancourt DE, Hawkes R. Patterned Purkinje cell degeneration in mouse models of Niemann–Pick type C disease. *Journal of Comparative Neurology* (2003) 456:279-291.
- ❖ Sattler R, Rothstein JD. Regulation and dysregulation of glutamate transporters. *Handbook of Experimental Pharmacology* (2006) 175:277–303.
- ❖ Schiffmann R. Niemann-Pick disease type C. From bench to bedside. *JAMA* (1996) 276(7):561-564.
- ❖ Schilling K, Oberdick J, Rossi F, Baader SL. Besides Purkinje cells and granule neurons: an appraisal of the cell biology of the interneurons of the cerebellar cortex. *Histochemistry and Cell Biology* (2008) 130:601–615.
- ❖ Schulz C, Gomez Perdiguero E, Chorro L, Szabo-Rogers H, Cagnard N, Kierdorf K, Prinz M, Wu B, Jacobsen SE, Pollard JW, Frampton J, Liu KJ, Geissmann F. A lineage of myeloid cells independent of Myb and hematopoietic stem cells. *Science* (2012) 336:86–90.
- ❖ Schwartz PM, Borghesani PR, Levy RL, Pomeroy SL, Segal RA. Abnormal cerebellar development and foliation in BDNF^{-/-} mice reveals a role for neurotrophins in CNS patterning. *Neuron* (1997) 19:269–281.
- ❖ Scott C, Ioannou YA. The NPC1 protein: structure implies function. *Biochimica et Biophysica Acta* (2004) 1685:8–13.
- ❖ Sedel F, Saudubray JM, Roze E, Agid Y, Vidailhet M. Movement disorders and inborn errors of metabolism in adults: a diagnostic approach. *Journal of Inherited Metabolic Disease* (2008) (3):308-318.
- ❖ Seifert G, Schilling K, Steinhauser C. Astrocyte dysfunction in neurological disorders: a molecular perspective. *Nature Reviews Neuroscience* (2006) 7:194–206.
- ❖ Sekerková G, Ilijic E, Mugnaini E. Time of origin of unipolar brush cells in the rat cerebellum as observed by prenatal bromodeoxyuridine labeling. *Neuroscience* (2004) 127:845–858.
- ❖ Sekerková G, Ilijic E, Mugnaini E. Time of origin of unipolar brush cells in the rat cerebellum as observed by prenatal bromodeoxyuridine labeling. *Neuroscience* (2004) 127:845–858.
- ❖ Sévin M, Lesca G, Baumann N, Millat G, Lyon-Caen O, Vanier MT, Sedel F. The adult form of Niemann-Pick disease type C. *Brain* (2007) 130(1):120-133.
- ❖ Simat M, Ambrosetti L, Lardi-Studler B, Fritschy JM. GABAergic synaptogenesis marks the onset of differentiation of basket and stellate cells in mouse cerebellum. *European Journal of Neuroscience* (2007) 26:2239–2256.
- ❖ Sofroniew MV, Vinters HV. Astrocytes: biology and pathology. *Acta Neuropathologica* (2010) 119:7–35.
- ❖ Sofroniew MV. Molecular dissection of reactive astrogliosis and glial scar formation. *Trends in Neurosciences* (2009) 32:638–647.
- ❖ Sokol J, Blanchette-Mackie J, Kruth HS, Dwyer NK, Amende LM, Butler JD, Robinson E, Patel S, Brady RO, Comly ME. Type C Niemann-Pick disease. Lysosomal accumulation and defective intracellular mobilization of low density lipoprotein cholesterol. *Journal of Biological Chemistry* (1988) 263:3411–3417.
- ❖ Solecki DJ, Liu XL, Tomoda, T, Fang Y, Hatten ME. Activated Notch2 signaling inhibits differentiation of cerebellar granule neuron precursors by maintaining proliferation. *Neuron* (2001) 31: 557–568.

- ❖ Solomon D, Winkelman AC, Zee DS, Gray L, Buttner-Ennever J. Niemann–Pick type C disease in two affected sisters: ocular motor recordings and brain-stem neuropathology. *Annals of the New York Academy Sciences* (2005) 1039:436-445.
- ❖ Sotelo C, Rossi F. Purkinje cell migration and differentiation. In: Manto, M., Gruol, D.L., Schmähmann, J.D., Koibuchi, N., Rossi, F. Handbook of the Cerebellum and Cerebellar Disorders. *Springer, New York, Heidelberg* (2012) pp. 147–178.
- ❖ Sotelo C. Cellular and genetic regulation of the development of the cerebellar system. *Progress in Neurobiology* (2004) 72:296–339.
- ❖ Spacek J. Three-dimensional analysis of dendritic spines. III. *Glial sheath. Anatomy and Embryology* (1985) 171: 245–252.
- ❖ Spiegel R, Raas-Rothschild A, Reish O, Regev M, Meiner V, Bargal R, Sury V, Meir K, Nadjari M, Hermann G, Iancu TC, Shalev SA, Zeigler M. The clinical spectrum of fetal Niemann–Pick type C. *American Journal of Medical Genetics* (1999) 149A:446-450.
- ❖ Steinberg SJ, Ward CP, Fensom AH. Complementation studies in Niemann-Pick disease type C indicate the existence of a second group. *Journal of Medical Genetics* (1994) 31(4):317-320.
- ❖ Stevens B, Allen NJ, Vazquez LE, Howell GR, Christopherson KS, Nouri N, Micheva KD, Mehalow AK, Huberman AD, Stafford B, Sher A, Litke AM, Lambris JD, Smith SJ, John SW, Barres BA. The classical complement cascade mediates CNS synapse elimination. *Cell* (2007) 131:1164–1178.
- ❖ Storey JD. Strong control, conservative point estimation and simultaneous conservative consistency of false discovery rates: a unified approach. *Journal of the Royal Statistical Society* (2004) 66:87–205.
- ❖ Sudarov A, Joyner AL. Cerebellum morphogenesis: the foliation pattern is orchestrated by multi-cellular anchoring centers. *Neural Development* (2007) 2:26.
- ❖ Sueyoshii N, Maehara T, Ito M. Apoptosis of Neuro2a cells induced by lysosphingolipids with naturally occurring stereochemical configurations. *Journal of Lipid Research* (2001) 42:1197–1202.
- ❖ Sun X, Marks DL, Park WD, Wheatley CL, Puri V, O'Brien JF, Kraft DL, Lundquist PA, Patterson MC, Pagano RE and Snow K. Niemann-Pick C variant detection by altered sphingolipid trafficking and correlation with mutations within a specific domain of NPC1. *American Journal of Human Genetics* (2001) 68:1361-1372.
- ❖ Suzuki K. Twenty five years of the “psychosine hypothesis”: a personal perspective of its history and present status. *Neurochemical Research* (1998) 23:251–259.
- ❖ Suzuki S, Kiyosue K, Hazama S, Ogura A, Kashihara M, Hara T, Koshimizu H, Kojima M. Brain-derived neurotrophic factor regulates cholesterol metabolism for synapse development. *Journal of Neuroscience* (2007) 27:6417–6427.
- ❖ Suzuki S, Numakawa T, Shimazu K, Koshimizu H, Hara T, Hatanaka H, Mei L, Lu B, Kojima M. BDNF-induced recruitment of TrkB receptor into neuronal lipid rafts: roles in synaptic modulation. *The Journal of cell biology* (2004) 167:1205–1215.
- ❖ Swinnen N, Smolders S, Avila A, Notelaers K, Paesen R, Ameloot M, Brone B, Legendre P, Rigo JM. Complex invasion pattern of the cerebral cortex by microglial cells during development of the mouse embryo. *Glia* (2013) 61:150–163.
- ❖ Takayasu Y, Iino M, Takatsuru Y, Tanaka K, Ozawa S. Functions of glutamate transporters in cerebellar Purkinje cell synapses. *Acta Physiologica* (2009) 197:1–12.

- ❖ Takikita S, Fukuda T, Mohri I, Yagi T, Suzuki K. Perturbed myelination process of premyelinating oligodendrocyte in Niemann-Pick type C mouse. *Journal of Neuropathology and Experimental Neurology* (2004) 63:660–673.
- ❖ Tarugi P, Ballarini G, Bembi B, Battisti C, Palmeri S, Panzani F, Di Leo E, Martini C, Federico A, Calandra S. Niemann-Pick type C disease: mutations of NPC1 gene and evidence of abnormal expression of some mutant alleles in fibroblasts. *Journal of Lipid Research* (2002) 43:1908-1919.
- ❖ te Vruchte D, Lloyd-Evans E, Veldman RJ, Neville DC, Dwek RA, Platt FM, van Blitterswijk WJ, Sillence DJ. Accumulation of glycosphingolipids in Niemann-Pick C disease disrupts endosomal transport. *Journal of Biological Chemistry* (2004) 279(25):26167-26175.
- ❖ Tettamanti G, Bassi R, Viani P, Riboni. Salvage pathways in glycosphingolipid metabolism. *Biochimie* (2003) 85: 423–437.
- ❖ Tilleux S, Hermans E. Down-regulation of astrocytic GLAST by microglia-related inflammation is abrogated in dibutyryl cAMP-differentiated cultures. *Journal of Neurochemistry* (2008) 105:2224–2236.
- ❖ Trendelenburg G, Vanier MT, Maza S, Millat G, Bohner G, Munz DL, Zschenderlein R. Niemann-Pick type C disease in a 68-year-old patient. *Journal of Neurology, Neurosurgery and Psychiatry* (2006) 77(8):997-998.
- ❖ Truett GE, Heeger P, Mynatt RL, Truett AA, Walker JA, Warman ML. Preparation of PCR-quality mouse genomic DNA with hot sodium hydroxide and tris (HotSHOT). *Biotechniques* (2000) 29(1):52-54.
- ❖ Ullian EK, Sapperstein SK, Christopherson KS, Barres BA. Control of synapse number by glia. *Science* (2001) 291:657– 661.
- ❖ Vaillant C, Monard D. Shh pathway and cerebellar development. *Cerebellum* (2009) 8(3): 291-301.
- ❖ Vance JE. Lipid imbalance in the neurological disorder, Niemann-Pick C disease. *FEBS Letters* (2006) 580:5518-52411
- ❖ Vanier MT, Duthel S, Rodriguez-Lafrasse C, Pentchev P, Carstea ED. Genetic heterogeneity in Niemann-Pick C disease: a study using somatic cell hybridization and linkage analysis. *American Journal of Human Genetics* (1996) 58(1):118-125.
- ❖ Vanier MT, Millat G. Niemann-Pick disease type C. *Clinical Genetics* (2003) 64:269-281.
- ❖ Vanier MT, Millat G. Structure and function of the NPC2 protein. *Biochimica et Biophysica Acta* (2004) 1685:14–21.
- ❖ Vanier MT, Gissen P, Bauer P, Coll MJ, Burlina A, Hendriksz CJ, Latour P, Goizet C, Welford RW, Marquardt T, Kolb SA. Diagnostic tests for Niemann-Pick disease type C (NP-C): A critical review. *Molecular Genetics and Metabolism* (2016) 118(4):244-254.
- ❖ Vanier MT, Rodriguez-Lafrasse C, Rousson R, Gazzah N, Juge MC, Pentchev PG, Revol A, Louisot P. Type C Niemann-Pick disease: spectrum of phenotypic variation in disruption of intracellular LDL-derived cholesterol processing. *Biochimica et Biophysica Acta* (1991) 1096:328–337.
- ❖ Vanier MT. Complex lipid trafficking in Niemann-Pick disease type C, *Journal of Inherited Metabolic Disease* 38 (2015) 187–199.
- ❖ Vanier MT. Complex lipid trafficking in Niemann-Pick disease type C. *Journal of Inherited Metabolic Disease* (2015) 38:187–199.

- ❖ Vanier MT. Niemann Pick disease type C. *Orphanet Journal of Rare Disease* (2010) 5:16.
- ❖ Vanier MT. Niemann Pick disease type C. *Orphanet. J. Rare Dis.*, (2010) 5:16.
- ❖ Vanier MT. Phenotypic and genetic heterogeneity in Niemann-Pick disease type C: current knowledge and practical implications. *Wiener klinische Wochenschrift* (1997) 109:68-73.
- ❖ Vela JM, Dalmau I, Gonzalez B, Castellano B. Morphology and distribution of microglial cells in the young and adult mouse cerebellum. *Journal of Comparative Neurology* (1995) 361:602–616.
- ❖ Vèlez-Fort M, Audinat E, Angulo MC. Central role of GABA in neuron–glia interactions. *Neuroscientist* (2012) 18:237–250.
- ❖ Vite C, Bagel J, Swain G, Prociuk M, Sikora T, Stein V, O'Donnell P, Ruane T, Ward S, Crooks A, Li S, Mauldin E, Stellar S, De Meulder M, Kao ML, Ory DS, Davidson C, Vanier MT, Walkley SU. Intracisternal cyclodextrin prevents cerebellar dysfunction and Purkinje cell death in feline Niemann-Pick type C1 disease. *Science Translational Medicine* (2015) 7:276ra226.
- ❖ Vöikar V, Rauvala H, Ikonen E. Cognitive deficit and development of motor impairment in a mouse model of Niemann-Pick type C disease. *Behavioral Brain Research* (2002) 132:1–10.
- ❖ Vranesic I, Iijima T, Ichikawa M, Matsumoto G, Knöpfel T. Signal transmission in the parallel fiber Purkinje cell system visualized by high-resolution imaging. *PNAS USA* (1994) 91: 13014-13017.
- ❖ Walkley SU, Suzuki K. Consequences of NPC1 and NPC2 loss of function in mammalian neurons. *Biochim. Biophys. Acta* (2004) 1685:48-62.
- ❖ Wallace VA. Purkinje-cell-derived Sonic hedgehog regulates granule neuron precursor cell proliferation in the developing mouse cerebellum. *Current Biology* (1999) 9:445–448.
- ❖ Walterfang M, Fahey M, Desmond P, Wood A, Seal ML, Steward C, Adamson C, Kokkinos C, Fietz M, Velakoulis D. White and gray matter alterations in adults with Niemann-Pick disease type C: a cross-sectional study. *Neurology* (2010) 75:49–56.
- ❖ Walterfang W, Fietz M, Abel L, Bowman E, Mocellin R, Velakoulis D. Gender dimorphism in siblings with schizophrenia-like psychosis due to Niemann–Pick disease type C. *Journal of Inherited Metabolic Disease* (2009) 32(1):S221-226.
- ❖ Wang F, Xu Q, Wang W, Takano T, Needergard M. Bergmann glia modulate Purkinje cell bistability via Ca²⁺-dependent K⁺ uptake. *PNAS USA* (2012) 109:7911–7916.
- ❖ Wang ML, Motamed M, Infante RE, Abi-Mosleh L, Kwon HJ, Brown MS, Goldstein JL. Identification of surface residues on Niemann-Pick C2 essential for hydrophobic handoff of cholesterol to NPC1 in lysosomes. *Cell Metabolism* (2010) 12:166-173.
- ❖ Wassif CA, Cross JL, Iben J, Sanchez-Pulido L, Coughnoux A, Platt FM, Ory DS, Ponting CP, Bailey-Wilson JE, Biesecker LG, Porter FD. High incidence of unrecognized visceral/neurological late-onset Niemann-Pick disease, type C1, predicted by analysis of massively parallel sequencing data sets. *Genetical Medicine* (2016) 18(1):41-48.
- ❖ Watanabe Y, Akaboshi S, Ishida G, Takeshima T, Yano T, Taniguchi M, Ohno K, Nakashima K. Increased levels of GM2 ganglioside in fibroblasts from a patient with juvenile Niemann-Pick disease type C. *Brain Development* (1998) 20(2):95-97.

- ❖ Watari H, Blanchette-Mackie EJ, Dwyer NK. Niemann Pick C1 protein: obligatory roles for N-terminal domains and lysosomal targeting in cholesterol mobilization. *PNAS USA* (1999) 96: 805-810.
- ❖ Watase K, Hashimoto K, Kano M, Yamada K, Watanabe M, Inoue Y, Okuyama S, Sakagawa T, Ogawa S, Kawashima N, Hori S, Takimoto M, Wada K, Tanaka K. Motor discoordination and increased susceptibility to cerebellar injury in GLAST mutant mice. *Europe Journal of Neuroscience* (1998) 10:976-988.
- ❖ Weber A, Schachner M. Maintenance of immunologically identified Purkinje cells from mouse cerebellum in monolayer culture. *Brain Research* (1984) 311:119-130.
- ❖ Wechsler-Reya RJ, Scott MP. Control of neuronal precursor proliferation in the cerebellum by Sonic Hedgehog. *Neuron* (1999) 22: 103-114.
- ❖ Weisheit G, Gliem M, Endl E, Pfeffer PL, Busslinger M, Schilling K. Postnatal development of the murine cerebellar cortex: formation and early dispersal of basket, stellate and Golgi neurons. *European Journal of Neuroscience* (2006) 24:466-478.
- ❖ Welford RW, Garzotti M, Lourenço CM, Mengel E, Marquardt T, Reunert J, Amraoui Y, Kolb SA, Morand O, Groenen P. Plasma lysosphingomyelin demonstrates great potential as a diagnostic biomarker for Niemann-Pick disease type C in a retrospective study. *PLOS One* (2014) 9:e114669.
- ❖ Wewetzer K, Rauvala H, Unsicker K. Immunocytochemical localization of the heparin-binding growth-associated molecule (HB-GAM) in the developing and adult rat cerebellar cortex. *Brain Research* (1995) 693:31-38.
- ❖ Weyer A, Schilling K. Developmental and cell type-specific expression of the neuronal marker NeuN in the murine cerebellum. *Journal of Neuroscience Research* (2003) 73:400-409.
- ❖ Wigley R, Hamilton N, Nishiyama A, Kirchhoff F, Butt AM. Morphological and physiological interactions of NG2-glia with astrocytes and neurons. *Journal of Anatomy* (2007) 210:661-670.
- ❖ Wraith JE, Baumgartner MR, Bembi B, Covanis A, Levade T, Mengel E, Pineda M, Sedel F, Topcu M, Vanier MT, Widner H, Wijburg FA, Patterson MC. Recommendations on the diagnosis and management of Niemann-Pick disease type C. *Molecular Genetics and Metabolism* (2009) 98:152-165.
- ❖ Wulff P, Schonewille M, Renzi M, Viltono L, Sassoè-Pognetto M, Badura A, Gao Z, Hoebeek FE, van Dorp S, Wisden W, Farrant M, De Zeeuw CI. Synaptic inhibition of Purkinje cells mediates consolidation of vestibulo-cerebellar motor learning. *Nature Neuroscience* (2009) 12(8):1042-1049.
- ❖ Xie X, Brown MS, Shelton JM, Richardson JA, Goldstein JL, Liang G. Amino acid substitution in NPC1 that abolishes cholesterol binding reproduces phenotype of complete NPC1 deficiency in mice. *PNAS USA* (2011) 108:15330-15335.
- ❖ Xu ZQ, Sun Y, Li HY, Lim Y, Zhong JH, Zhou XF. Endogenous proBDNF is a negative regulator of migration of cerebellar granule cells in neonatal mice. *European Journal of Neuroscience* (2011) 33(8):1376-84.
- ❖ Xu-Friedman MA, Harris KM, Regehr WG. Three-dimensional comparison of ultrastructural characteristics at depressing and facilitating synapses onto cerebellar Purkinje cells. *Journal of Neuroscience* (2001) 21:6666-6672.
- ❖ Yam PT, Charron F. Signaling mechanisms of non-conventional axon guidance cues: the Shh, BMP and Wnt morphogens. *Current Opinion in Neurobiology* (2013) 23(6):965-973.

- ❖ Yamada K, Fukaya M, Shibata T, Kurihara H, Tanaka K, Inoue Y, Watanabe M. Dynamic transformation of Bergmann glial fibers proceeds in correlation with dendritic outgrowth and synapse formation of cerebellar Purkinje cells. *Journal of Comparative Neurology* (2000) 418:106–120.
- ❖ Yamada K, Watanabe M. Cytodifferentiation of Bergmann glia and its relationship with Purkinje cells. *Anatomical Science International* (2002) 77:94–108.
- ❖ Yamamoto T, Ninomiya H, Matsumoto M, Ohta Y, Nanba E, Tsutsumi Y, Yamakawa K, Millat G, Vanier MT, Pentchev PG, Ohno K. Genotype-phenotype relationship of Niemann-Pick disease type C: a possible correlation between clinical onset and levels of NPC1 protein in isolated skin fibroblasts. *J Med Genet.* (2000) 37:707-711.
- ❖ Yamanaka H, Yanagawa Y, Obata K. Development of stellate and basket cells and their apoptosis in mouse cerebellar cortex. *Neuroscience Research* (2004) 50:13–22.
- ❖ Yan X, Lukas J, Witt M, Wree A, Hübner R, Frech M, Köhling R, Rolfs A, Luo J. Decreased expression of myelin gene regulatory factor in Niemann-Pick type C 1 mouse. *Metabolic Brain Disease* (2011) 26:299–306.
- ❖ Yévenes LF, Klein A, Castro JF, Marín T, Leal N, Leighton F, Alvarez AR, Zanlungo S. Lysosomal vitamin E accumulation in Niemann-Pick type C disease. *Biochimica et Biophysica Acta.* (2012) 1822(2):150-160.
- ❖ Yu T, Lieberman AP. Npc1 acting in neurons and glia is essential for the formation and maintenance of CNS myelin. *PLOS Genetics* (2013) 9:e1003462.
- ❖ Yuasa S, Kawamura K, Kuwano R, Ono K. Neuron–glia interactions during migration of Purkinje cells in the mouse embryonic cerebellum. *International Journal of Developmental Neuroscience* (1996) 14: 429–438.
- ❖ Yuasa S, Kawamura K, Ono K, Yamakuni T, Takahashi Y. Development and migration of Purkinje in the mouse cerebellar primordium. *Anatomy and Embryology* 184:195–212.
- ❖ Yuasa S. Bergmann glial development in the mouse cerebellum as revealed by tenascin expression. *Anatomy and Embryology* (1996) 194:223–234.
- ❖ Zaaraoui W, Crespy L, Rico A, Faivre A, Soulier E, Confort-Gouny S, Cozzone PJ, Pelletier J, Ranjeva JP, Kaphan E, Audoin B. In vivo quantification of brain injury in adult Niemann-Pick Disease Type C. *Molecular Genetics and Metabolism* (2011) 103(2):138-41.
- ❖ Zervas M, Somers KL, Thrall MA, et al. Critical role for glycosphingolipids in Niemann-Pick disease type C. *Current Biology* 2001;11(16):1283–7.
- ❖ Zhang J, Liu Q. Cholesterol metabolism and homeostasis in the brain. *Protein Cell.* (2015) 6:254–264.
- ❖ Zhang JR, Coleman T, Langmade SJ, Scherrer DE, Lane L, Lanier MH, Feng C, Sands MS, Schaffer JE, Semenkovich CF, Ory DS. Niemann-Pick C1 protects against atherosclerosis in mice via regulation of macrophage intracellular cholesterol trafficking. *Journal of Clinical Investigation* (2008) 118:2281–2290.
- ❖ Zhang L, Goldman JE. Generation of cerebellar interneurons from dividing progenitors in white matter. *Neuron* (1996a) 16:47–54.
- ❖ Zhang M, Strnatka D, Donohue C, Hallows JL, Vincent I, Erickson RP. Astrocyte-only Npc1 reduces neuronal cholesterol and triples life span of Npc1^{-/-} mice. *Journal of Neuroscience Research* (2008) 86:2848–2856.

- ❖ Zhang X, Santuccione A, Leung C, Marino S. Differentiation of postnatal cerebellar glial progenitors is controlled by Bmi1 through BMP pathway inhibition. *Glia* (2011) 59:1118–1131.
- ❖ Zhao S, Hu X, Park J, Zhu Y, Zhu Q, Li H, Luo C, Han R, Cooper N, Qiu M. Selective expression of LDLR and VLDLR in myelinating oligodendrocytes. *Developmental Dynamics* (2007) 236:2708–2712.
- ❖ Zhou S, Davidson C, McGlynn R, Stephney G, Dobrenis K, Vanier MT, Walkley SU. Endosomal/lysosomal processing of gangliosides affects neuronal cholesterol sequestration in Niemann-Pick disease Type C. *American Journal of Pathology* (2011) 179:890–902.